Synthesis of $[Re(CO)_2]^{+/2+}$ Precursors and Substitution Reactions as a Convenient Route to Complexes with the *cis*-$\{Re(CO)_2\}$ Core

Dissertation

zur

Erlangung der naturwissenschaftlichen Doktorwürde

(Dr. sc. nat.)

vorgelegt der

Mathematisch-naturwissenschaftlichen Fakultät

der

Universität Zürich

von

Lukas Kromer

von Winterthur ZH

Promotionskomitee

Prof. Dr. Roger Alberto (Vorsitz)

Prof. Dr. Roland Sigel

Prof. Dr. Peter Hamm

Zürich, 2008

to my family

Table of Content

Summary

The in the meantime well developed organometallic and coordination chemistry of $[M(OH_2)_3(CO)_3]^+$ (M = Re, Tc) raised the fundamental question if a comparable chemistry would exist with M(I) but less CO ligands. Since the CO ligands determine the behaviour of the metal centre to a very large extent, there was in particular an interest in principally similar complexes of the $[MX_4(CO)_2]^n$ (X = Cl^-, Br^-, solvent) type. They are frequently suggested as intermediates in photochemical reactions of $[M(CO)_3]^+$. Considering the importance of the $[M(CO)_3]^+$ core, one might also expect a similar role of complexes with less CO for pharmaceutical applications. In order to have a number of building blocks available for biomolecule labelling, such new cores could complement the known ones but the development of novel cores is widely neglected. Though, a new core would increase the possibilities of labelling biological vectors. Although several $[M(CO)_2]^+$ complexes have been described, there is a lack of potent precursor complexes, allowing to synthesise complexes for possible application in radiopharmaceutical-, bioinorganic- and photochemistry.

A versatile route for the synthesis of a $\{Re(CO)_2\}^+$ precursor complex was found by the use of $(Et_4N)[ReBr_4(CO)_2]$ as a starting material. The reduction of $(Et_4N)[ReBr_4(CO)_2]$ with Mg° or TDAE in acetonitrile led to $(Et_4N)[ReBr_2(NCCH_3)_2(CO)_2]$ **1** and $[ReBr(NCCH_3)_3(CO)_2]$ **1a**. Changing to the weakly coordinating solvent DME and in the presence of additional ligands such as imidazole, the complex $(Et_4N)[ReBr_2(CO)_2(imz)_2]$ **1c** was formed. All three compounds are soluble in water, air stable and substitution labile and can be considered as precursor complexes. The direct carbonylation of high valent starting materials such as $[ReO_4]^-$ or $[ReOCl_4]^-$ showed, that some $\{Re(CO)_2\}^+$ complexes were obtained but their isolation proved difficult.

The water-soluble and air stable complexes **1** and **1a** showed a well-defined substitution reactivity pattern with several types of ligands. In water, methanol or acetonitrile, solvent molecules replaced the bromide ligands to form $[Re(NCCH_3)_2(CO)_2(sol)_2]^+$. These two positions *trans* to the CO ligands were of sufficient lability for substitution

whereas the two axial acetonitrile ligands in **1** and **1a** were not. Accordingly, the reaction of imidazole, benzimidazole and 9-ethylguanine with **1** formed the corresponding complexes $[Re(NCCH_3)_2(CO)_2(imz)_2]^+$ **3**, $[Re(NCCH_3)_2(CO)_2(bzimz)_2]^+$ **4** and $[Re(NCCH_3)_2(CO)_2(9EtG)_2]^+$ **5**. Complex **1** showed strong affinity with the imidazole moiety, which is present in biomolecules in form of histidine and DNA bases such as adenine or guanine although an interaction with DNA or plasmides was not observed. Once coordinated, the imidazole ligand in **3** was not substituted by a competing ligand. α,α'-diimines but also terpyridine coordinated bidentate to **1** by substitution of the two bromide ligands, forming the complexes $[Re(NCCH_3)_2(CO)_2(bpy)]^+$ **8**, $[Re(NCCH_3)_2(CO)_2(phd)]^+$ **9**, $[Re(NCCH_3)_2(CO)_2(pham)]^+$ **10**, $[(Re(NCCH_3)_2(CO)_2)_2(tpphz)]^{2+}$ **11** and $[Re(NCCH_3)_2(CO)_2(terpy)]^+$ **12** in different colours but without strong luminescence properties. With bidentate pyridine-carboxylic acid containing ligands neutral complexes such as $[Re(2\text{-pic})(NCCH_3)_2(CO)_2]$ **13** and $[Re(2,5\text{-dipic})(NCCH_3)_2(CO)_2]$ **14** could be obtained, again substituting the two bromides in *trans* position to the carbonyl ligands. Finally, with the tetradentate ligand bis-(2-pyridylmethyl)glycine BPG, it was possible to replace the axial CH_3CN ligands and the two bromides to form the "true" $[Re(CO)_2]$ complex $[Re(BPG)(CO)_2]$ **15**. The neutral complex $[ReBr(NCCH_3)_3(CO)_2]$ **1a** behaved the same in all reactions since in solution, the ligands *trans* to the carbonyl ligands are exchanged by solvent molecules and ready for substitution reactions.

Under CO pressure and in water, complex **1** accommodated one more CO ligand and the unexpected *mer*-$[ReBr(NCCH_3)_2(CO)_3]$ complex **2** formed. Thermodynamically, the *fac*-geometry would be preferred but the acetonitrile ligands in trans position are stable (or robust) enough to withstand being replaced by CO. It seems therefore that the complex **2** is the kinetic and not the thermodynamic product. Substitution reactions with **2** showed a similar reactivity than **1**. Substitution reaction released one of the CO ligands and, with bidentate ligands, the bromide to produce the complexes already found when starting from **1** or **1a**. Accordingly, bidentate α,α'-diimine ligands gave **8** and **9**. With imidazole, only substitution of CO could be obtained. The reaction was performed in organic solvents such as THF from which the neutral complex **6** readily

precipitated. Reactivity with terpyridine however showed a strong dependence of the starting complex. Starting with **2**, a *meridional* coordination of the terpyridine ligand was observed and the two acetonitriles and one CO ligand were replaced, forming $[ReBr(CO)_2(terpy)]$ **12a**. As described above, the reaction of **1** with terpy resulted in an only bidentate coordination.

The $[ReBr_2(CO)_2(imz)_2]^-$ complex (**1c**) can also be considered as starting material for the synthesis of $[Re(CO)_2]^+$ complexes. **1c** reacted with 2 equivalents of 2-pic to form $(HImz)[Re(2\text{-pic})_2(CO)_2]$ **16**. The reaction of **1c** with bipyridine led in the formation of $[Re(bpy)(CO)_2(imz)_2]Br$ (**16a**) with the imidazole ligands in *trans* position to each other.

The clear 2-electron reduction from Re(III) to Re(I) induced the question if it would be possible to synthesise an assumed Re(II) intermediate by a directed one-electron reduction. By the reaction of only ½ eq. of TDAE with $(Et_4N)[ReBr_4(CO)_2]$ in pyridine or acetonitrile lead to the formation of rare 17 electron Re(II) complexes indeed. $[ReBr_2(CO)_2(NC_5H_5)_2]$ (**17**) and $(Et_4N)[ReBr_3(NCCH_3)(CO)_2]$ (**18**) are two air stable representatives with potential substitution lability.

To make the complexes described above useful for radiopharmaceutical purposes, several attempts with ^{99m}Tc were performed to obtain and identify $\{^{99m}Tc(CO)_2\}^+$ compounds as produced with rhenium. However, since the 99mTc solutions are highly diluted, the reactions turned out to be less directed than in the rhenium case. The standard synthesis of $[^{99m}Tc(OH_2)_3(CO)_3]^+$ but in the presence of acetonitrile and ligands such as imidazole or bipyridine gave several peaks in HPLC. The peaks were sharp and reproducible but could hardly be brought into coincidence with known rhenium complexes. Some of them were identified as tricarbonyl complexes by co-injection with the corresponding characterized $\{Re(CO)_3\}^+$ compounds but none of them could be assigned to retention times of $Re(CO)_2\}^+$ complexes described above. Other changes such as lowering the amount of CO, changing the reducing agent or performing a one-pot synthesis with tetradentate chelators did not lead to any improvements in the synthesis of $[^{99m}Tc(CO)_2]^+$ complexes. Thus, complexes of the

form $[^{99m}Tc(NCCH_3)_2(CO)_2L_2]^+$ remain elusive and further work is required to introduce the $[^{99m}Tc(CO)_2]^+$ core into radiopharmaceutical chemistry.

Zusammenfassung

Das bis heute nur am Rande untersuchte Fragment $[M(CO)_2]^+$ (M = Re, Tc) tritt vor allem in der Chemie des $[M(CO)_3]^+$ Fragmentes immer wieder in Erscheinung, sei es als Zwischenprodukt bei Substitutionsreaktionen oder in katalytischen Reaktionen. Zusätzlich besteht in der Nuklearmedizin eine Nachfrage nach neuen Fragmenten, welche die Markierung von anderen Molekülen und die Entwicklung von neuen Synthesestrategien erlauben. Einige bereits bekannte $[M(CO)_2]^+$ Komplexe zeigen ein interessantes photochemisches Verhalten, doch fehlt eine einfache Molekülvorstufe welche den Zugang zu einer breiten Auswahl an Komplexen für mögliche Anwendungen in der radiopharmazeutischen-, bioanorganischen- und Photochemie zulässt.

Die Reduktion von $(Et_4N)[ReBr_4(CO)_2]$ bewies sich als eine gute Methode um eine solche Vorstufe zu synthetisieren. Die Reaktion in Acetonitril mit Mg° oder TDAE als Reduktionsmittel ergab die beiden Komplexe $(Et_4N)[ReBr_2(NCCH_3)_2(CO)_2]$ **1** und $[ReBr(NCCH_3)_3(CO)_2]$ **1a**. Die Verwendung des schwach koordinierenden Lösungsmittels DME und die Zugabe von Imidazol zur Reaktionslösung führte zum Komplex $(Et_4N)[ReBr_2(CO)_2(imz)_2]$ **1c**. Alle drei Komplexe sind wasserlöslich, luftstabil und gehen Ligandubstitutionsreaktionen ein. Somit können diese als Ausgangsverbindungen für weitere $[Re(CO)_2]^+$ Komplexe betrachtet werden. Andere Synthesewege wie die Decarbonylierung von $[Re(CO)_3]^+$ Komplexe oder die Reduktion und Carbonylierung von Edukten in höheren Oxidationsstufen ergaben ebenfalls $[Re(CO)_2]^+$ Komplexe, welche aber nicht isoliert werden konnten. Ein derartiger Syntheseweg würde auch die Chemie an $[Tc(CO)_2]^+$ Komplexen zugänglich machen, wozu aber weitere Unersuchungen nötig sind.

Löste man die drei Verbindungen **1**, **1a** und **1c** in Wasser, Methanol oder Acetonitril, wurden die Bromidliganden durch Lösungsmittelmoleküle ersetzt. An diesen Stellen konnten durch Substitutionsreaktionen mit unterschiedlichen Liganden gezielt erneut stabile Komplexe synthetisiert. Die Umsetzung von **1** mit Liganden wie Imidazol,

Benzimidazol und 9-Ethyl-guanine ergab die entsprechenden Komplexe **3**, **4** und **5**. Imidazol oder imidazolähnliche Moleküle sind Bausteine in Biomolekülen wie Histidine oder der DNA-Basen Adenin und Guanin. Trotz der Affinität zum Imidazol-Fragment wurde eine Wechselwirkung von **1** mit Plasmid-DNA nicht beobachtet. Die Reaktion von **1** mit α,α'-Diiminen, aber auch mit Terpyridin, zeigte erneut eine zweifache Substitution an den Koordinationsstellen der Bromide, was zu den Komplexen **8**, **9**, **10**, **11** und **12** führte. Die intensiv gefärbten Verbindungen zeigen aber keine ausgeprägte Fluoreszenz. Mit zweizähnigen Liganden welche eine Pyridin- und eine Karbonsäure-Einheit enthalten wurden die neutralen Komplexe **13** und **14** erhalten. Wurde aber der vierzähnige Ligand bis-(2-pyridylmethyl)glycin (BPG) verwendet, konnten alle vier Liganden ausser den Carbonylen substituiert und der neutrale Komplex **15** isoliert werden. Die Verbindung **1a** zeigte dasselbe Verhalten und dieselbe Reaktivität wie **1**, werden doch in Lösung ebenfalls die beiden zu den Carbonyl Liganden *trans*-stehenden Liganden durch Lösungsmittelmoleküle ersetzt.

Setzte man eine wässrige Lösung von **1** mit 20 bar CO unter Druck, liess sich *mer*-$[ReBr(NCCH_3)_2(CO)_3]$ **2** darstellen. Verwendete man **2** in THF als Ausgangsverbindung, erhielt man ebenfalls $[Re(CO)_2]^+$ Komplexe. Die beiden *trans*-ständigen Carbonylliganden destabilisieren sich gegenseitig durch ihre π-Akzeptorenstärke wodurch eine Substitution von einem der beiden Carbonylliganden leichter wird. Die Reaktion mit den zweizähnigen α,α'-Diiminen ergab die selben Produkte **8** und **9** wie aussgehend von **1**. Bei der Reaktion mit Imidazol erfolgte nur eine einfache Substitution eines Carbonylliganden. Aufgrund des Lösungsmittels THF wurde der neutrale Komplex **6** gebildet, welcher aus der Reaktionslösung ausfiel. Der grösste Unterschied zeigte die Reaktion von **2** mit Terpyridin. Die Bindung erfolgte in einer dreifachen, *meridionalen* Koordination und substituierte beide Acetonitril-Liganden. Der neutrale Komplex $[ReBr(CO)_2(terpy)]$ (**12a**) fiel aus der Reaktionslösung aus, hingegen reagierte Terpyridin mit **1** nur zweifach zum Komplex **12**.

Die Ausgangsverbindung $(Et_4N)[ReBr_2(CO)_2(imz)_2]$ **1c** reagierte mit 2-Picolinsäure unter einer vierfachen Substitution am Metallzentrum zu $(HImz)[Re(2\text{-}pic)_2(CO)_2]$ **16**. Mit Bipyridine reagierte **1c** zu $[Re(bpy)(CO)_2(imz)_2]Br$ wobei eine Umlagerung der

Imidazol-liganden aus *cis* in *trans* Position zueinander erfolgte. Mit anderen Liganden wurden keine klaren Resultate erhalten und die entstandenen Produkte konnten nicht isoliert werden.

Die Reduktion von $(Et_4N)[ReBr_4(CO)_2]$ um ein Elektron mit TDAE in Pyridine oder Acetonitril führte zu bis anhin nur spärlich untersuchten Re(II)-Komplexen. Die beiden sogar luftstabilen 17 Elektronen Komplexe $[ReBr_2(CO)_2(NC_5H_5)_2]$ (**17**) und $(Et_4N)[ReBr_3(NCCH_3)(CO)_2]$ (**18**) sind zwei Vertreter dieser Spezies. **18** zeigte Paramagnetismus und könnte als substitutionslabile Ausgangsverbindung für eine Vielzahl von Re(II)-Komplexen dienen.

Die Synthese einer möglichen $[^{99m}Tc(CO)_2]^+$ Verbindung wurde in verschiedenen Experimenten versucht. Die Zugabe von 10% Acetonitril zu der Synthese von $[^{99m}Tc(OH_2)_3(CO)_3]^+$ und die Komplexierung der entstandened Produkte mit Liganden wie Imidazol oder Bipyridin, zeigte neue, definierte Verbindungen gemäss HPLC. Durch Koinjektionen bekannter Rheniumverbindungen konnten einige Verbindungen einer $[^{99m}Tc(CO)_3]^+$ Spezies zugeordnet werden. Hingegen konnte keine definitive Aussage über mögliche $[^{99m}Tc(CO)_2]^+$ Komplexe gemacht werden. Auch ein Wechsel des Reduktionsmittels, die Bereitstellung von weniger CO oder die Zugabe eines vierzähnigen Liganden ergab keine eindeutigen Hinweise für eine $[^{99m}Tc(CO)_2]^+$ Verbindung.

Die ersten $[Re(CO)_2]^{+/2+}$ Ausgangsverbindungen für weitere Komplexe mit der $[Re(CO)_2]$-Einheit wurden präsentiert und eine mögliche Verwendung für photochemische-, bioanoganische- oder radiopharmazeutische Experimente anhand von Substitutionsreaktionen ausgelotet. Die erhaltenen Komplexe wurden sorgfälltig analysiert und charakterisiert. Obwohl noch viele Fragen offen stehen, gibt diese Arbeit einen breiten Einblick in eine bisher fast unbekannte Klasse von metallorganischen Rheniumkomplexen und hinterlässt viele Ideen für weiterführende Projekte.

1. Introduction

General information about the rhenium, technetium and carbonyl complexes were taken from textbooks.[1-4]

1.1. Rhenium and technetium

Rhenium and technetium are two representatives of the group VII transition metals but their natural abundance is very different. Rhenium has a widespread abundance but with concentrations lower than 0.001%. Relatively rich in rhenium are molybdenum ores such as MoS_2. While roasting this ores, rhenium is evolved as oxide in the ashes, which can be earned as $(NH_4)[ReO_4]$. As metals, rhenium and technetium have a high density (21.03, 11.49 g cm^{-3}) and very high melting (3180, 2172° C) and boiling points (5870, 4700° C). After tungsten, rhenium has the second highest melting point of the metals.
Natural rhenium consists of the isotopes ^{185}Re (37.4%) and ^{187}Re (62.6%). Therefore, for example in mass spectroscopy, the isotope-pattern indicates the presence of rhenium in the analysed samples. The mass spectrum shown in figure 1 representing $[Re(NCCH_3)_2(CO)_2(C_3H_4N_2)_2]^+$ contains two main peaks with a mass difference of 2 mass units, which are around 2:3 in intensity. The radionuclides ^{186}Re and ^{188}Re are both artificially produced and used in radiotherapy.

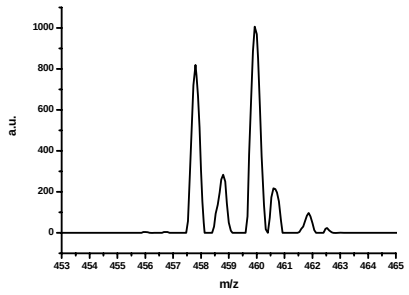

Figure 1: Typical ESI^+ mass spectrum of a rhenium compound $[Re(NCCH_3)_2(CO)_2(C_3H_4N_2)_2]^+$, which shows the natural abundance of the two rhenium isotopes ^{185}Re and ^{187}Re.

Technetium does practically not exist in nature. There are only short-living traces from the spontaneous fission of uranium-235. Within the ten different artificial isotopes of technetium, the two isotopes ^{99}Tc (β^-, $\tau_{1/2}$ = 2.12•10^5 y, coordination chemistry) and ^{99m}Tc (γ, $\tau_{1/2}$ = 6.05 h, medicine) are of practical importance. The metastable ^{99m}Tc is produced by the bombardment of ^{98}Mo with neutrons via ^{99}Mo, which decays further to ^{99m}Tc under β^- emission. The metastable ^{99m}Tc isotope "decays" to its ground state isotope ^{99}Tc under photon emission. More commonly, $[^{99}MoO_4]^{2+}$ is extracted during the PUREX-process as a fission product of uranium in nuclear reactors. Also $[^{99}TcO_4]^-$ is extracted during the PUREX-process waste solution in up to 6% yield. A 100 MW uranium power plant produces around 4 g ^{99}Tc a day. With the growing number of power plants, the amount of ^{99}Tc in the world is increasing but also the radioactive waste storage problem. The current waste form today is the vitrification but during this process, technetium is transformed either to the volatile Tc_2O_7 or it is converted to soluble $[TcO_4]^-$, which has high mobility in ground waters. The discharge of radionuclides to the sea is a problem which is followed by an increasing concentration of ^{99}Tc, *e.g.* in lobster, near the British Nuclear Fuel site (BNFL) in Sellafield.[5] Methods to reduce the ^{99}Tc waste (by neutron capture to the stable ^{100}Ru)[6] or to solve the problems while vitrification (conditioning in polyoxometallate)[7] are under investigation.

In an oxygen atmosphere both metals burn at temperatures higher then 400° C to the volatile species M_2O_7 and under oxidising conditions to pertechnetate or perrhenate $[MO_4]^-$. Reaction with F_2, Cl_2 or sulphur, the metals are forming TcF_5/TcF_6, ReF_6/ReF_7, MCl_6, and MS_2.

Both rhenium and technetium are stable as compounds in the oxidation states from –3 to +7 whereas the compounds in higher oxidation states usually occur in almost all coordination forms with four to nine ligands (*e.g.* $[MH_9]^{2-}$). Within a range of oxidation states zero to two, the complexes are octahedral and complexes with negative oxidation states have a coordination number lower then six.

Rhenium is used in technology as a cathode in electron producing systems or as mirrors, which are highly resistant and highly reflective. Rhenium is of high interest on actual research (ca. 800 publications in 2007) mainly in the field of material science, catalysis, photochemistry and radiotherapy, whereas technetium is of high interest in nuclear medicine with 1100 publications in 2007.[8]

1.2. Carbonyl complexes

1.2.1. Carbon monoxide as a ligand

Carbonyl complexes are compounds containing CO as a coordinated ligand. Carbon monoxide is a common ligand in organometallic transition metal chemistry. The bonding of CO to a metal consists of two contributions. The first contribution is a two-electron donation of the lone pair on carbon (coordination exclusively through the oxygen is extremely rare) into a vacant metal d-orbital. This electron donation makes the metal more electron rich, and in order to compensate for this increased electron density, a filled metal d-orbital may interact with the empty π* orbital on the carbonyl ligand to delocalise electron density over the ligands. This second component is called π-backbonding or π-backdonation. The two binding modes are shown in figure 2.

The two components of this bonding are synergistic. The more σ-donation by the carbonyl (or other σ-donors on the metal centre), the stronger the π-backbonding interaction. It must be noted that although this involves the occupation of a π* orbital on the CO, it is still a bonding interaction as far as the metal centre is concerned. There is a fundamental similarity between the nature of carbonyl-metal bonding and that of alkenes, acetylenes, phosphines and dihydrogen. The occupation of the π* in CO does lead to a decreased bond order in CO. As might be expected, the stronger π-backdonation, the lower the CO bond order. The reduced bond order in CO results in lengthening of the CO bond and a decrease in the carbonyl stretching frequency in the IR.

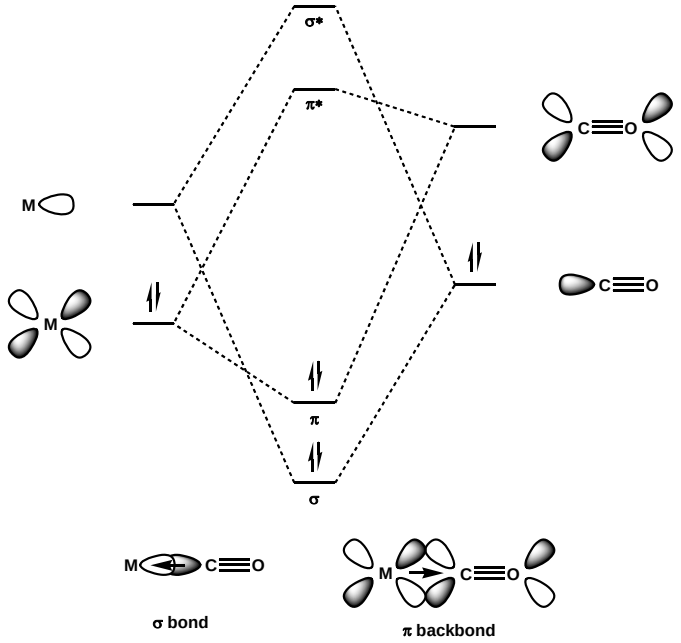

Figure 2: Molecular orbital diagram of a metal-carbonyl bond.

Carbon monoxide typically binds in an end-on fashion through carbon. However, bridging carbonyls are not uncommon and often undergo exchange with terminal carbonyls. An overview of the different binding modes of CO is given in figure 3 and the range of their IR stretching frequencies is listed in Table 1.

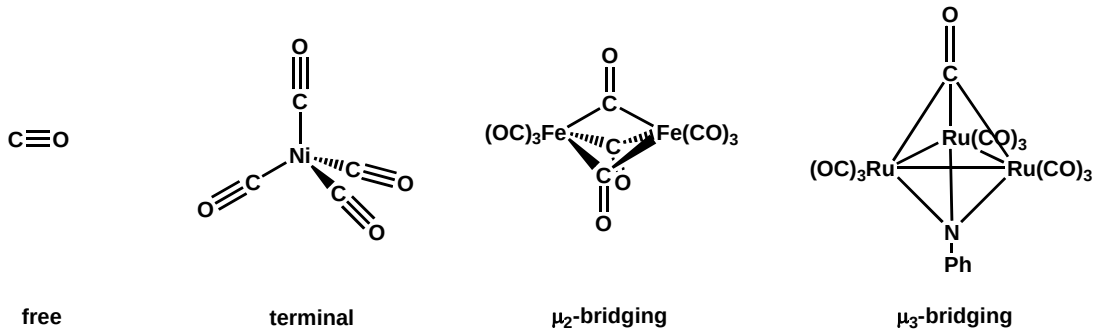

Figure 3: Different binding modes of carbonyl ligands to metal centres.

In IR spectroscopy, carbonyl ligands show very distinct and intensive bands. For binary carbonyl complexes, the number of IR and Raman CO stretching frequencies and their pattern often permits a structural assignment. Symmetric and antisymmetric vibrations are well separated and the number of CO stretches expected for possible geometries/isomers could be predicted.

Table 1: IR symmetric stretching frequencies of carbonyl ligands depending on their binding mode.

binding mode	typical IR stretching frequencies
Uncoordinated or "free" CO	2143 cm^{-1}
Terminal M-CO	2125 to 1850 cm^{-1}
Doubly bridging (μ_2)	1850 to 1750 cm^{-1}
Triply bridging (μ_3)	1675 to 1600 cm^{-1}

Two convenient trends are observed in the IR spectra of carbonyl complexes, both consistent with the concept of π-backbonding discussed above:

- With reduction to a lower oxidation state of the metal centre by one electron, the CO stretching frequency decreases by approximately 80 cm^{-1}.
- The better the σ-donating capability (or worse the π-acceptor ability) of the other ligands on the metal, the lower the CO stretching frequency.

1.2.2. Syntheses of metal carbonyl complexes

Metal carbonyls can be synthesised in a variety of methods. Three examples of the most commonly methods are shown in scheme 1:

- For Ni and Fe, metal carbonyls can be synthesised by the direct interaction of CO gas with the metal (Eq. 1).
- The reduction of a metal precursor complex in the presence of CO or using CO as the reductant (Eq. 2).
- The reaction of carbon monoxide with various metal complexes, most typically filling a vacant coordination site or performing a ligand substitution reaction (Eq. 3).

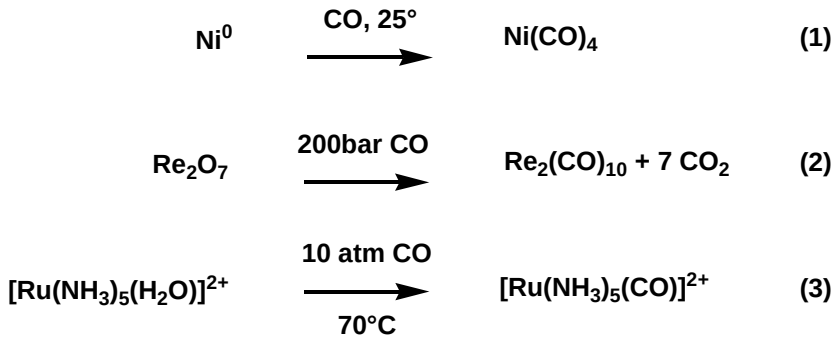

Scheme 1: Synthesis of metal carbonyl complexes.[9-11]

1.3. Rhenium carbonyl complexes

Rhenium carbonyl complexes are used in various fields of research such as catalysis or photochemistry,[12-14] and as analogues to radioactive technetium compounds for radiopharmaceutical application.[15-17] The usual starting material for the synthesis of rhenium carbonyl complexes is rhenium oxide, Re_2O_7 or perrhenate, $[ReO_4]^-$. The dinuclear compound $Re_2(CO)_{10}$ can be obtained via a high pressure carbonylation reaction in an autoclave[10] and $(Et_4N)_2[ReBr_3(CO)_3]$ via a low pressure carbonylation with CO at atmospheric pressure and borane as reducing agent.[18] Starting with these rhenium compounds, an enormous variety of carbonyl complexes are accessible.

1.3.1. Rhenium carbonyl complexes in catalysis

The activation of H_2 by transition metal species for the homogeneous hydrogenation of organic substrates is one of the most widely studied class of catalysed organometallic reactions[19, 20] and rhenium carbonyl complexes are under investigation as catalysts.[21, 22] Their activated hydride complexes are studied such as *e.g.* unsaturated $[Re(CO)_{5-n}(PMe_3)_n]^+$ cations (n = 2, 3, and 4) or their solvent-stabilised analogues, which were explored for a heterolytic activation of dihydrogen for the hydrogenation of imines.[23]

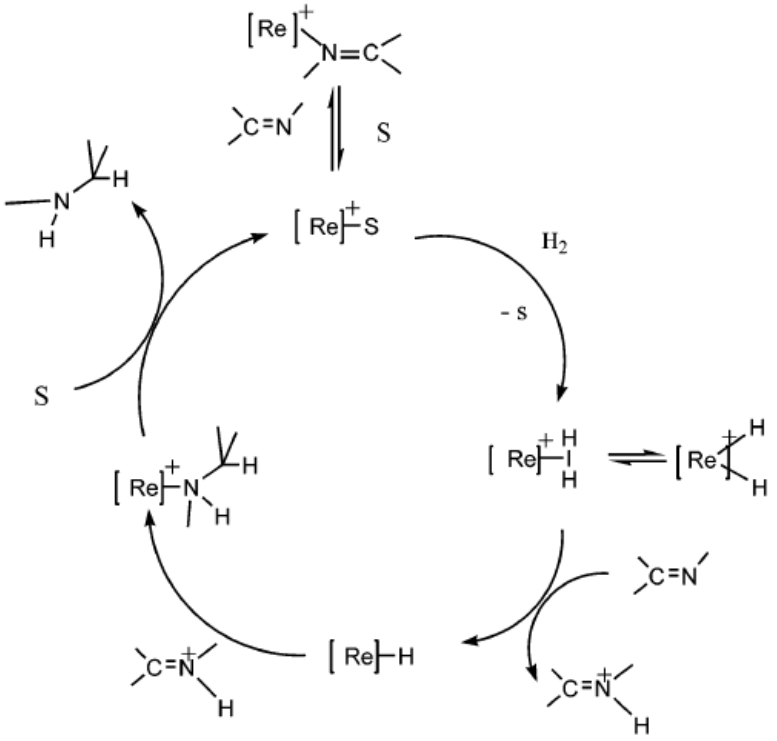

Scheme 2:[23] Anticipated mechanism of the catalytic imine hydrogenation.

Beside hydrogenation reactions, the development of efficient and recyclable catalytic systems to convert atmospheric carbon dioxide (CO_2) into useful chemicals and fuels is an important research topic in recent years. The activation of CO_2 using transition metal complexes as catalysts has been extensively studied.[24, 25] In particular, tricarbonyl-rhenium(I)-diimine complexes have been found to be able to catalyse the electro- and photochemical reduction of CO_2 efficiently[26-30] due to their long-lived excited state lifetimes and high quantum yields. The chemical fixation of CO_2 with epoxides[31] by recyclable tricarbonyl rhenium(I) complexes with an anchored pyrrolidinium ionic liquid moiety show the use of rhenium carbonyl complexes in catalysis (scheme 3).

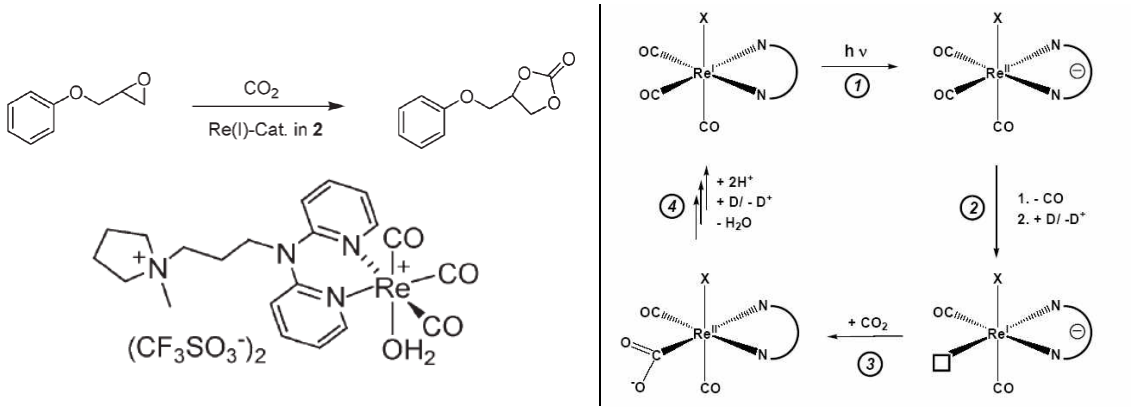

Scheme 3: Rhenium catalyst for the CO_2 fixation with epoxides (left)[31] and the photocatalytic cycle of the CO_2 to CO conversion (right).[32]

1.3.2. Rhenium and technetium tricarbonyl complexes

The tricarbonyl complexes of rhenium and technetium *fac*-$[MX_3(CO)_3]^{2-}$ (M = Re, Tc; X = Br, Cl) are accessible via the halogenation of $[M_2(CO)_{10}]$ to $[ReX(CO)_5]$[33] and substitution of two carbonyl ligands with $(Et_4N)X$ at high temperatures.[34] To avoid high-pressure carbonylation with toxic CO gas to synthesise $[M_2(CO)_{10}]$, a low-pressure method was developed.

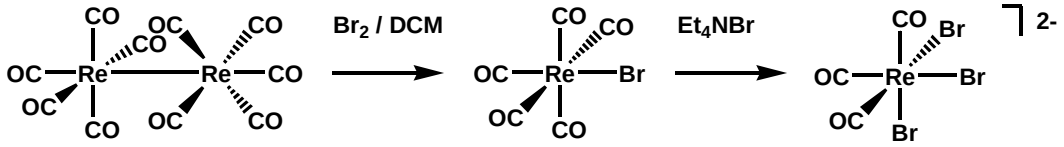

Scheme 4: Synthesis of $[ReBr_3(CO)_3]^{2-}$ starting from dirhenium decacarbonyl.

Starting from $[MO_4]^-$ or $[MOCl_4]^-$ in organic solvents and at atmospheric CO pressure, BH_3 is versatile for the reduction process Re(V) to Re(I). Borane has enough reducing power to reduce the metal centre oxidation state from +VII to +I and the resulting borate is not coordinating to Re(I). By bubbling CO trough a THF solution in the presence of BH_3·THF and halide anions, *fac*-$[MX_3(CO)_3]^{2-}$ is formed.[18] For the low-pressure preparation methods, the mechanism of the reaction remains unclear. No intermediate complex in an oxidation state higher than +I could be detected in significant amounts. Depending of the halide concentration, hydrido or halide-bridged complexes such as $[Tc(\mu\text{-}H)_3(CO)_4]_3$ or $[Tc_2(\mu\text{-}Cl)_3(CO)_6]^-$ are obtained as intermediates. Both lead to the

corresponding complex $[TcCl_3(CO)_3]^{2-}$ in the presence of excess chloride in an appropriate solvent.[35]

For nuclear medicine purposes, organic solvents are not suitable and the synthesis of $\{^{99m}Tc(CO)_3\}^+$ has to be performed in saline. At tracer level, this is done with $NaBH_4$ under CO.[36] Since the development of a carbonylation kit containing $Na_2[BH_3COO]$ (BC), there is no need for gas CO anymore. BC acts as reducing agent and CO delivering moiety in one. Within 30 minutes at 95° C, $[^{99m}Tc(OH_2)_3(CO)_3]^+$ is formed in a yield higher than 98% direct from $[^{99m}TcO_4]^-$ for radiopharmaceutical use.[37] The later kit is known under the trade name Isolink™.

Dissolved in water, the *fac*-$[MX_3(CO)_3]^{2-}$ complexes exchange the halide ligands by water to form the "aqua-ions" $[M(OH_2)_3(CO)_3]^+$. As aqua-ions, they are stable in air over weeks. They are Brönstedt acidic and deprotonation of coordinated water ligands leads to terminal hydroxyl ligands, which tend to form μ-OH or μ-O species. At basic conditions and depending of the procedure, the trimeric $[Re_3(\mu_3\text{-}OH)(\mu\text{-}OH)_3(CO)_9]^-$ and the dimeric $[Re_2(\mu\text{-}OH)_3(CO)_6]^-$ were obtained.[34]
The aqua-complex is ready for substitution with several types of ligands, especially with *facial* coordinating tridentate ligands such as 1,4,7-trithiacyclononane[38] or so called scorpionates.[39] The self-exchange of the coordinated water ligands ($k_{ex} = 5.5 \pm 0.3 \times 10^{-3}$ s^{-1})[40] makes the $[M(CO)_3]^+$ core accessible for incoming ligands with functional groups like (aromatic) amines, carboxylic acids, thiols, cyanides and other σ-donors.

1.4. Rhenium and technetium in radiopharmacy

In radiopharmacy, rhenium and technetium play an important role. Due to their radioactive isotopes with almost ideal values in half-life-time and energy (table 2), they can be used either in therapy ($^{186/188}Re$, β^-) or in imaging (^{99m}Tc, γ).

Table 2: Half-lifetime and radiation energy of rhenium and technetium isotopes suitable for radiopharmaceutical applications.

Isotope	radiation	$\tau_{1/2}$	E [keV]
^{186}Re	β^-	89.25 h	1100
^{188}Re	β^-	16.98 h	2100
^{99m}Tc	γ	6.0 h	141

Both ^{188}Re and ^{99m}Tc can be obtained from generators. The generator uses an artificially produced parent nuclide with a half-life-time between two days and two months, which decays to a daughter nuclide with a shorter half-life-time. From the law of radioactive decay, this constellation is called a secular equilibrium. Secular equilibrium is a situation in which the quantity of a radioactive isotope remains constant because its production rate is equal to its decay rate (due to the decay of the parent isotope). Since for both generators the parent nuclide is a β^--emitter, the daughter nuclide is of different charge and can be separated by chromatographic methods. For both, rhenium and technetium, generators are on the market using the ^{188}W/^{188}Re and ^{99}Mo/^{99m}Tc cascade (figure 4,5).

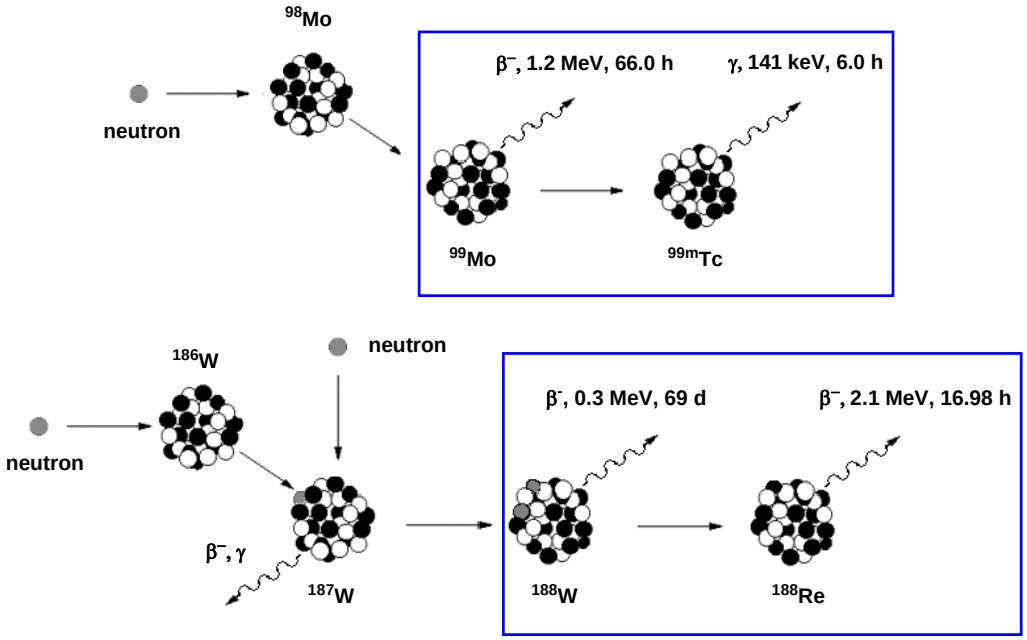

Figure 4: The two decay cascades forming a secular equilibrium used in the ^{188}W/^{188}Re and the ^{99}Mo/^{99m}Tc generator.

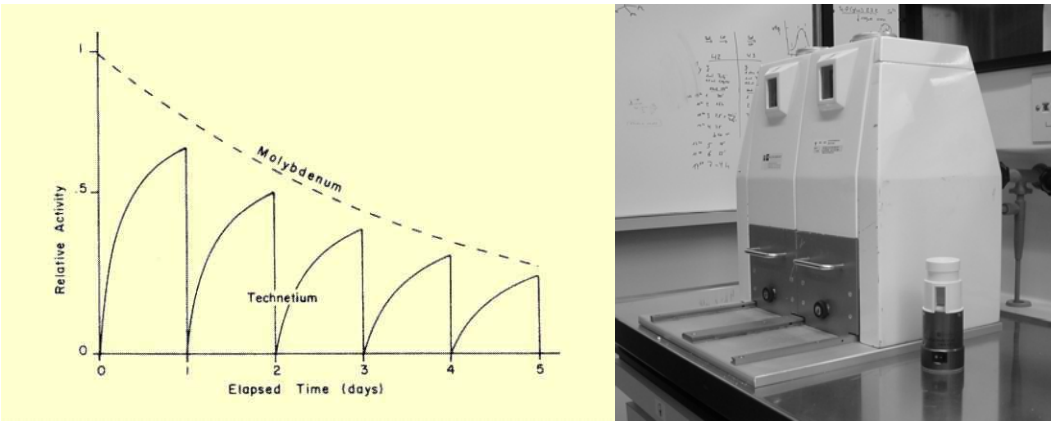

Figure 5: Scheme of the activity in a $^{99}Mo/^{99m}Tc$ generator with secular equilibrium (left) and a picture of a double generator containment with the elution tool (right).

^{99m}Tc is used in Single Photon Emission Computer Tomography (SPECT). For routine use, it is important to have a kit formulation of the desired product. Adding of the $[^{99m}TcO_4]^-$ solution and eventually heating, the radiopharmaceutical can be obtained in one step. Due to the low concentrations, the structures of some of the compounds are still not known but nevertheless in clinical application. With the use of multiple head gamma cameras, high resolution scans for perfusion disease-, inflammation- and tumour imaging at very low radiation doses for the patients is possible (table 3 and figures 6-8).

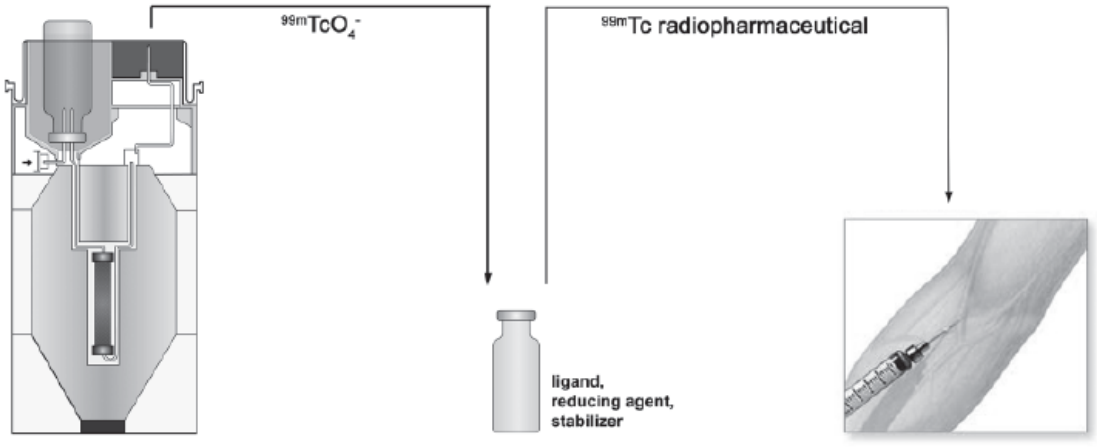

Figure 6: The kit-strategy for ^{99m}Tc radiopharmaceutical: $[^{99m}TcO_4]^-$ is eluted from the generator (left) and added to reagents formulated in a kit (middle). Without multistep purification, the radiopharmaceutical should be ready for application (right).

Table 3: Overview of some ^{99m}Tc radiopharmaceuticals with their medicinal application.

Organ	Compound	Trade name (example)	Application
Brain	hexamethyl propylenamino oxime HMPAO	Neurospect Ceretec	Brain perfusion
	ethyl cysteinate dimer ECD	Neurolite	Brain perfusion
Heart	1,2-*bis*[*bis*(2-ethoxyethyl) phosphino]ethane	Myoview	Heart perfusion
	methoxy-isobutyl-isonitril (MIBI)	Cardiolite	Heart perfusion
Lung	diethylenetriamine pentaacetic acid	DTPA-Aerosol	Lung ventilation scintigraphy
Kidney	Betiatide	TechneScan®MAG3	Kidney scintigraphy
Skeleton	methylene diphosphonate	MDP Osteosol	Bone scan

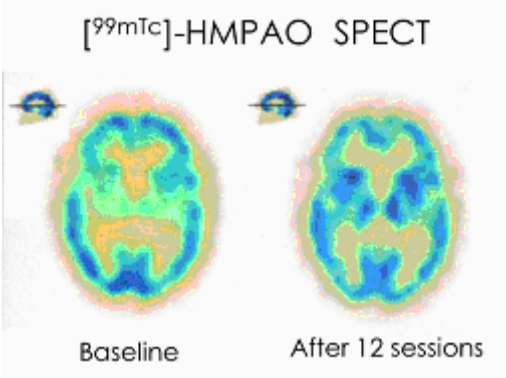

Figure 7:[41] SPECT-image of a brain perfusion scan with ^{99m}Tc-HMPAO before and after treatement.

The kit formulation of many radiopharmaceuticals consists of stannous chloride reducing $[^{99m}TcO_4]^-$ to the oxidation state +VI, +V or +IV. With two tetrofosmin ligands 1,2-*bis*[*bis*(2-ethoxyethyl) phosphino]ethane, a octahedral {O=Tc=O} complex is formed (figure 8, right). With the tetradentate ligand betiatide (*N*-[*N*-[*N*-[(benzoylthio) acetyl]glycyl]glycyl]glycine), the square pyramidal $\{Tc=O\}^{3+}$ complexes is formed (figure 8, middle) and with methoxy-isobutyl-isonitrile ligands the $\{Tc(CNR)_6\}^+$ complex (figure 8, left).

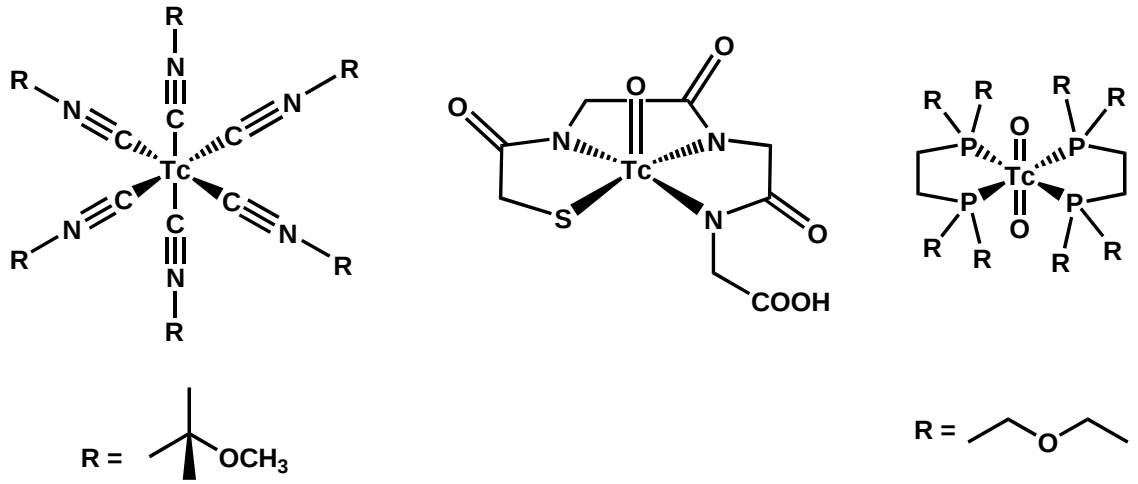

Figure 8: Representatives of commercially available ^{99m}Tc-based radiopharmaceuticals: cardiolite, technescan and myoview (from left to right).

Radiopharmaceutical containing the $\{^{99m}Tc(CO)_3\}^+$ core are still under investigation. As mentioned above, the "IsoLink™ Carbonyl Labelling Agent" or the combination $NaBH_4$/CO allows an easy access to the solvated tricarbonyl species $[^{99m}Tc(OH_2)_3(CO)_3]^+$ in a yield higher than 98% in water. Several strategies to label targeting molecules were developed the past few years.

Several groups are developing suitable and tailor-made ligand systems for the $\{M(CO)_3\}^+$ fragment.[42-47] Single molecule labelling can be obtained via tridentate linker molecules such as *e.g.* histidine-[48], aliphatic triamine-[49] or the mixed pyridine-amine-carboxylic acid (NNO)[50] moieties.

The [2+1] mixed ligand approach developed by Mundwiler,[17] allowed to combine two different functions at one metal centre. For cell specific nuclear targeting, a DNA-intercalator could be labelled via a bidentate ligand. A cell specific biomolecules can be attached to the sixth position allowing a receptor specific targeting.[49, 51-53]

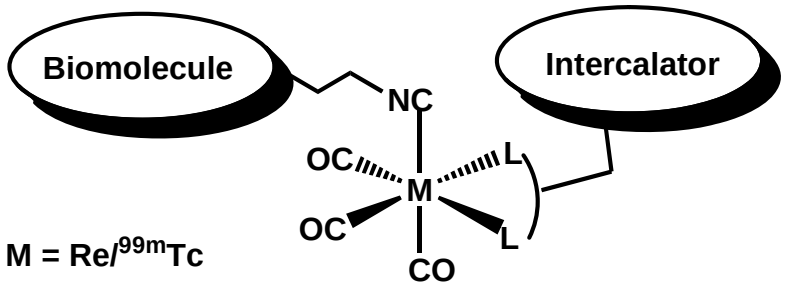

Figure 9: Scheme of the [2+1] mixed ligand approach for the tricarbonyl moiety for nuclear targeting.

Over expressed receptors in tumor tissues or bacterial inflammations are targeted. Indeed, at places of enhanced proliferation, characteristically for tumors and inflammation, the demand for *e.g.* vitamin B_{12} is increased. The use of B_{12} as a Trojan horse is obvious.[54] Further, two-third of breast tumours have high estrogen receptor (ER) levels, which can be targeted with the hydroxytamoxifen scaffold.[55]

1.5. Complexes comprising the $\{M(CO)_2\}^+$ moiety

Complexes containing the $\{M(CO)_2\}^+$ (M = Re, ^{99}Tc) moiety are known since a long time. Usually, these compounds are synthesised by decarbonylation of tricarbonyl complexes but not directly from substitution labile $\{M(CO)_2\}^+$ precursors or from higher valent starting materials via carbonylation.[56-59] Photoinduced reactions are known. Photoexcitation transform *e.g. fac*-[ReCl(bpy)$(CO)_3$] into its *meridional* isomer *mer*-[ReCl(bpy)$(CO)_3$] which subsequently exchanges CO with acetonitrile, phosphines or pyridine.[60] Many complexes containing cyclopentadienyl or phosphine ligands were prepared. Such complexes are in general difficult to substitute. An exception is represented by the Re(III) complex $[ReBr_4(CO)_2]^-$. As will be discussed later, reduction leads to precursor complexes for the $\{Re(CO)_2\}^+$ core.

To obtain $\{Re(CO)_2\}^+$ complexes, special conditions or compounds with special reactivity are necessary:

- The synthesis of $[Re(CO)_2(bpy)_2]^+$ was achieved by adding [Re(OTf)$(CO)_3$(bpy)] to an excess of molten bpy at 273° C.[56] (scheme 5, top)
- [Cp*M$(CO)_2(PR_3)$] is synthesised from [Cp*M$(CO)_3$] in THF using UV-light to activate the loss of one CO.[57] (scheme 5, middle)
- The reaction of a bidentate ligand with *mer*-[M$Cl(CO)_3(PPh_3)_2$] lead to the formation of $[M(CO)_2(PPh_3)_2(L_2)]$ due to the *trans* effect in *meridional* tricarbonyl complexes.[58] (scheme 5, bottom)

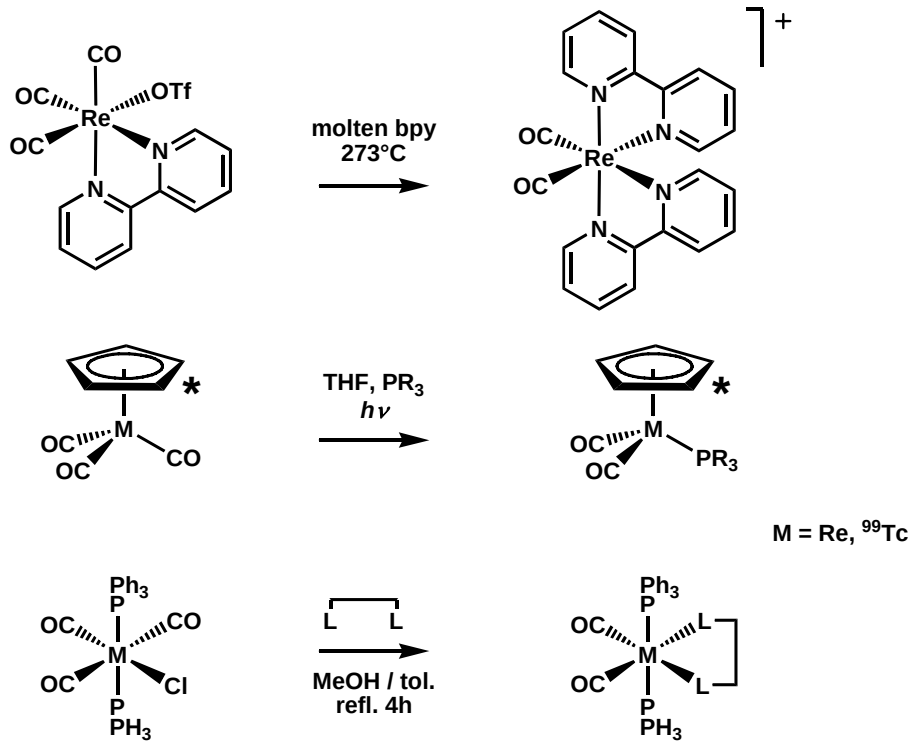

Scheme 5: Synthesis of $\{M(CO)_2\}^+$ complexes under special conditions.[56-58]

These complexes have specific physico-chemical properties but they cannot be considered as precursors since they are not substitution labile.

Complexes like $[Re(CO)_2(bpy)_2]^+$ or diphosphine analogues of the general formula $[Re(CO)_2(bpy)(P\text{-}P)]^+$ showed generally high redox stability and reversible one electron oxidation from +0.9 to +1.4 V. Longer luminescence lifetimes and higher quantum yields were measured for these kind of compounds as compared to similar $\{Re(CO)_3\}^+$ complexes.[56, 61] These features make $\{Re(CO)_2\}^+$ complexes interesting for photocatalysis.

Using *mer*-$[TcCl(CO)_3(PPh_3)_2]$ as starting material several $\{Tc(CO)_2\}^+$ complexes were accessible. The tridentate amines 1,4,7-triazacyclononane and hydrido-tris(pyrazolyl)borate coordinated in a *facial* geometry and one chloride, one CO and one phosphine was displaced. Complexes of the composition $[Tc(CO)_2(PPh_3)(NNN)]^{+/0}$ are formed.[62]

2. Perspectives and Objectives

Based on the knowledge about $[M(CO)_3]^+$ complexes (M = Re, Tc), there is indeed a need for a $[M(CO)_2]^+$ precursor which allows systematically exchange of ligands to fine-tune the properties of the resulting compounds. $[M(CO)_2]^+$ complexes have been frequently suggested as intermediates in photochemical reactions with $[M(CO)_3]^+$ but access to corresponding model complexes proved difficult or impossible. For pharmaceutical applications, core based chemistry is scarce and a focus should be put on the synthesis of new cores and not only on ligand tuning. A substitution labile precursor would allow getting information about the general behaviour of a relatively unknown class of complexes. Although a few $[M(CO)_2]^+$ complexes exist, there is a lack of a potent precursor for the synthesis of complexes with novel properties.

We aimed at finding an approach for the synthesis of air and water-stable $[Re(CO)_2]^+$ complexes in a good yield and purity. Their behaviour in solution (water in particular) and their fundamental coordination chemistry should give evidence about it's the potential as precursors. The use of selected ligands in substitution reactions would give a first idea about possible application in photochemistry, radiopharmaceutical and bioinorganic chemistry.

First attempts showed that the reduction of $[ReBr_4(CO)_2]^-$ in acetonitrile with Zn° or $[Cp_2Co]$, led to $[Re(CO)_2]^+$ complexes such as $[CoCp_2][ReBr_2(NCCH_3)_2(CO)_2]$ or $[Re(NCCH_3)_4(CO)_2][ZnBr_2]$. The low yields and purity as well as the unpleasant heterometallic salts demanded further investigations.

Using rhenium as a model, the results should be the base for finding a direct synthesis of $[M(CO)_2]^+$ from high-valent precursors and to consequently translate the approach for the synthesis of $[^{99m}Tc(CO)_2]^+$ at tracer level.

3. Results and Discussion

3.1. Abbreviation

TEABr	tetraethyl-ammoniumbromide
TBABr	tetrabutyl-ammoniumbromide
$TBAPF_6$	tetrabuthyl-ammoniumhexafluorophosphate
TFA	trifluoroacetate [F_3CCOOH]
TMNO	trimethylamine-*N*-oxide
TDAE	*tetrakis*-dimethylaminoethylene $((CH_3)_2N)_2C=C(N(CH_3)_2)_2$
ReImz	*trans*-*cis*-*cis*-$(Et_4N)[ReBr_2(CO)_2(imz)_2]$
DME	1,2-dimethoxyethane
DMF	*N*,*N*-dimethylformamide
THF	tetrahydrofuran
diglyme	*bis*-(2-methoxyethyl)ether
RT	room temperature
r.t.	retention time
atm	atmospheric pressure
sol	solvent (as a ligand)
Cp	cyclopentadienyl-
Cp*	pentamethylcyclopentadienyl-
BPG	bis(2-pyridylmethyl)glycine

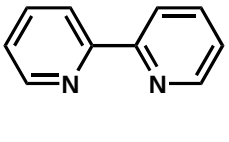

bpy

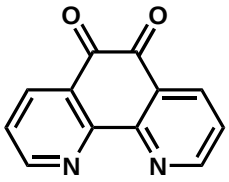

phd

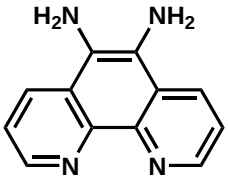

pham

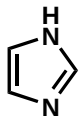

imz

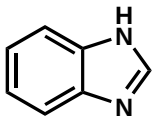

bzimz

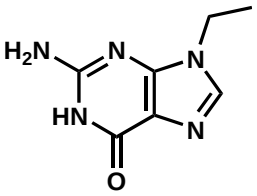

9EtG

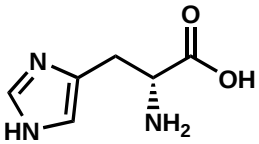

L-His

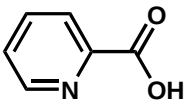

2-pic

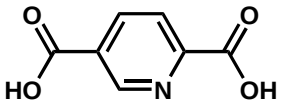

2,5-dipic

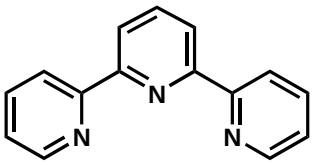

terpy

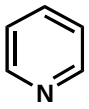

py

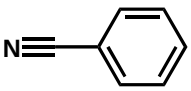

NCBz

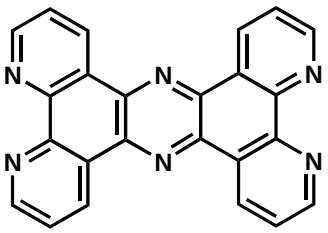

tpphz

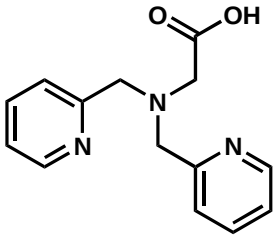

BPG

3.2. Synthesis of starting materials

The synthesis of $(Et_4N)[ReBr_4(CO)_2]$ was achieved by an oxidative decarbonylation of $[ReBr_3(CO)_3]^{2-}$ with Br_2.[63] The synthesis was easily upscaled to 2 g $[ReBr_3(CO)_3]^{2-}$, 250 ml CH_2Cl_2, 0.4 ml Br_2). After recrystallisation from CH_2Cl_2/Et_2O yields up to 80% could be verified.

Scheme 6: Synthesis of the starting material $(Et_4N)[ReBr_4(CO)_2]$.

The other starting materials $(Et_4N)_2[ReBr_3(CO)_3]$[34] and $(Bu_4N)[ReOCl_4]$[18] were synthesised according to literature procedures and the starting materials $(Bu_4N)[TcOCl_4]$, $(Bu_4N)[ReO_4]$, $(Et_3NH)[ReCl_4(NCCH_3)_2]$ and $[ReCl_4(NCCH_3)_2]$ were available in our group. All the starting materials are shown in figure 11.

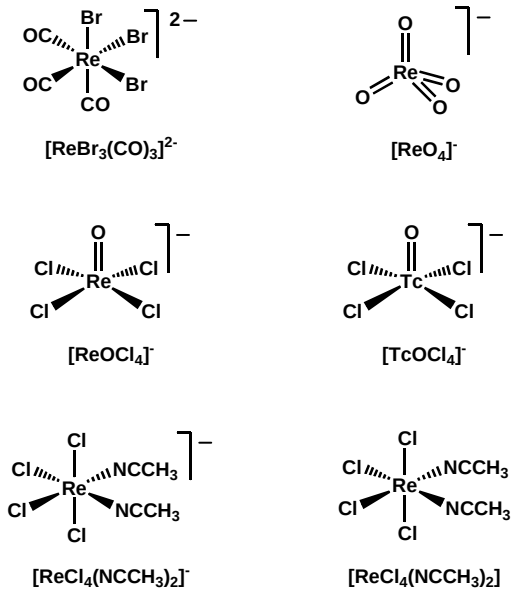

Figure 10: Starting materials used during this work.

3.3. Complexes synthesised in this work

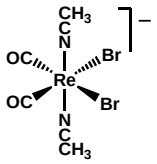

1

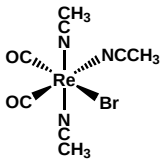

1a

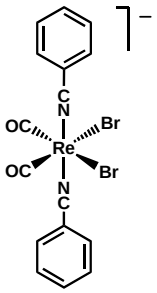

1b

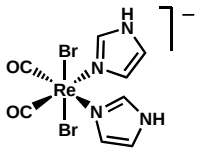

1c

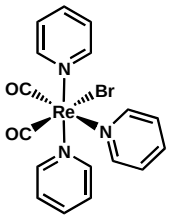

1d

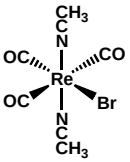

2

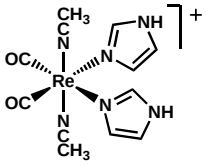

3

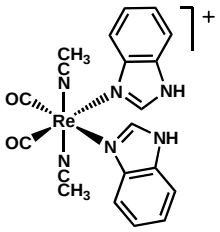

4

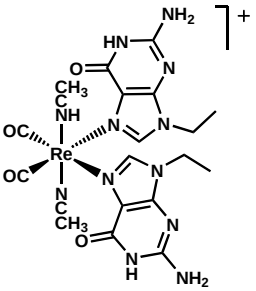

5

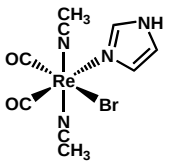

6

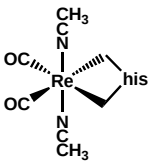

7

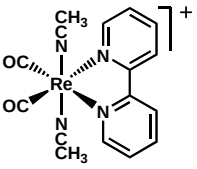

8

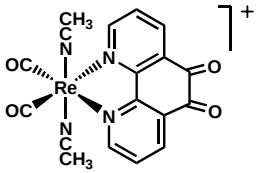

9

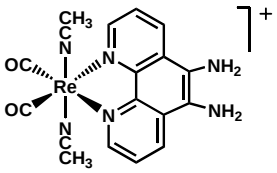

10

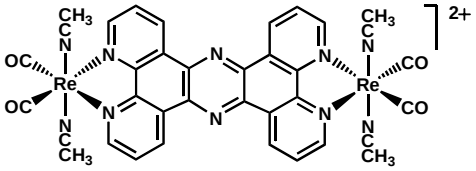

11

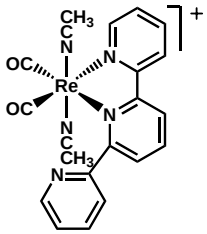

12

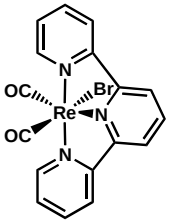

12a

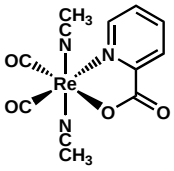

13

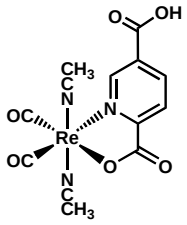

14

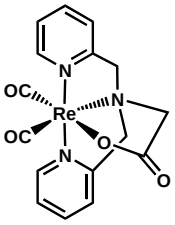

15

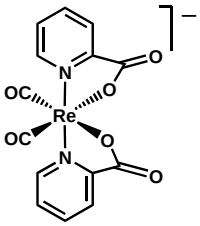

16

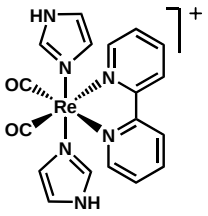

16a

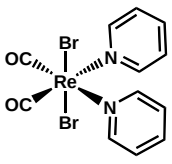

17

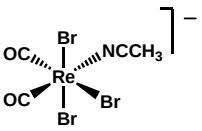

18

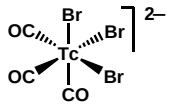

19

3.4. Formation of $\{Re(CO)_2\}^+$ complexes

Generally, there are two different ways to obtain $\{Re(CO)_2\}^+$ complexes: Either by decarbonylation of polycarbonyl complexes such as $(Et_4N)_2[ReBr_3(CO)_3]$ or $ReBr(CO)_5$, or by carbonylation and reduction of high valent precursor complexes. A known method (scheme 7) is the oxidation of $(Et_4N)_2[ReBr_3(CO)_3]$ by bromine, forming the dark red complex $(Et_4N)[Re^{(III)}Br_4(CO)_2]$ with concurrent CO evolution.[63] For the reduction back to oxidation state +I, a versatile reducing agent in a suitable solvent had to be found. The origin for a successful reaction lies in the solvent in which the reducing agent is soluble, the number of electrons it provides and in the formation of side products that can easily be handled. Most of our investigations follow the direction of reducing $[ReBr_4(CO)_2]^-$ in different solvents with different reducing agents. With respect to an analogue technetium complex, a different method has to be chosen because the synthesis of the $Tc(+III)(CO)_2$ complex is known to occur with a very low yield. The main product of this reaction is $[Tc(V)Br_6]^-$.[unpubl. results]

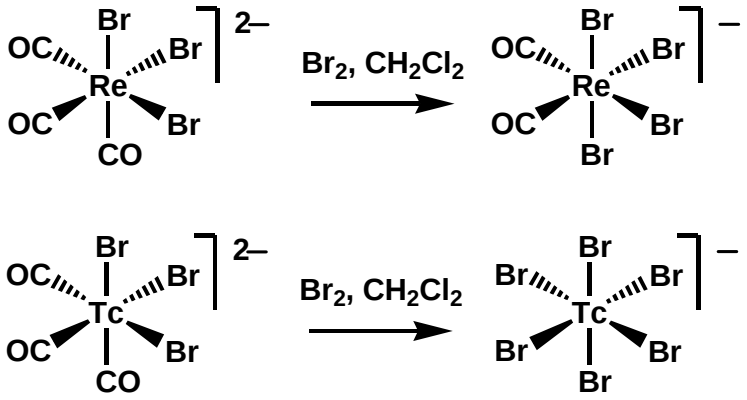

Scheme 7: Oxidation of $[MBr_3(CO)_3]^{2-}$ (M = Re, ^{99}Tc) complexes with bromine.

The smartest way would be a direct synthesis starting from perrhenate via reduction in the presence of CO. Both, high and low pressure carbonylation reactions are known to yield different rhenium and technetium carbonyl complexes. A high pressure reaction led in the formation of $Re_2(CO)_{10}$ whereas the low pressure carbonylation with BH_3-THF as reducing agent formed the well known tricarbonyl complexes $[MX_3(CO)_3]^{2-}$ (M = ^{99}Tc, Re) Beside permetallate, also M(+V) compounds like $[MOCl_4]^-$ are versatile

starting materials forming as well tricarbonyl complexes while treating with BH_3-THF in a CO saturated solution.[18]

3.5. Reduction of $(Et_4N)[Re^{(III)}Br_4(CO)_2]$

Preliminary investigations by Lukas Candreia and Nikos Agorastos have shown that either an electrochemical reduction or the reduction with cobaltocene of $(Et_4N)[Re^{(III)}Br_4(CO)_2]$ in acetonitrile led to the formation of $\{Re(CO)_2\}^+$ complexes. In an electrochemical reduction experiment $[Re^{(III)}Br_4(CO)_2]^-$ was dissolved (1 mM) in 40ml of acetonitrile with 0.1 M $TBAPF_6$ as an electrolyte. –1 V *vs.* Ag/Ag^+ was applied until the current decreased from initial 100 mA to a stable value of about 15 mA. During the reduction, the colour changed from dark red to green/yellow. The crude product was purified by extraction of $TBAPF_6$ with dichloromethane and the solvent dried *in vacuo*. The crude product still contained $TBAPF_6$ but in IR spectroscopy we could determine the carbonyl stretching frequencies at 1898 and 1797 cm^{-1} which gave first information about the range of $\nu_{(CO)}$ for $\{Re(CO)_2\}^+$ complexes in IR spectroscopy. Due to the low concentration of the reactant, the small volume of the reaction and the high amount of electrolyte, an electrochemical reduction is clearly not the method of choice for a bulk synthesis.

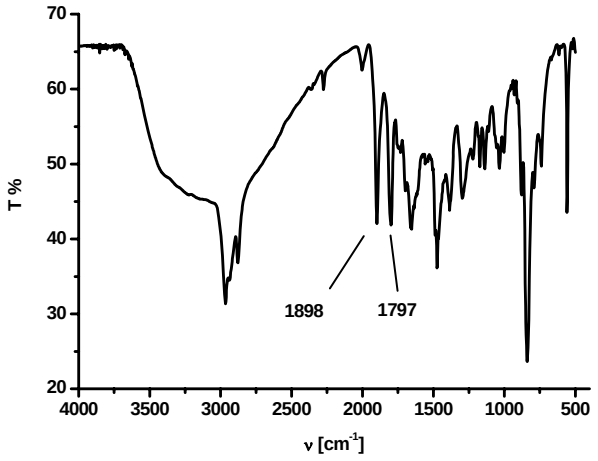

Figure 11: IR spectra of the electrochemical reduction of $[ReBr_4(CO)_2]^-$.

To follow these initial experiments, several reducing agents were tried in different solvents but with the main focus on acetonitrile due to the preliminary experiments.

3.5.1. Synthesis of $[ReBr(NCCH_3)_3(CO)_2]$ and $(Et_4N)[ReBr_2(NCCH_3)_2(CO)_2]$

For a bulk synthesis metals such as zinc or magnesium-powder as reducing agents were chosen.[64] To activate the magnesium, the oxide layer was removed by washing with 1 M HCl and the reduction was performed in acetonitrile for 16 h. The residual metal was filtered off but the separation of the $\{Re(CO)_2\}^+$ compound from the Zn(II) or Mg(II) salt was difficult. To separate the complex from the residual salt, several methods were tried. Unfortunately both, complex and salt, had similar solubility in many solvents. Additionally, $Zn^{(II)}$ or $Mg^{(II)}$ may act as a counter ion of the rhenium complex. Resulting $MgBr_2$ shows a strong signal in IR with a characteristic band for the crystal-water at 1630 cm^{-1} and was used as an indication for the success of the separation. With a column separation over silica gel with acetonitrile, pure $\{Re(CO)_2\}^+$-precursor $[ReBr(NCCH_3)_3(CO)_2]$ (**1a**) was obtained in a 40% yield with IR carbonyl stretching frequencies at 1940 and 1840 cm^{-1}.

Alternatively, the crude product was refluxed in ethanol dissolving the magnesium salt. The rhenium complex remained suspended with a yield up to 70%. Carbonyl stretching frequencies at 1893 and 1794 cm^{-1} indicated a different composition. From elemental analysis the composition $(Et_4N)[ReBr_2(NCCH_3)_2(CO)_2]$ (**1**) was calculated. This precursor was much easier to prepare in a much higher yield than **1a** why most of the following reactions were prepared with **1**. Both complexes **1** and **1a** were soluble in water and methanol and air stable.

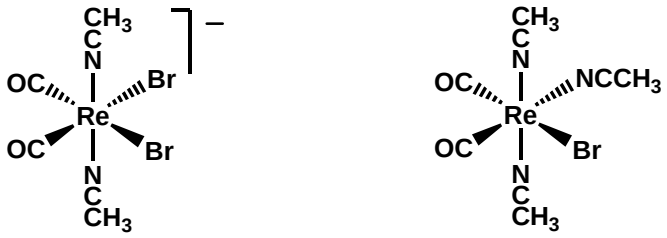

1 **1a**

Figure 12: The two $[Re(CO)_2]^+$ precursors **1** and **1a**.

From the reduction by Zn° in acetonitrile a crude product with similar CO stretching frequencies (1944, 1865 cm^{-1}) than in **1a** was obtained.

1a crystallised from CH_3CN/Et_2O in the hexagonal space group $P6_3$ as colourless needles in a distorted octahedral coordination. The crystal structure in figure 13 shows a strong bending of the two axial acetonitrile ligands: N(1)-Re(1)-N(2) 167.53(19)°. Considering the crystal packing, six molecules are forming a cycle with bent acetonitrile ligands. If this effect is due to the crystal packing or this packing a result of the bent acetonitrile ligands is hardly to decide. The Re(1)–N(1,2) bond lengths of average 2.074(5) Å of the two acetonitrile ligands standing in axial position show clearly that they are stronger bounded compared to the one standing in *trans* position of the carbonyl ligands which has a Re(1)-N(3) bond length of 2.144(7) Å. This fact fits with the standard *trans*-effect theory and shows a lability of the third acetonitrile. The bromide Br(1a) is disordered in a 95:5 ratio with the acetonitrile ligand in plane with the carbonyl ligands.

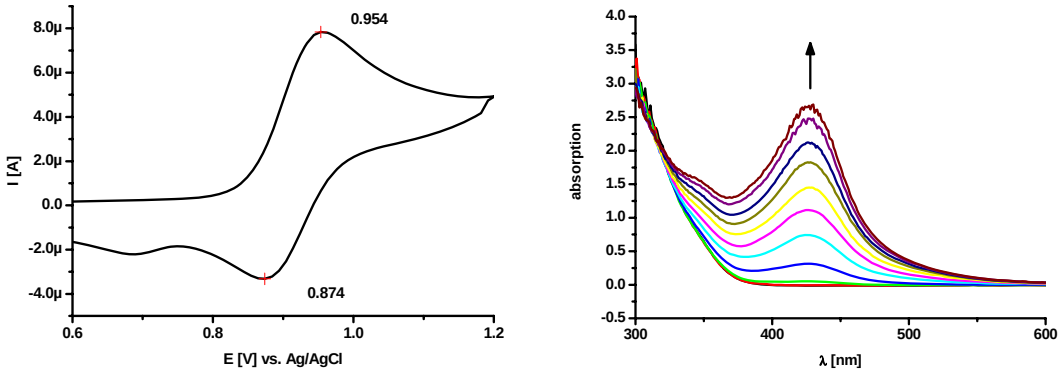

Figure 14: Cyclic voltammogram *vs.* Ag/Ag^+ (left) and UV-spectra of the electrochemical oxidation (right) of **1** in DMF.

While a heterogeneous reduction with zinc or magnesium is time consuming and the workup complicated, the need for another reducing agent is evident. Experiments with cobaltocene and $CrCl_2$ showed only minor improvements. In literature, the organic reducing agent *tetrakis*-dimethylaminoethylene (TDAE) as a two electron donor was found to be a good alternative due to its solubility in a wide range of solvents.[64] The ability of TDAE to readily donate 2 electrons is due to the presence of the four amino groups, which stabilize the positive charge by partial transfer of their free electron pairs onto the two central *C* atoms.[65] The half wave potentials are –0.75 and –0.61 V *vs.* aq. SCE.[66] The remarkably negative potential at which TDAE is oxidized is the evidence for a strong electron donor. Furthermore it is known that TDAE reduces metal-carbonyl complexes like $Co_2(CO)_8$ or $[CpMo(CO)_3]_2$ under the formation of the octamethyloxamidinium salts $[C_{10}H_{24}N_4][Co(CO)_4]_2$ or $[C_{10}H_{24}N_4][CpMo(CO)_3]_2$.[67]

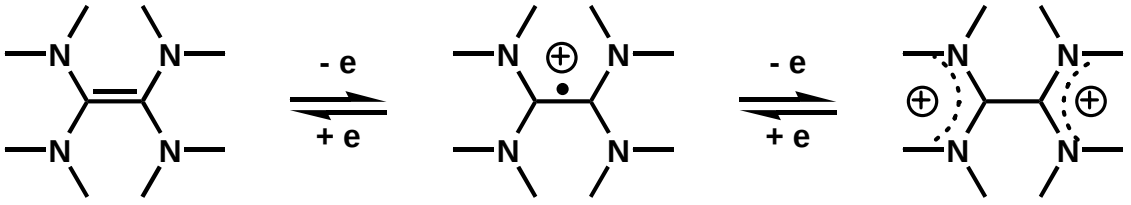

Scheme 8: Oxidation pathway of TDAE.

The reduction of $(Et_4N)[Re^{(III)}Br_4(CO)_2]$ in acetonitrile with 1.1 equivalent of TDAE proceeded very fast. Within 10 minutes, the resulting $(TDAE)Br_2$ salt, which is only

slightly soluble in acetonitrile, was filtered off. With the two above mentioned workup methods, again both **1** and **1a** were obtained but in yields up to 90%. The characteristic strong IR band of the (TDAE)Br_2 salt with 1635 cm^{-1} is indicative about the purity of the products. Changing the reducing agent to TDAE improved the synthesis of **1** and **1a** concerning reaction time, handling and yield.

3.5.2. IR spectroscopy of rhenium carbonyl complexes

Most of the analytics of this work was done by IR, showing whether a Re(I), Re(II) or Re(III) complex and whether a mono-, di- or tricarbonyl complex was obtained. Characteristic values are the wavenumbers and the shape of the symmetric and asymmetric CO stretching frequency (see figure 15 and 16). On the one hand, the lower the electron density at the metal centre, the lower the CO backbonding and therefore the higher the CO stretching frequencies. $[ReBr_4(CO)_2]^-$ shows the symmetric band at 2076 cm^{-1} whereas $[ReBr_2(NCCH_3)_2(CO)_2]^-$ at 1897 cm^{-1}. To compare, the $[ReBr_3(CO)_3]^{2-}$ complexes have the stretching frequency at around 2000 cm^{-1} due to the additional backbonding carbonyl group, which withdraws electron density from the metal centre. The stretching frequencies of {Re(II)$(CO)_2$} complexes (discussed below) are in the range of the tricarbonyl complexes with symmetric vibrations at around 1990 cm^{-1}. Thus, one more carbonyl ligand is able to almost compensate one charge at the metal centre by π-backbonding. Due to the number of vibrations, the shape is characteristic for rhenium carbonyl complexes.

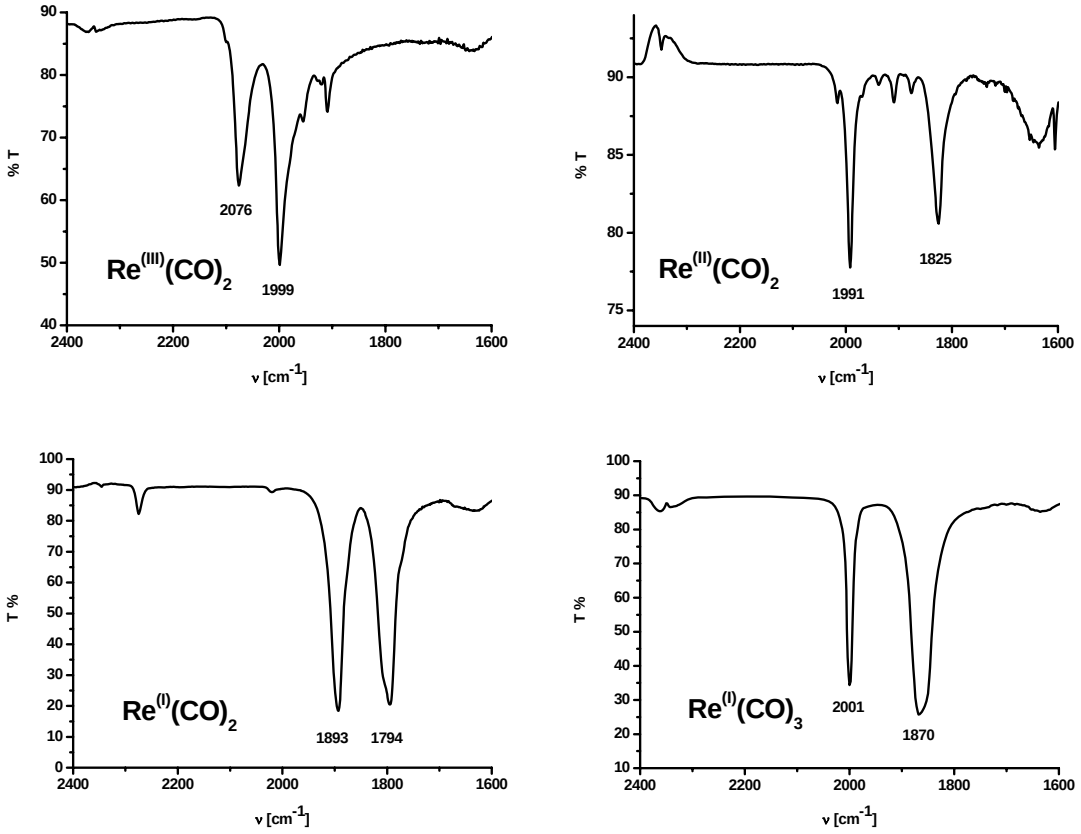

Figure 15: IR spectra of $Re^{(+I/+II/+III)}(CO)_{2,3}$ complexes, with the corresponding symmetric and antisymmetric stretching frequencies (from top left to bottom right) [cm^{-1}]: $(Et_4N)[ReBr_4(CO)_2]$[63] 2076, 1999; $[ReBr_2(CO)_2(py)_2]$ (**17**)[this work] 1991, 1825; $(Et_4N)[ReBr_2(NCCH_3)_2(CO)_2]$ (**1**)[68 and this work] 1893, 1794; $(Et_4N)_2[ReBr_3(CO)_3]$[34] 2001, 1870.

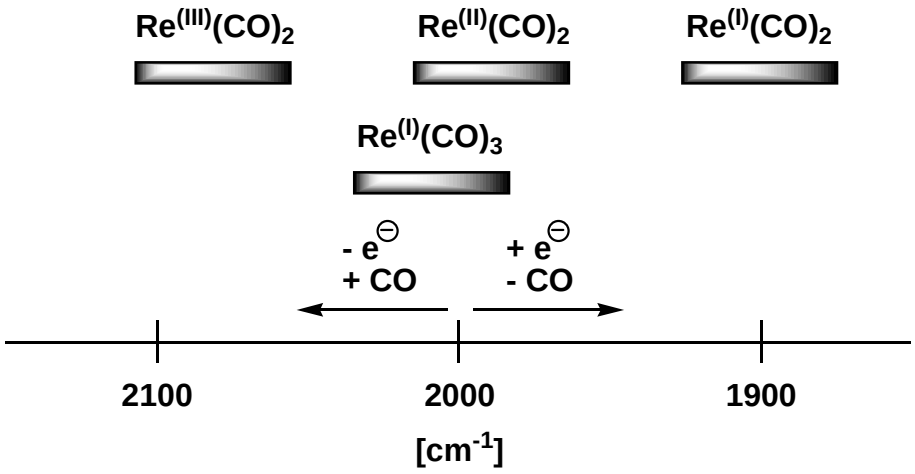

Figure 16: Change of the symmetric carbonyl stretching frequencies, influenced by the oxidation state and the number of carbonyl ligands.

3.5.3. Further reductions of $(Et_4N)[ReBr_4(CO)_2]$

The reduction was also carried out in solvents other than acetonitrile. In methanol, water and toluene no defined $Re(I)(CO)_2$ complexes could be identified. The IR always showed several sets of carbonyl stretching frequencies between 2070 and 1770 cm^{-1}. This meant, that besides the reduction to Re(I) also a single electron reduction to Re(II) or disproportion reactions to tricarbonyl complexes is possible. In weakly or non-coordinating solvents, charge compensation can only be achieved if $(Et_4N)^+$ and $(TDAE)^{2+}$ are acting both as counter ions and theoretically a mixed cation $[ReBr_4(CO)_2]^{3-}$ complex should be formed. Only in dimethoxyethane as a weakly coordinating solvent, a crude product with a nice $\{Re(CO)_2\}^+$ pattern with bands at 1865 and 1775 cm^{-1} could be isolated (see figure 17). The four negative charges explain the low frequencies. The obtained products were not stable and decomposed during workup. In IR spectroscopy, several $\{Re(CO)_3\}^+$ species were observed as decomposition products, indicating a disproportion reaction.

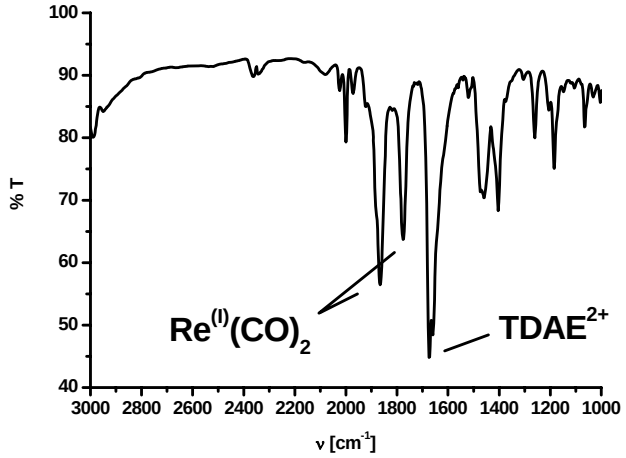

Figure 17: IR spectra of the product of the reduction of $[ReBr_4(CO)_2]^{2-}$ by TDAE in dimethoxyethane.

Using TDAE as a reducing agent but applying other nitriles as solvent was more successful and the corresponding benzonitrile complex could be isolated as $(Et_4N)[ReBr_2(NCC_6H_5)_2(CO)_2]$ (**1b**) (scheme 9). It seems that the axial nitrile ligands or other ligands, are crucial for the stability of $\{Re(CO)_2\}^+$ complexes. Considering the

high electron density at the metal centre as compared to the tricarbonyl complexes, electron-accepting ligands reduce the electron density. Since nitrile functions have both donating and accepting properties, the complexes are stable enough to compensate the π-backbonding strength of one carbonyl ligand.

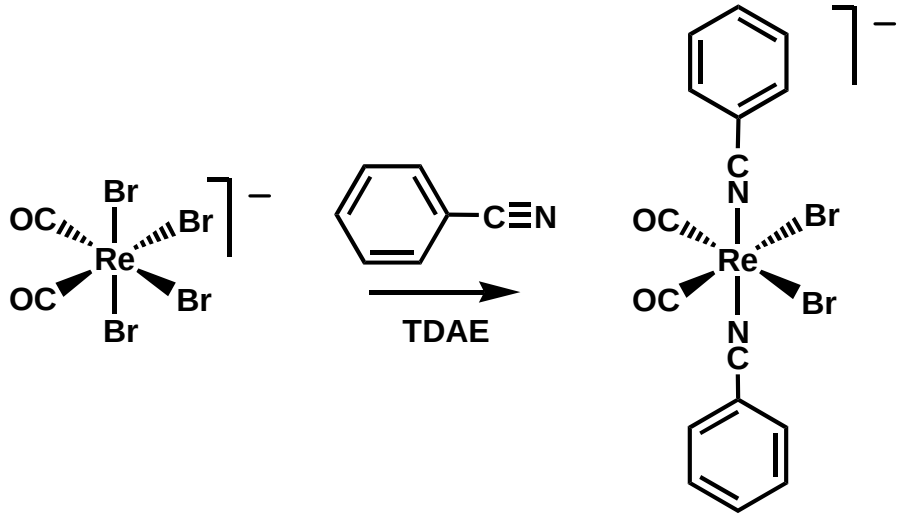

Scheme 9: Reduction of $[ReBr_4(CO)_2]^{2-}$ by TDAE in benzonitrile.

3.5.4. Synthesis of $(Et_4N)[ReBr_2(CO)_2(imz)_2]$

In order to stabilise the $\{Re(CO)_2\}^+$ complex in a different way than by nitriles, another strategy was chosen. The solvent was changed to less coordinating dimethoxyethane (DME). The addition of a supporting ligand with electron accepting abilities should led to new $\{Re(CO)_2\}^+$ complexes. The reduction of $(Et_4N)[ReBr_4(CO)_2]$ with TDAE in DME and an excess of imidazole as ligand resulted in a precipitate containing a mixture of a $\{Re(CO)_2\}^+$ complex and $(TDAE)Br_2$ salt. A pure rhenium compound remained after washing the residue with water. Single crystal x-ray analysis showed, that the imidazole ligands are not in axial position like in the nitrile complexes but the two bromides (figure 18). This new compound *trans-cis*-$(Et_4N)[ReBr_2(CO)_2(imz)_2]$ (**1c**) is air stable, well soluble in acetonitrile and pyridine, slightly soluble in alcohol and water and insoluble in dichloromethane and THF. Complex **1c** crystallises in the monoclinic space group $P2_1/n$ as colourless needles by slow evaporation of a methanol solution. The Re-N bond length is with 2.226(6) and 2.231(5) Å quite elongated as compared to the Re-N bond lengths in the corresponding acetonitrile complex *trans-cis*-

$[Re(NCCH_3)_2(CO)_2(imz)_2]Br$ (**3**) with 2.198(5) and 2.200(5) Å.[68] The IR stretching frequencies of the carbonyl ligands in KBr were again shifted to very low wavenumbers. With 1870 and 1767 cm^{-1}, they are the lowest values for carbonyl frequencies observed in this work. The two bromides and the two imidazole ligands seemed to be labile for substitution reactions. In water, the liquid IR showed a symmetric stretching frequency at 1884 cm^{-1}. There was no change by adding of Ag^+ salts, implying a substitution of the two bromides by solvent molecules in solution. In acetonitrile, after heating to 60° C for 2h, a crude product was obtained, which showed IR frequencies (1917, 1824 cm^{-1}) shifted to higher wavenumbers, comparable with the known complex **3** (1916, 1827 cm^{-1}).

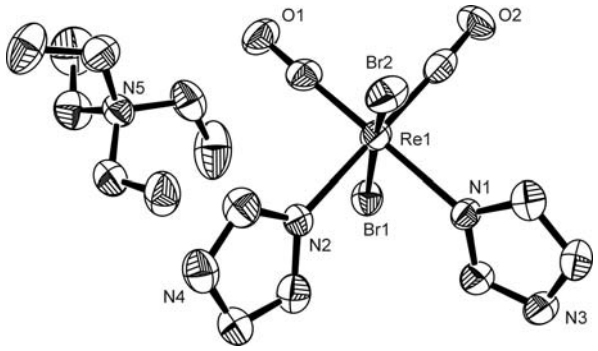

Figure 18: ORTEP plot of complex **1c** (Ellipsoids are drawn at 50% probability and hydrogen atoms are omitted for clarity). Selected bond lengths are [Å]: Re(1)-N(1) 2.231(5); Re(1)-N(2) 2.226(6); Re(1)-Br(1) 2.6054(8); Re(1)-Br(2) 2.6129(8).

In other solvents like THF, CH_2Cl_2 or methanol, the reduction of $(Et_4N)[ReBr_4(CO)_2]$ with TDAE gave no defined product. In DME but with changing the ligands led to defined products according IR spectroscopy. With benzimidazole, a crude product still contaminated with $(TDAE)Br_2$, was obtained with ν_{CO} at 1865 and 1771 cm^{-1}. From the reduction in presence of bipyridine, the IR spectrum of the product exhibited a typical $\{Re(CO)_2\}$ pattern but too high in frequencies compared to known complexes. We are now able to assign this frequencies to a $\{Re(CO)_2\}^{2+}$ complex which was not expected at that time. The experiments concerning the $\{Re(CO)_2\}^{2+}$ complexes are discussed in more detail in chapter 3.14.

Table 4, CO stretching frequencies of imidazole like complexes obtained by different pathways.

compound	$\nu_{(CO)sym}$ [cm^{-1}]	$\nu_{(CO)asym}$ [cm^{-1}]
$[ReBr_2(CO)_2(imz)_2]^-$ (**1c**)	1870	1767
$[ReBr_2(CO)_2(bzimz)_2]^-$	1865	1771
$[Re(NCCH_3)_2(CO)_2(imz)_2]^+$ (**3**)	1916	1827

The determination of the redox potentials of **1c** was hardly possible since difference pulse measurements (DP) of a 1 mM solution with 0.1 M TBAPF6 as an electrolyte showed up to six signals between –250 mV and +1350 mV with varying intensities, a sign for solvatation effects. After heating the solution at 60° C overnight, the solution showed one main signal with an irreversible oxidation at ~770 mV and a smaller one around 400 mV which remains as a main signal after precipitating the bromides by Ag^+.

3.5.5. Synthesis of "$[ReBr(CO)_2(py)_3]$"

Changing to pyridine as solvent and ligand like the nitriles, the reduction with 1 eq. TDAE depicted again a nice $\{Re(CO)_2\}^+$ pattern in the IR with carbonyl stretching frequencies at 1875 and 1785 wavenumbers. The crude complex is soluble in acetone and from layering with water, single crystals suitable for x-ray diffraction studies could be obtained. The product crystallised as a big brown prism in the monoclinic space group $P2_1/n$. The structure is shown in figure 19 and consists of a neutral rhenium complex with two carbonyls, three pyridines and one bromide $[ReBr(CO)_2(py)_3]$ (**1d**). Compared to the complexes **1a** and **1c**, the composition is similar to the acetonitrile complex **1a**. The two axial pyridine ligands have a shorter Re-N bond length then the one *trans* to the carbonyl ligands but all bonds are around 0.09 Å longer then in **1a** (table 5). The bromide is disordered in 60:40% with its *trans*-carbonyl group.

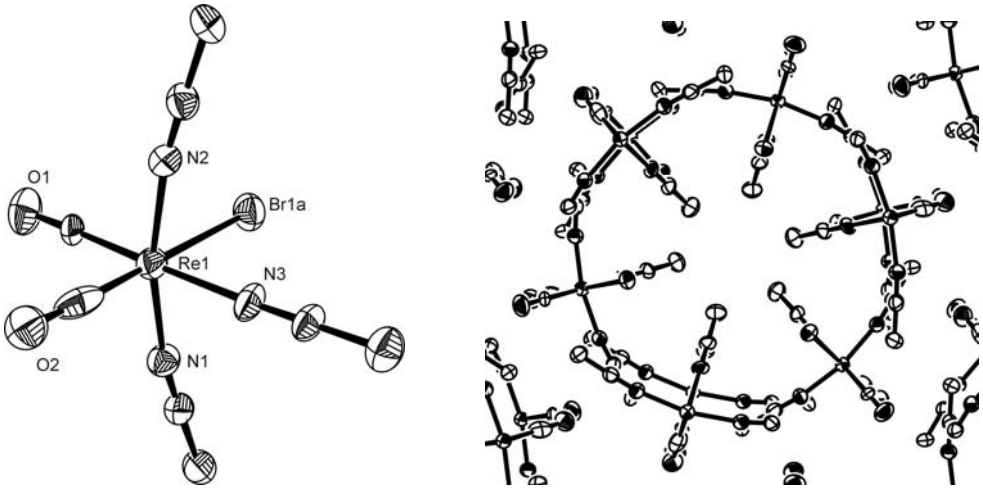

Figure 13: ORTEP plot and crystal packing of complex **1a** (Ellipsoids are drawn at 50% probability and hydrogen atoms are omitted for clarity). Selected bond lengths are [Å]: Re(1)-N(1) 2.073(5), Re(1)-N(2) 2.075(5), Re(1)-N(3) 2.144(7), Re(1)-Br(1a) 2.6622(12).

In cyclic voltammetry, complex **1** showed partly reversible one electron oxidation at 914 mV *vs.* Ag/Ag^+ (figure 14, left). Additionally, spectro-electrochemical oxidation at 960 mV (figure 14, right) indicated the formation of a new species with a yellow colour (λ_{max} = 427 nm). But with time, the solution lost colour again and the product could not be isolated and analysed. With the right coordination sphere and the right reaction conditions, a stable $\{Re(II)(CO)_2\}$ compound should be possible and will be discussed in chapter 3.14.

A two-electron oxidation of **1** with Br_2 in DCM led again to the starting material $[ReBr_4(CO)_2]^-$ as shown by equal carbonyl stretching frequencies in IR.

The IR spectra of the crystals did not show anymore the above-mentioned frequencies of the product, but the bands are with 1890 and 1796 cm^{-1} shifted to higher wavenumbers. This inconsistency caused discussions about the original product. Concerning the standard rules of influence of ligands to carbonyl stretching frequencies, the crude product was likely to consist of the di-bromide complex salt.

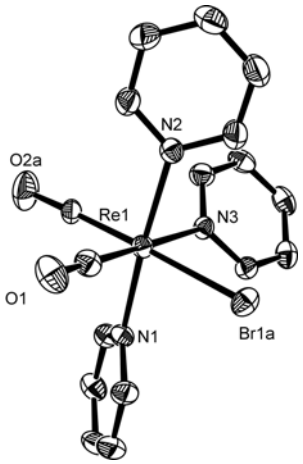

Figure 19: ORTEP plot of complex **1d** (Ellipsoids are drawn at 50% probability and hydrogen atoms are omitted for clarity).

Table 5: Selected bond lengths of complex **1d** in comparison with **1a**.

bond length [Å]	**1d**	**1a**
Re(1)-N(1)	2.157(3)	2.073(5)
Re(1)-N(2)	2.169(2)	2.075(5)
Re(1)-N(3)	2.220(2)	2.144(7)
Re(1)-Br(1a)	2.6138(8)	2.6622(12)

Instead of working in pure pyridine, the reaction was performed in DME adding pyridine as a ligand. Again, a precipitation was obtained with carbonyl stretching frequencies different from **1d** (1875 and 1778 cm^{-1} *vs.* 1890 and 1796 cm^{-1} (**1d**)). The bands for $(TDAE)^{2+}$ were still visible and remained with slightly lower intensity after washing with water. Elemental analysis was consistent with $(TDAE)[ReBr_2(CO)_2(py)_2]_2$ (Found: C, 30.77; H, 3.58; N, 8.12. Calc. for $C_{34}H_{46}Br_4N_8O_4Re_2$: C, 30.87; H, 3.51; N, 8.47).

3.5.6. Summary of the reductions of $(Et_4N)[ReBr_4(CO)_2]$

The reduction of $(Et_4N)[ReBr_4(CO)_2]$ is a versatile method to obtain new $\{Re(CO)_2\}^+$ complexes in good yields. They were stable under air and in solution and are substitution labile (see below). A stabilising ligand, in this cases a nitrile-, imidazole- or pyridine was necessary to compensate for the stabilising effect of a third carbonyl in a *facial* coordination. Nevertheless, five new substitution labile complexes were synthesised and characterised. Behaviour and substitution patterns of **1**, **1a**, **1c** will be discussed in chapter 3.10. - 3.12., whereas for **1b** its presumed to have similar behaviour like **1**. Further complexes like **1d** can be obtained by again changing the reaction conditions shown with the different pyridine-complex. With the mentioned examples a general overview and further possibilities but also limitations are given.

3.6. Decarbonylation of $\{Re(CO)_3\}^+$ complexes

A versatile method for obtaining $\{Re(CO)_2\}^+$ complexes would be decarbonylation of corresponding $\{Re(CO)_3\}^+$ complexes without oxidation of the metal centre. In literature, several methods have been described and we adapted these methods to our particular complexes.

3.6.1. Decarbonylation of $\{Re(CO)_3\}^+$ complexes by TMNO

Decarbonylation can be achieved with amine oxides like trimethyl amine oxide (TMNO). TMNO oxidises CO to CO_2, which is replaced by the reduced amine, solvent molecule or a ligand. Several examples are known from literature, especially from the chromium triade but also from manganese.[69]

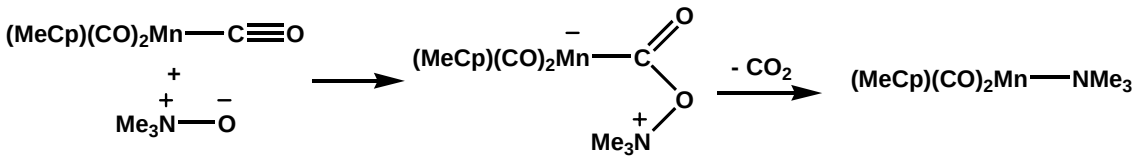

Scheme 10: Decarbonylation reaction of $[(MeCp)Mn(CO)_3]$ by TMNO.[69]

According to literature, this method requires an electrophilic CO carbon. Carbonyl complexes with symmetric stretching frequencies lower than 2000 cm^{-1} do not react anymore with amine oxides. Thus, $(Et_4N)_2[ReBr_3(CO)_3]$ with a carbonyl frequency of 1999 cm^{-1} would be at the borderline. For rhenium the following is known: hexamethyl-benzene tricarbonyl-rhenium is decarbonylated by TMNO and forms in the presence of $(Bu_4N)Cl$ the corresponding dicarbonyl-chloride complex $[ReCl(CO)_2(C_6(CH_3)_6]$ in low yield (10-30%).[70]

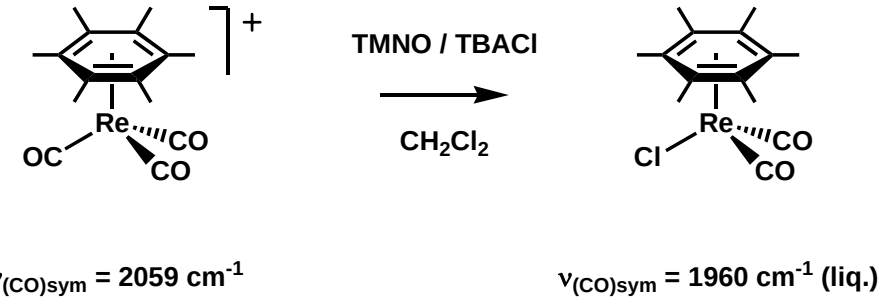

Scheme 11: Decarbonylation of $[((H_3C)_6C_6)Re(CO)_3]^+$ by TMNO.

Nevertheless, attempts to decarbonylate $[ReBr_3(CO)_3]^{2-}$ and some tricarbonyl-arene compounds by TMNO were performed in different solvents and at different temperatures with and without precipitation of the bromides by silver salts. Beside the example known from literature, all the investigations didn't show any change in the IR, meaning no clear shift to lower frequencies and remaining of a general $\{Re(CO)_3\}^+$ pattern.

Table 6: Overview over the reaction conditions of the performed decarbonylation reactions.

$\{Re(CO)_3\}^+$	solvent	temp.	silver salt	result
$[ReBr_3(CO)_3]^{2-}$	CH_3CN	RT	-	$\{Re(CO)_3\}^+$
	CH_3CN	50° C		$\{Re(CO)_3\}^+$
$[ReBr_3(CO)_3]^{2-}$	H_2O	RT	$AgNO_3$	$\{Re(CO)_3\}^+$
$[ReBr_3(CO)_3]^{2-}$	H_2O	90° C	AgO_3SCF_3	$\{Re(CO)_3\}^+$
$[Re(CO)_3(tol)]^+$	CH_2Cl_2	reflux	-	$\{Re(CO)_3\}^+$
$[Re(CO)_3(C_6(CH_3)_6)]^+$	CH_2Cl_2	RT	-	$[ReCl(CO)_2(C_6(CH_3)_6)]$

3.6.2. Decarbonylation of $[ReBr_3(CO)_3]^{2-}$ under harsh conditions

A few more successful methods were described in literature but they all use very harsh conditions or phosphine containing ligand systems.[56] They did start from $[ReBr(CO)_5]$ and synthesised first the corresponding tricarbonyl complex with bipyridine or phenanthroline. In a second step, diphosphines were added and refluxed in *o*-dichlorobenzene (bp. = 173° C) to form mixed $[Re(CO)_2(P,P)(N,N)]^+$ complexes. A second method was to mix the tricarbonyl-bpy-complex with a large excess of bpy, melt the reaction mixture and heated to reflux ($bp._{(bpy)}$ = 273° C) to obtain the corresponding $[Re(CO)_2(N,N)_2]^+$ complex.

Nevertheless, $(Et_4N)_2[ReBr_3(CO)_3]$ was dissolved in acetonitrile and the bromides were precipitated with Ag^+ to yield the fully solvated complex $[Re(NCCH_3)_3(CO)_3]^+$. The solution was then heated up to 150° C in a small autoclave and IR spectra were measured over a period of 16 hours. But a change in the IR was not detectable. A similar reaction in water did not show any improvement.

3.6.3. Decarbonylation of $[ReBr_3(CO)_3]^{2-}$ by light - hν

A last method was inspired by the fact that $[Cp^*Re(CO)_3]$ in THF is evolving CO under irradiation with light to form the solvated intermediate $[Cp^*Re(CO)_2(THF)]$.[71]

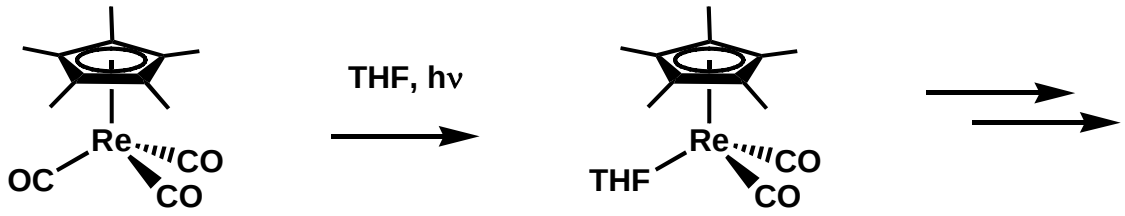

Scheme 12: Decarbonylation of $[(Cp^*)Re(CO)_3]$ by light in THF.

Therefore, $(Et_4N)_2[ReBr_3(CO)_3]$ was dissolved in THF and the bromides precipitated by Ag^+ and removed by filtration. The dissolved complex was then irradiated in a irradiation-aperture with a 600 W Quartz-lamp for several minutes. The IR bands for the $\{Re(CO)_3\}^+$ disappeared but no other carbonyl pattern was growing in. Therefore we concluded that complete decomposition of the carbonyl complex took place.

In summary, the decarbonylation experiments confirmed the prediction that only rhenium carbonyl complexes with CO bands higher than 2000 cm^{-1} can be decarbonylated. Neither the CO oxidation by TMNO, harsh conditions or the use of light was successful. These are methods for special cases. To synthesise $\{Re(CO)_2\}^+$ complexes, other general strategies have to be chosen.

3.7. Carbonylation of high valent rhenium complexes

The reduction of high valent rhenium and technetium complexes such as TBA[$MOCl_4$] or TBA[MO_4] (M = Re, ^{99}Tc) with BH_3-THF under CO atmosphere resulted in tricarbonyl complexes. Using diglyme as a weakly coordinating solvent and a non-coordinating reducing agent gave the desired *fac*-$[MCl_3(CO)_3]^{2-}$. Due to several colour changes, a multistep reaction with an initial reduction to M(+III) and stepwise carbonylation was suggested.[18] TBA[$TcOCl_4$] in the presence of strongly coordinating and reducing compounds like triphenylphosphine did not yield the thermodynamically favoured *facial* tricarbonyl but the *meridional*-$[MCl(CO)_3(PPh_3)_2]$ (M = Re, ^{99}Tc).[62] Whereas a stepwise reaction with first a reduction with triphenylphosphine gave $[TcCl_3(NCCH_3)(PPh_3)_2]$ forming under CO atmosphere the monocarbonyl complex $[TcCl_3(CO)(PPh_3)_2]$.[72]

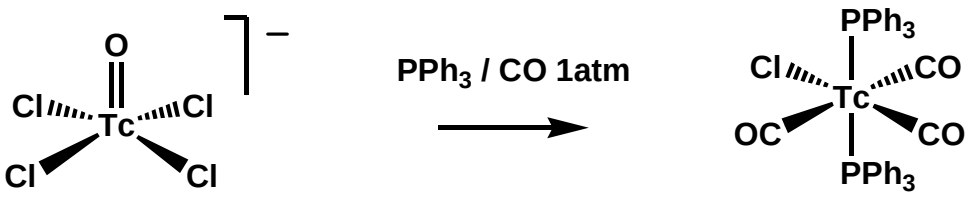

Scheme 13: Formation of *mer*-$[Tc(CO)_3]^+$ with PPh_3 under CO atmosphere.

Meridional carbonyl complexes should be very substitution labile at least at the positions *trans* to CO. In IR spectroscopy $[TcCl(CO)_3(PPh_3)_2]$ showed a weak band at 2057 and two strong bands at 1962 and 1919 cm^{-1} respectively.

In most of the $\{Re(CO)_2\}^+$ complexes obtained in this work, the acetonitrile ligands are strongly bound. The use of acetonitrile in carbonylation reactions of high valent starting materials, could perhaps provide a three fold carbonylation or at least give access to a *meridional* complex. Several starting materials in different oxidation states and various reducing agents were examined. Furthermore, CO was applied from atmospheric up to 20 bar of pressure and all reactions were carried out in acetonitrile.

3.7.1. Carbonylation of $(Bu_4N)[ReOCl_4]$

Oxo-tetrachlororhenate is a convenient starting material. It is easily prepared from perrhenate in high yields and it is soluble in a wide range of solvents. To obtain $\{Re(CO)_2\}^+$ complexes, a four electron reduction is necessary. In analogy to the low pressure synthesis of $[ReCl_3(CO)_3]^{2-}$, the first experiment was performed with H_3B-THF as reducing agent but in acetonitrile instead of diglyme.[18] Carbon monoxide was bubbled trough the solution to generate H_3B-CO and to deliver enough CO during the whole reaction. The crude product of this reaction showed no IR CO stretching frequency in the region between 2000 and 1750 cm^{-1}. Thus neither a $\{Re(CO)_3\}^+$ nor a $\{Re(CO)_2\}^+$ species was formed.

Changing reducing agent and CO pressure gave products with different IR bands in the carbonyl region but an assignment was not possible. A typical spectra is shown in figure 20 and an overview of the experiments with $TBA[ReOCl_4]$ is given in table 7.

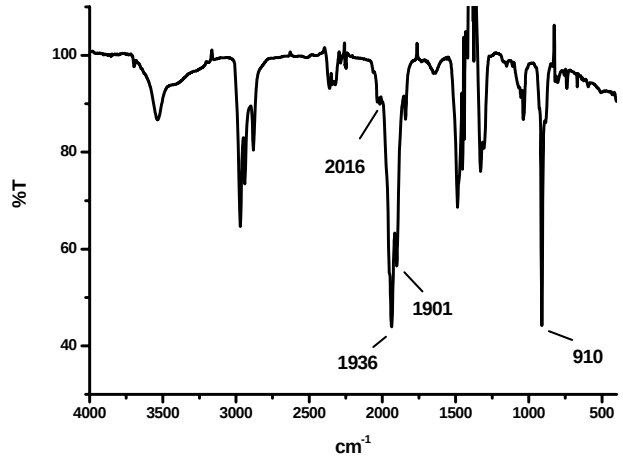

Figure 20: IR spectra of the carbonylation reaction of $[ReOCl_4]^-$ with Mg° as a reductant.

Table 7: Carbonyl stretching frequencies of the crude products from the carbonylation reactions of $[ReOCl_4]^-$.

reductant	$p_{(CO)}$	IR bands [cm^{-1}]
H_3B-THF	atm	-
Mg°	3 bar	2016, 1952 (sh), 1936, 1901
Zn°	atm	1927
TDAE	atm	2001, 1921, 1868, 1802

3.7.2. Carbonylation of other rhenium starting materials

When starting form $[ReCl_4(NCCH_3)_2]$ carbonyl frequencies were detectable in liquid IR during the reaction with Mg° at a CO pressure of 3 bar. With 1943 and 1870 cm^{-1}, they were not comparable with the known $\{Re(CO)_2\}^+$ complexes.

$[ReCl_4(NCCH_3)_2]$ requests an odd number of electrons to achieve the oxidation state +I. Therefore the starting material was first reduced to $(HEt_3N)[ReCl_4(NCCH_3)_2]$ which would then need two electrons. The reducing agent for the carbonylation reaction was Mg° and a CO pressure of 20 bar was applied. After more then 20 h under CO the IR spectrum of the product (figure 21) exhibited two CO bands in the region of

$\{Re(CO)_2\}^+$ complexes. With 1904 and 1809 cm^{-1}, they were comparable with complex **1**.

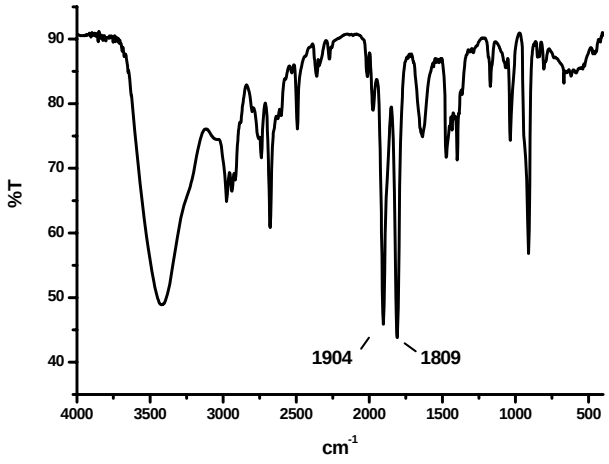

Figure 21: IR spectra of the carbonylation reaction of $[ReCl_4(NCCH_3)_2]^-$ with Mg° as a reductant.

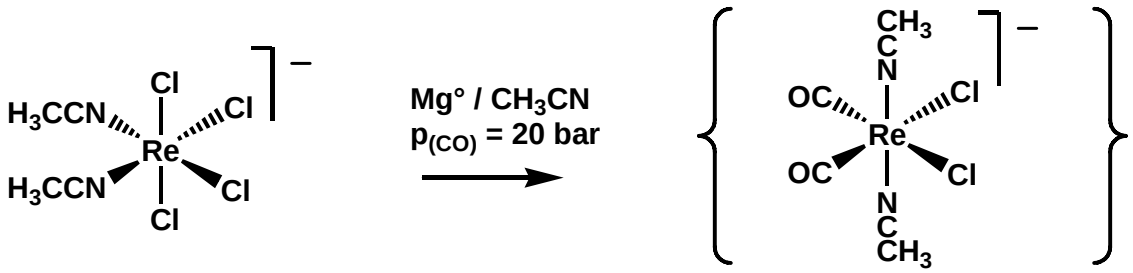

Scheme 14: Reduction oft the rhenium(+III) compound $[ReCl_4(NCCH_3)_2]^-$ with magnesium in acetonitrile under 20 bar of carbon monoxide.

This reaction showed that a direct carbonylation of "higher" valent rhenium precursors was possible even if $(HEt_3N)[ReCl_4(NCCH_3)_2]$ is not an easily accessible precursor.

Table 8: IR stretching frequencies of the crude products from the carbonylation reactions with other starting materials.

starting material	reductant	$p_{(CO)}$	IR bands [cm^{-1}]
$HNEt_3[ReCl_4(NCCH_3)_2]$	Mg°	20 bar	1904, 1809
$TBA[ReO_4]$	H_3B-THF	atm	-
$TBA[^{99}TcOCl_4]$	Zn°	atm	2258 $_{(CN)}$, 2031, 1949, 1857 $_{(CO)}$

Starting from perrhenate in acetonitrile, the direct adaptation of the tricarbonyl synthesis with reduction by H_3B-THF under CO did not show any carbonyl frequencies in the IR.

3.7.3. Carbonylation of $(Bu_4N)[^{99}TcOCl_4]$

Changing to technetium, the reduction of TBA[$^{99}TcOCl_4$] was performed with Zn° under CO in acetonitrile. In the IR spectrum in figure 22, the crude product showed traces of a $\{Tc(CO)_2\}^+$ complex but one could also formulate a *meridional* tricarbonyltechnetium complex. Most reasonable is a superposition of several carbonyl complexes. Interestingly, there is also a band at 2258 cm^{-1}, which is assigned to a ν(CN) of coordinated acetonitrile.

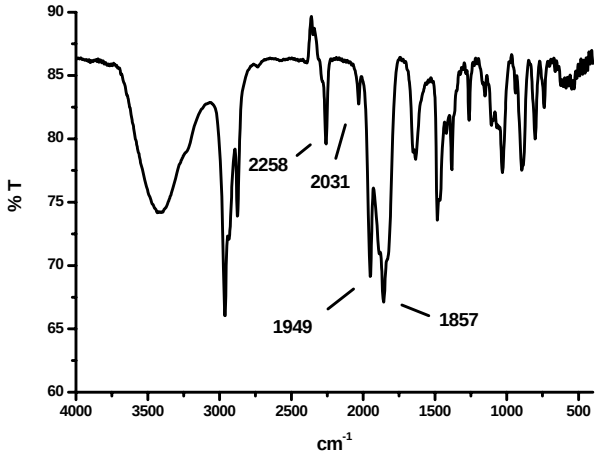

Figure 22: IR spectra of the carbonylation reaction of [$^{99}TcOCl_4$]$^-$ with Zn° as a reductant.

Summarising the outcome of this reactions, starting from $[ReCl_4(NCCH_3)_2]$ as well as from $(Bu_4N)[MOCl_4]$, some carbonyl compounds were accessible but none of the compounds could be isolated and structurally identified. All the results are suggestions based on carbonyl stretching frequencies from IR spectra. The obtained crude products seemed to be mixtures of $\{Re(CO)_2\}^+$ and $\{Re(CO)_3\}^+$ compounds assigned by the band at around 2010 cm^{-1} for the symmetric stretching frequency of tricarbonyl and some bands between 1800 and 1950 cm^{-1} in the IR spectrum.

3.8. Conclusion for the formation of $\{Re(CO)_2\}^+$ complexes

A versatile route to various *cis*-$\{Re(CO)_2\}^+$ complexes was found by the reduction of $(Et_4N)[ReBr_4(CO)_2]$ in the presence of ligands like acetonitrile or imidazole. From these reactions, several complexes were synthesised mainly $(Et_4N)[ReBr_2(NCCH_3)_2(CO)_2]$ **1**, $[ReBr(NCCH_3)_3(CO)_2]$ **1a** and $(Et_4N)[ReBr_2(CO)_2(imz)_2]$ **1c** and structurally characterized. Basic investigations and substitution reaction with these complexes will be discussed in the next chapters. Other synthetic approaches via decarbonylation reactions did not yield defined $\{Re(CO)_2\}^+$ complexes. On the other hand, a direct carbonylation of high valent starting materials revealed, that CO complexes were formed. More details about the reaction mechanism and the influence of changing conditions must be known in order to direct the reaction towards a well defined product.

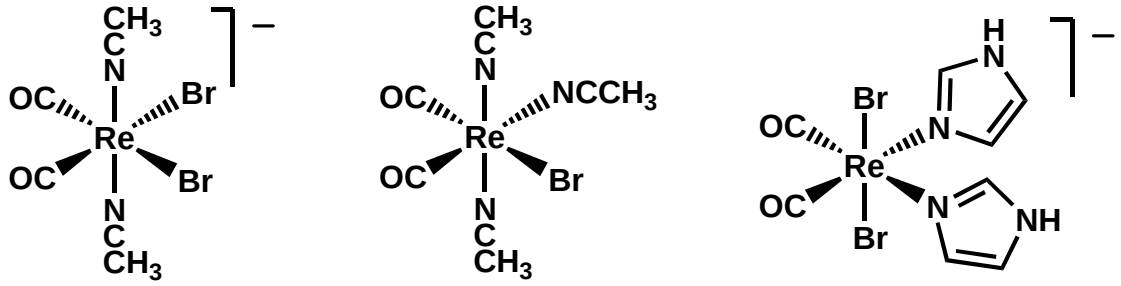

1 **1a** **1c**

Figure 23: The three $\{Re(CO)_2\}^+$ precursors **1**, **1a** and **1c**.

3.9. Reactivity of *cis*-$\{Re(CO)_2\}^+$ based complexes

3.9.1. Behaviour of $(Et_4N)[ReBr_2(NCCH_3)_2(CO)_2]$ in coordinating solvents

Versatile precursors for application in organometallic chemistry must be soluble in different solvents and a number of ligands should be substitution labile. For bioorganometallic chemistry or radiopharmacy, water stability is of utmost importance. Complexes should comprise ligands such as halides, which are easily replaced by water, thus, forming sort of organometallic aqua-ions. As in the case of $[Re(OH_2)_3(CO)_3]^+$, these water molecules can be replaced by donors from biomolecules or from ligands attached to targeting molecules (labelling).[73] Therefore, the behaviour of **1** in water represented a crucial test for potential applicability. Re(I) and Tc(I) with low spin d6 configurations are in general considered to be soft metal centres (B type). However, the electron withdrawing effect of the CO ligands is likely to shift this behaviour towards a preference for more medium-hard O and N ligands such as water, amines or acetonitrile. Therefore, the halides are not too strongly bound and are expected to be replaced by solvent molecules. This assumption was confirmed by the behaviour of **1** in water. As evident from IR-spectroscopy, the halides were readily exchanged by H_2O thereby forming the complex *trans*-*cis*-$[Re(NCCH_3)_2(OH_2)_2(CO)_2]^+$ (Figure 24).

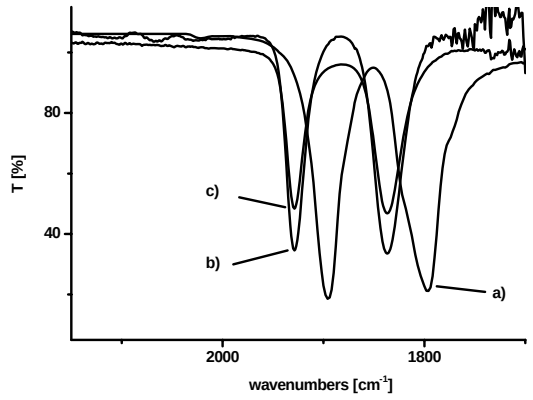

Figure 24: IR study of the behaviour of **1** in water: a) The spectrum of solid **1** in KBr shows the two CO stretching frequencies at 1893 and 1794 cm^{-1}; b) An aqueous solution of **1** exhibits the same pattern substantially blue-shifted to higher wave numbers (1928, 1836 cm^{-1}); c) The spectra remains unchanged when the bromides are precipitated with Ag^+ confirming the identity of the two complexes present in aqueous solution prior to and after precipitation of the Br^-.

A similar behaviour was also observed with other coordinating solvents such as CH_3CN or CH_3OH. The bromides were readily substituted by solvent molecules and complexes of the general composition *trans-cis*-$[Re(NCCH_3)_2(sol)_2(CO)_2]^+$ formed. These solvent-complexes were stable in solution over several days. Heating an aqueous solution up to 150° C in an autoclave, the aqua-complex remained intact, none of the other ligands were exchanged and no decomposition was observed. They were also unreactive against air (oxygen). Passing oxygen through an aqueous solution for more than one hour did not oxidize any of the complexes as shown by HPLC or in the infrared spectra.

Metal aqua-ions usually act as Brönstedt acids, especially the first row transition metals. Even though mono-cationic species are not very acidic. Deprotonation of coordinated water tends to the formation of μ-OH or μ-O bridged polymeric clusters.[34, 74] In water, $[Re(OH_2)_3(CO)_3]^+$ is known to form different clusters such as $[Re_3(\mu_3\text{-}OH)(\mu\text{-}OH)_3(CO)_9]^-$ and $[Re_2(\mu\text{-}OH)_3(CO)_6]^-$ at basic conditions starting from pH ≈ 8.
The pH-curve in figure 25 of the titration of a 0.1 M KNO_3 solution of **1** (10^{-3} M) with 0.1 M KOH shows a consumption of $[OH]^-$ by deprotonation of coordinated water molecules as compared with a reference experiment (titration of a 0.1 M KNO_3 solution with 0.1 M KOH).

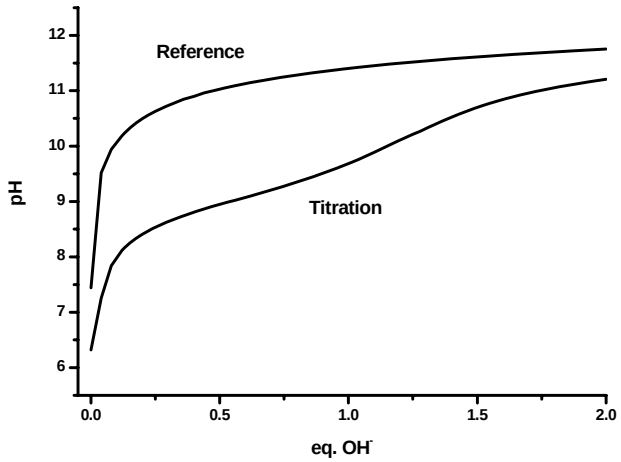

Figure 25: Alkaline titration of a 0.1 M KNO_3 solution of **1** (1 mM) with 0.1 M KOH.

After the addition of 1 equivalent of base, the solution became turbid. A precipitate was formed and the pH value was increasing faster. The filtered and washed precipitate was not soluble anymore in any solvent. A suggested reaction pathway is shown in scheme 15. It seems that after single deprotonation of the aquo-complex $[Re(OH_2)_2(NCCH_3)_2(CO)_2]^+$, a dinuclear, μ-OH bridged, neutral complex was formed. It is well known that such clusters are sometimes very insoluble due to the presence of lipophilic organic and very hydrophilic OH ligands. This mixture is sometimes not compatible with corresponding solvents.

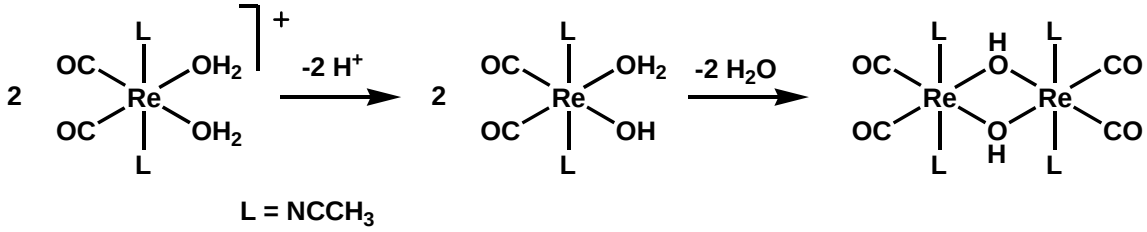

Scheme 15: Suggested pathway of μ-OH formation according to the results of the alkaline titration of **1**.

The IR spectrum in figure 27 (left) shows a sharp band at 3606 cm^{-1}, which was assigned to a bridging hydroxide. The carbonyl stretching frequencies are only slightly shifted to lower wavenumbers as compared to **1**, indicating a minor change of the electronics at the metal centre. Elemental analysis and atomic absorption spectrometry (AAS) rather suggested $[Re_2(\mu\text{-}OH)(\mu\text{-}Br)(NCCH_3)_4(CO)_4] \cdot 3H_2O$ (figure 26) then $[Re_2(\mu\text{-}OH)_2(NCCH_3)_4(CO)_4]$ as was expected.

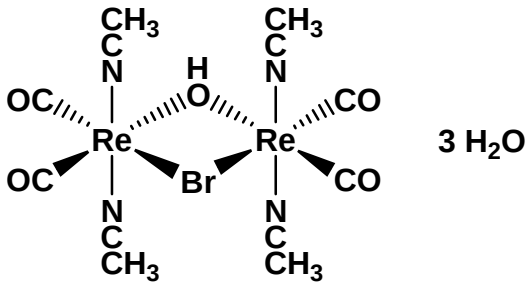

Figure 26: Suggested composition according elemental analysis and atomic absorption spectrometry of the product obtained by alkaline titration. Elemental analysis: (Found: C, 17.8; H, 2.3; N, 7.1. Calc. for $C_{12}H_{19}BrN_4O_8Re_2$: C, 18.02; H, 2.39; N, 7.01); AAS (1000 ppm in 0.2 M HNO_3) 45% rhenium, no sodium. Calc. for $C_{12}H_{19}BrN_4O_8Re_2$: 46.57%.

The structure of this hydrolysis product remains elusive since fast atom bombardment-mass spectrometry (FAB-MS) gave no further indication about the composition and it was not possible to grow crystals. The main conclusion of the observed behaviour for the potential application of **1** is, that with the substitution of the two Br^- by solvent molecules, **1** can be used as a reactive starting material for the synthesis of various complexes. While working in water, the pH value should be neutral or just slightly basic to avoid the formation of μ-OH bridged complexes.

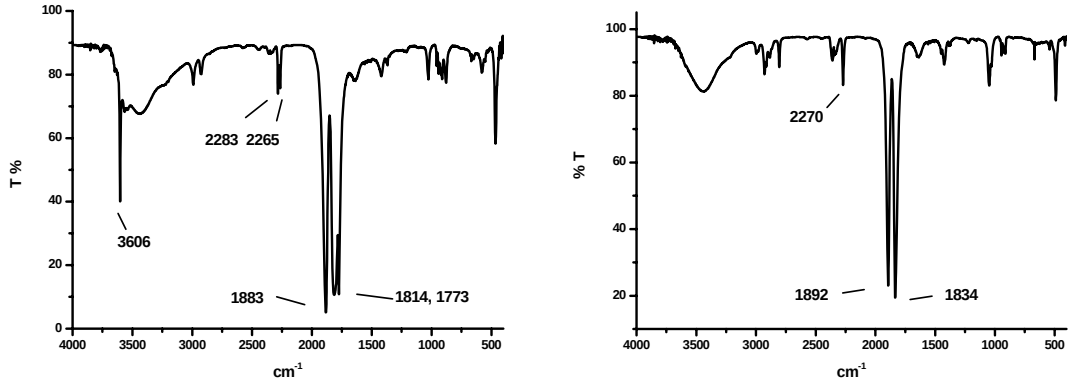

Figure 27: IR spectra of the hydroxy product (left) and the methoxy product (right).

To obtain more information, the same reaction was performed with NaOMe. Very frequently, structurally similar complexes with μ-OH and μ-OCH_3 exist. The reaction gave again a precipitate the infrared spectrum of which (figure 27, right) displays two sharp bands for the carbonyl stretching frequencies with the same small redshift to lower wavenumbers. The change to Na[OCH_3] did not improve the solubility of the resulting complex and it was not possible to obtain more structural information.

To grow crystals, the following techniques were used (figure 28): Standard vapour diffusion technique with ammonia as a volatile base and an aqueous solution of **1** proceeded to fast and amorphous precipitates formed. The layering of an aqueous solution of **1** with a cache layer of water and a NaOH solution did not change the rate of diffusion and reaction. As a final attempt, a gel crystallisation was set up, where the

different ions counter diffuse from two reservoirs slowly and should crystallise in the gel[75] but neither crystals nor precipitate could be detected.

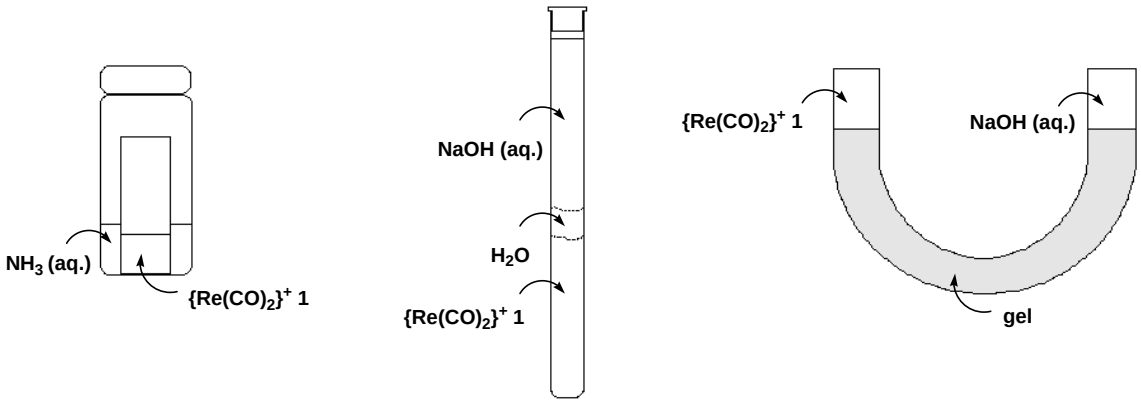

Figure 28: Three crystallisation set-ups for growing single crystals: vapour diffusion (left), layering (middle), gel crystallisation (right).

3.9.2. Reactivity of $(Et_4N)[ReBr_2(NCCH_3)_2(CO)_2]$ with CO

Many carbonyl complexes are synthesised by carbonylation with CO gas at medium to high pressure or by decarbonylation of binary carbonyl complexes. The direct synthesis of *cis*-$\{Re(CO)_2\}^+$ complexes either by decarbonylation of $\{Re(CO)_3\}^+$ or carbonylation of high valent starting materials was not successful (see chapter 3.7. and 3.8.). Since the Re(I) centre in $[Re(OH_2)_2(NCCH_3)_2(CO)_2]^+$ is of the soft type and the two water ligands are labile, reactivity of **1** with CO could be expected. Thermodynamic considerations implied that the carbonylation of *cis*-$\{Re(CO)_2\}^+$ should lead to a *facial* coordination after binding a third CO. Theoretical calculations showed, that the *fac*-$[Re(OH_2)_3(CO)_3]^+$ is by 103.8 kJ mol^{-1} more stable than the corresponding *meridional* isomer.[76] The comparison of the analogous technetium compounds with *cis*-$[Tc(CO)_2(OH_2)_4]^+$ is shown in figure 29. The *cis*-$[Tc(CO)_2]^+$ is by 18.1 kJ mol^{-1} more stable than *mer*-$[Tc(CO)_3]^+$ but by 91 kJ mol^{-1} less stable than *fac*-$[Tc(CO)_3]^+$.[77]

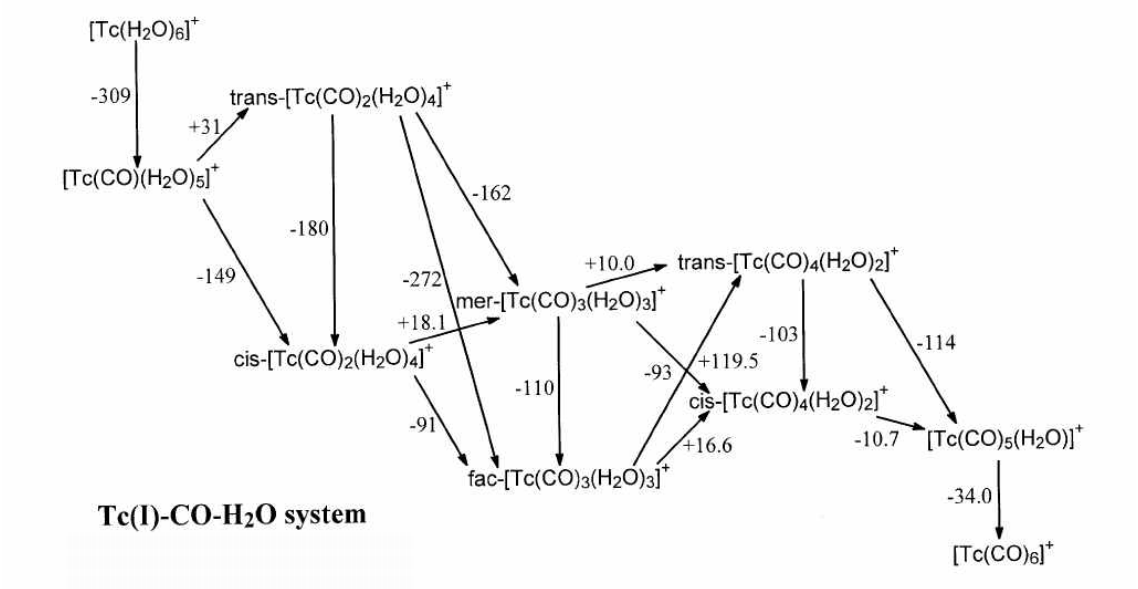

Figure 29:[77] Reaction network diagram on the $[Tc(CO)_i(OH_2)_{6-i}]^+$ system. ΔG in kJ mol^{-1}.

Several reactions of **1** in water with CO were performed. The CO pressure was stepwise increased and the reaction followed by IR spectroscopy. Passing CO through an aqueous solution of **1** caused no change in the carbonyl stretching frequencies in the liquid IR spectrum. A new band was growing in when 2 bar of CO in a small autoclave for 16 hours were applied. No precipitation occurred. Evaporating to dryness and washing the crude product with water gave a small amount of a colourless powder. The IR-bands indicated a *mer*-$[Re(CO)_3]^+$ species (figure 30). Applying 40 bar of CO gave a colourless powder of *mer*-$[ReBr(NCCH_3)_2(CO)_3]$ (**2**) in 80% yield as a precipitate. An overview of the experiments is given in table 9.

Table 9: Summary of the experiments of **1** with CO.

set up	time	$\nu_{(CO)}$ [cm^{-1}] (liq.)	. $\nu_{(CO)}$ [cm^{-1}] (KBr)	result	compound
1 in H_2O		1929, 1837	1893, 1794	-	-
atm CO	16 h	no change	-	-	**1**
2 bar CO	16 h	1972, 1929, 1837	2065, 1954, 1887, 1827	solution	traces of **2**
20 bar CO	16 h	-	2065, 1954, 1887, 1827	40% precipitate	**2**
40 bar CO	16 h	-	2065, 1954, 1887, 1827	80% precipitate	**2**

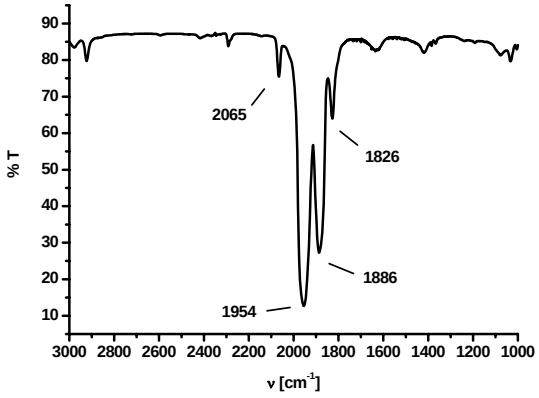

Figure 30: Typical IR spectrum (KBr) of a *meridional* tricarbonyl species, representing complex **2**.

Complex **2** is one of the relatively rare *mer*-$[Re(CO)_3]^+$ complexes. The neutral complex **2** is only soluble in CH_2Cl_2, chloroform or THF but insoluble in water and alcohol. Single crystals were obtained by diffusing cyclohexane into a THF solution of **2**. Complex **2** crystallised in the uncommon space group I2/*m*. A presentation of the structure is shown in figure 31. The asymmetric unit consists of a "L" formed by one acetonitrile, the rhenium atom and a disordered carbonyl and bromide. The full complex was generated by a two-fold axis and a mirror plane perpendicular to the two-fold axis. Therefore, the rhenium centre possesses perfect octahedral geometry.

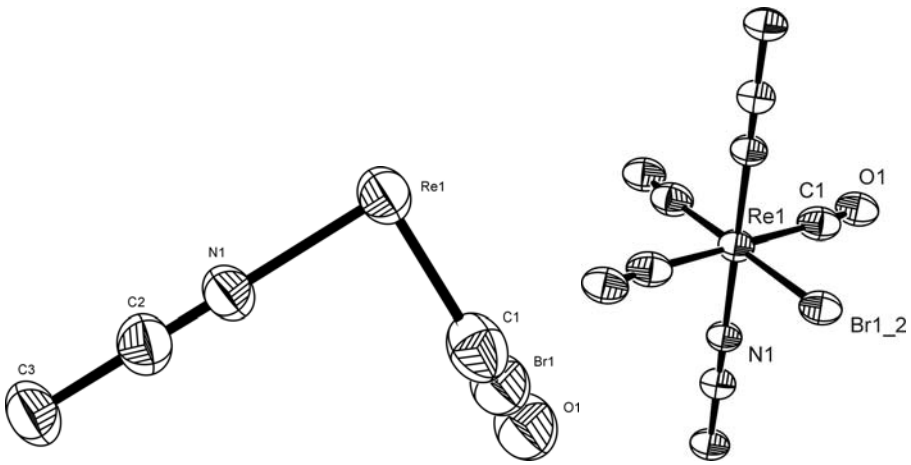

Figure 31: ORTEP plot of the asymmetric unit and the whole complex **2** (Ellipsoids are drawn at 50% probability and hydrogen atoms are omitted for clarity). The Re(1)-N(1) bond length is 2.087(8) Å

In fact, the formation of the thermodynamically unfavoured *meridional* complex clearly emphasised the importance of the strongly bound acetonitrile ligands. Although the facial geometry would be preferred, the acetonitrile ligands were not replaced. This observation will be important for ligand exchange reactions as outlined later. Immediate precipitation from water might be another reason why the unfavoured *meridional* complex did not convert to the more stable *facial* complex.

As a consequence of the strong *trans*-effect of the carbonyl ligands, the release of one CO is very likely and heating to reflux in acetonitrile yielded again the precursor complex **1a**. As will be shown later, it was an advantage for substitution reactions to start from the *mer*-$\{Re(CO)_3\}$ **2** because no separation of $(Et_4N)Br$ was needed. The only side product was free CO evolving from the solution.

3.10. Ligand substitution reactions with $(Et_4N)[ReBr_2(NCCH_3)_2(CO)_2]$ and *mer*-$[ReBr(NCCH_3)_2(CO)_3]$

To yield biologically interesting compounds, substitution reactions are the base to explore the reactivity of **1** or **2** with different kind of ligands. As is known from the chemistry with $[ReBr_3(CO)_3]^{2-}$, aliphatic amines and anions such as carboxylates coordinate only weakly to the metal centre.[73] However, aromatic amines show a fast complex formation and excellent thermodynamic and kinetic stability. For the chemistry of **1**, similar binding properties were predicted, since both, **1** and $[ReBr_3(CO)_3]^{2-}$, have similar properties in solution and are of equal oxidation state. Ligands of interest depend on their later purposes of application. For bioinorganic chemistry, the reactions with imidazole or amino acids as model ligands for naturally occurring biomolecules are of interest. If stable complexes with imidazole are formed, substituted imidazole ligands such as benzimidazole, purine bases like adenine or guanine can be studied. The cytotoxicity of Re(I) carbonyl complexes may involve binding to DNA bases after replacement of the labile ligands.[78, 79] Such a *cis*-platin like inter- or intrastrand crosslink causes replication arrest and cell death.[80] To mimic guanine in its natural appearance in DNA, 9-ethylguanine acts as a model. For photochemical purposes, conjugated heterocyclic aromatic systems such as bipyridine (bpy) and phenanthroline derivatives are relevant. These aromatic systems may allow metal to ligand charge transfers (MLCT), generating formally Re(II) complexes after charge transfer, which can potentially be reductively quenched.[28, 81, 82] Finally for labelling purposes mixed (N,O), (N,N,O) chelators such as 2-pyridinecarboxylic acid (2-pic) are of interest. Since the chemistry of substitution reactive complexes with the *cis*-$\{Re(CO)_2\}^+$ moiety is not very well explored, a comparison with the chemistry of *fac*-$\{Re(CO)_3\}^+$ is highly interesting.

3.10.1. Synthesis of complexes with ligands comprising the imidazole motif

It was previously shown in aqueous solution that a stepwise complexation by imidazole stops after the addition of two equivalents, yielding the complex $[ReBr(CO)_3(imz)_2]$.

Even excess imidazole did not result in the formation of $[Re(CO)_3(imz)_3]^+$ but the neutral complex $[ReBr(CO)_3(imz)_2]$ was the end product.[73]

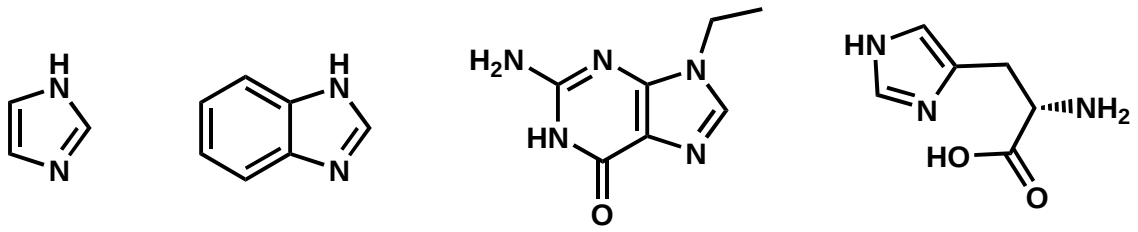

Figure 32: Imidazole and imidazole like ligands used in this work.

As discussed above, solvent molecules like water or methanol substituted the two Br^- in trans positions to the CO ligands in **1**. When **1** was heated to reflux in the presence of excess imidazole, the disubstituted product $[Re(NCCH_3)_3(CO)_2(imz)_2]Br$ (**3**) formed in 63% yield. Stepwise addition of imidazole (figure 33), revealed the stepwise formation of first the monosubstituted $[Re(NCCH_3)_2(OH_2)(CO)_2(imz)]^+$ and then the disubstituted product **3**. The reaction is irreversible and no re-coordination of Br^- and the formation of a neutral complex$[ReBr(NCCH_3)_2(CO)_2(imz)]$ was not observed.

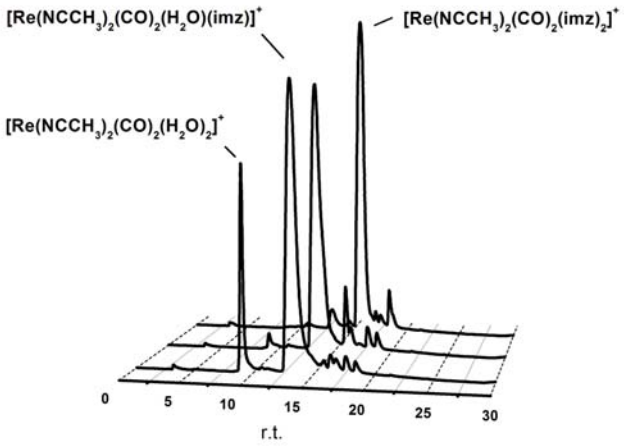

Figure 33: Stepwise coordination of imidazole to **1** analytically followed by HPLC.

Complex **3** is kinetically inert against further substitution. A ^{1}H-NMR challenge experiment with an excess of 1-methylimidazole over 6 h at RT and for 1 h at 50° C in

MeOD showed no change in the chemical shifts of the imidazole protons (figure 34) indicating that imidazole was not exchanged for 1-methylimidazole. The signal at 7.91 ppm is assigned to Hc_1 of coordinated imidazole and the one at 7.59 ppm to Hc_2 of the free 1-methylimidazole. The Hc proton of free imidazole would have a chemical shift at 7.66 ppm.

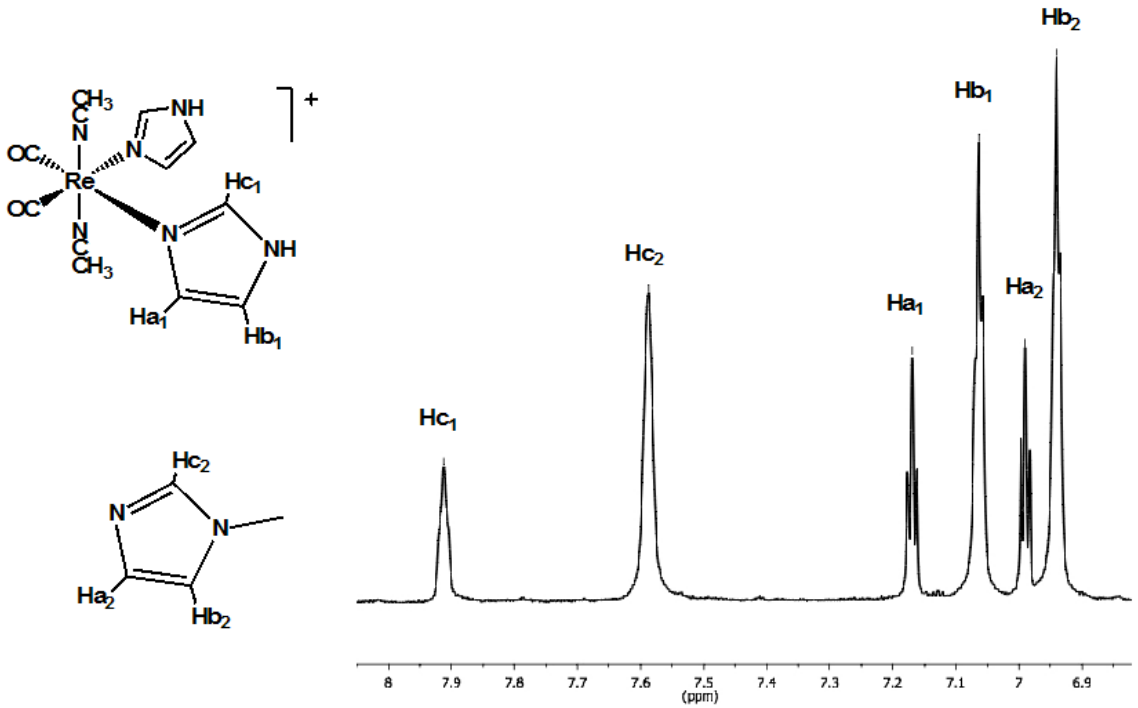

Figure 34: Challenge experiment of **3** with 1-methylimidazole.

Single crystals were obtained by diffusing hexane in a methanol solution of **3**. Complex **3** crystallised in the monoclinic spacegroup $P2_1/c$ as colourless needles. The structure in figure 35 shows an almost perfect octahedral geometry. Beside the N(3)-Re(1)-N(4) angle (83.05(18)°) between the sterically more demanding imidazole ligands the bond angles are all between 86.5° and 96.5°. The Re(1)-N(1,2) bond length are with 2.061(5) and 2.063(5) Å slightly shorter as in **1a** (2.073(5), 2.075(5)) and the Re(1)-N(3,4) is of 2.198(5) and 2.200(5) Å.

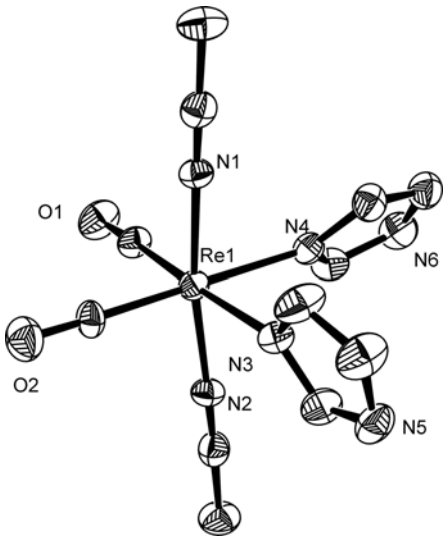

Figure 35: ORTEP plot and selected bond lengths of complex **3** (Ellipsoids are drawn at 50% probability, hydrogen atoms and the counter ion are omitted for clarity). Selected bond length are for [Å]: Re(1)-N(1) 2.061(5); Re(1)-N(2) 2.063(5); Re(1)-N(3) 2.200(5); Re(1)-N(4) 2.198(5).

The reaction with benzimidazole (bzimz), was also straightforward and gave the corresponding complex $[Re(NCCH_3)_2(CO)_2(bzimz)_2]Br$ (**4**). Single crystals could not be obtained but all other analytical methods such as elemental analysis and mass spectroscopy confirmed the authenticity of **4**.

Whereas the reactions with imidazole-based ligands were relatively rapid, the reaction with 9-ethylguanine (9EtG) was very slow. In solution, one 9EtG ligand of the two-fold substituted product $[Re(NCCH_3)_2(CO)_2(9EtG)_2]^+$ is in equilibrium with solvent molecules based on the sterical hindrance of the two bulky ligands detected by HPLC (figure 37). Nevertheless, single crystals of the di-substituted product $[Re(NCCH_3)_2(CO)_2(9EtG)_2]Br$ (**5**) were obtained by diffusing hexane in a methanol solution of the crude product.

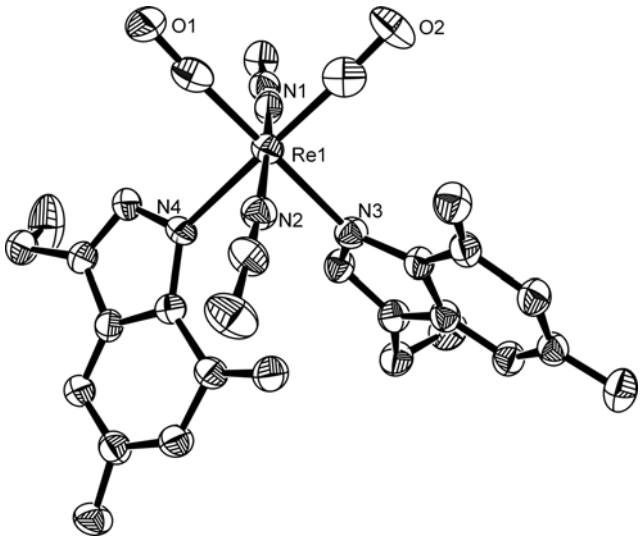

Figure 36: ORTEP plot of complex **5** (Ellipsoids are drawn at 50% probability, hydrogen atoms and the counter ion are omitted for clarity). Selected bond length are for [Å]: Re(1)-N(1) 2.072(6); Re(1)-N(2) 2.077(5); Re(1)-N(3) 2.204(5); Re(1)-N(4) 2.233(5).

5 crystallised in the monoclinic space group $P2_1/n$ as colourless plates. The structure is shown in figure 36. The Re–N(4) bond length with 2.233(5) Å is quite long as compared with Re–N(3) 2.205(5) in **5** or other imidazole-containing $[Re(CO)_2]^+$ complexes (table 10). The corresponding $[Re(OH_2)(CO)_3(9MeG)_2]^+$ complex (**5a**)[83] with 2.212(13) and 2.186(13) shows shorter Re–N bond length than **5**. This fact confirmed the lability of one of the 9EtG ligands. In order to act cytotoxic by cross-linking DNA-strands, a two-fold coordination of DNA bases to **1** is necessary. The lability of one 9EtG ligand in **5** may provide an influence of the topology of DNA.

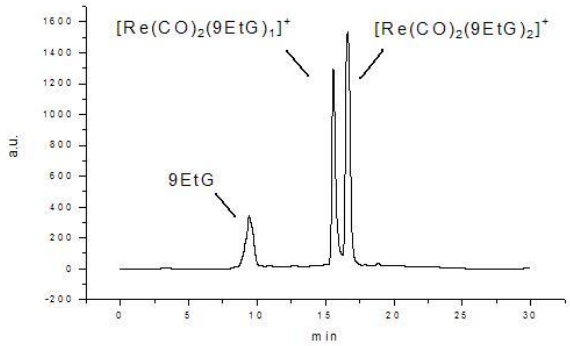

Figure 37: The HPLC-trace of single crystals of **5** dissolved in methanol shows an equilibrium between the mono- and disubstituted complexes $[Re(NCCH_3)_2(CO)_2(9EtG)(sol)]^+$ and $[Re(NCCH_3)_2(CO)_2(9EtG)_2]^+$.

As obvious from the reaction with 9EtG, complex **1** can bind up to two nucleobases. This is attractive, since a *cis*platin like interaction with DNA can be expected providing that G binding is stable or robust enough. Thus, we performed gel mobility shift assays, which can demonstrate the topological changes in DNA. The study of metal-DNA binding and of the changes induced by metal complexes on the tertiary structure of DNA by this technique is well established.[84-86] Different Pt and Ru complexes, for example, cause unwinding of supercoiled (sc) or winding of open circular (oc) plasmid DNA. These structural changes can be observed on the gel matrix. Unwinding of sc plasmid DNA for example causes relaxation of the DNA molecule and, consequently, the frictional force between DNA and the gel matrix during electrophoresis increases. Thus, the band corresponding to the DNA-metal adducts moves relatively slower than the one of native sc DNA. The opposite is true if a metal complex causes winding of oc plasmid DNA. In this case winding of oc DNA renders the molecule more compact, the frictional force is reduced and the band of the corresponding DNA-metal adduct moves relatively faster.

It has been described that *fac*-$[ReBr_3(CO)_3]^{2-}$ has a sc-effect on plasmid DNA (ΦX174 pDNA).[79] $[ReBr_3(CO)_3]^{2-}$ and **1a** were incubated at different concentrations with ΦX174 plasmid DNA (5 nM) for 22 h at 37° C. The gel mobility shift assay showed (figure 38) that **1a** had no supercoiling effect on the plasmid DNA (figure 38). The lability of the second DNA base in complex **5** was too distinct to cause a cross-link of plasmid DNA with **1a** and a single coordination did not induce a structural change.

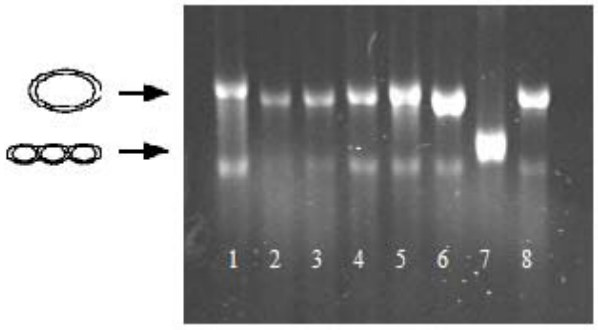

		complex concentration
1	pDNA	
2	pDNA + **1a**	$6.6 \cdot 10^{-7}$ M
3	pDNA + **1a**	$6.6 \cdot 10^{-6}$ M
4	pDNA + **1a**	$6.6 \cdot 10^{-5}$ M
5	pDNA +$[ReBr_3(CO)_3]^{2-}$	$6.6 \cdot 10^{-7}$ M
6	pDNA +$[ReBr_3(CO)_3]^{2-}$	$6.6 \cdot 10^{-6}$ M
7	pDNA +$[ReBr_3(CO)_3]^{2-}$	$6.6 \cdot 10^{-5}$ M
8	pDNA	

Figure 38: Gel mobility shift assay of 5 nM ΦX174 pDNA incubated with either **1** or $[ReBr_3(CO)_3]^+$ for 22 h at 37° C.

The reactions with 4 eq. imidazole and *mer*-[ReBr(NCCH$_3$)$_2$(CO)$_3$] **2** in THF, resulted in a colourless precipitate. According to the carbonyl stretching frequencies of 1910 and 1819 cm^{-1} in the IR spectrum support the formation of a {Re(CO)$_2$}$^+$ complex. Elemental analysis, proton NMR and mass spectrometry confirmed a neutral complex [ReBr(NCCH$_3$)$_2$(CO)$_2$(imz)] (**6**). Single crystals were obtained by diffusing hexane into a methanol solution of **6**, which crystallised in the monoclinic space group P2$_1$/*n* as colourless needles. The structure is shown in figure 39. The Re-N(3) bond length of the imidazole is with 2.200(4) Å in the same range as the other imidazole complexes (table 10). The formation of the monosubstituted complex **6** was a consequence of the solvent THF forcing a precipitation of the neutral complex whereas starting from **1** in water or methanol, the ionic complexes **3, 4** with two imidazole ligands was formed.

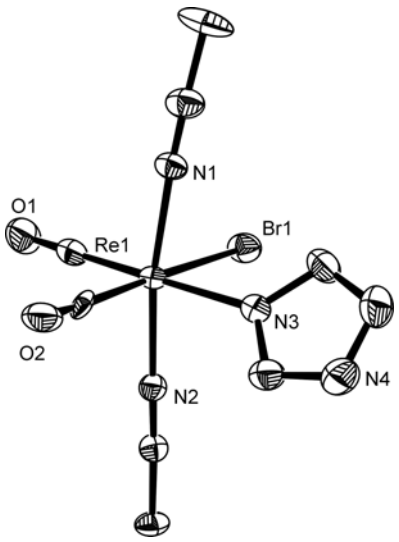

Figure 39: ORTEP plot of complex **6** (Ellipsoids are drawn at 50% probability and hydrogen atoms are omitted for clarity). It shows a disorder of Br(1) and C(2)-O(2) with a 96:4 ratio. Selected bond length are [Å]: Re(1)-N(1) 2.063(3); Re(1)-N(2) 2.064(3); Re(1)-N(3) 2.200(4).

The carbonyl stretching frequencies of all the imidazole or imidazole-like complexes (see table 10) are in the same range. The ligands comprising the imidazole moiety had minor influence on the electron density at the metal centre. The carbonyl stretching frequencies are slightly shifted to higher wavenumbers compared to **1**, since the imidazole moiety has electron-accepting capability as compared to Br$^-$. The symmetric vibrations are within 7 cm^{-1}, which is not unexpected considering the similarity of the ligands.

Table 10: Re-N bond length and carbonyl stretching frequencies of rhenium carbonyl complexes with imidazole like ligands.

	Re – N(3/4) distance [Å]		IR $\nu_{(CO)}$ [cm^{-1}]	
5a[83]	2.186(13)	2.212(13)	-	-
3	2.198(5)	2.200(5)	1916	1827
5	2.205(5)	2.233(5)	1917	1834
4	-	-	1918	1829
6	2.200(4)		1911	1820

As another imidazole containing ligand, L-histidine was reacted with **1** to study the interaction of **1** with amino acids. A binding to **1** via the imidazole-, amine- and carboxylate group would cause a substitution of an acetonitrile ligand and yield a neutral complex. The HPLC of the reaction of **1** with 1.1 eq. of the imidazole comprising L-histidine showed after 19 h stirring the pattern shown in figure 40 (left side). The addition of another 1.1 eq. did not induce any further change. Peak a) corresponds to be the starting material $[Re(NCCH_3)_2(OH_2)_2(CO)_2]^+$. Peaks b) and c) were collected and both analysed by MS. The two spectra showed the same peak patterns only different in intensity. Two main signals each with a typical Re-isotope pattern were observed (figure 40, right). The one with the ratios m/z = 477/479 was assigned to $[Re(NCCH_3)_2(CO)_2(his)]^+$ ($[M]^+$), the other one with m/z = 436/438 to $[M-CH_3CN]^+$.

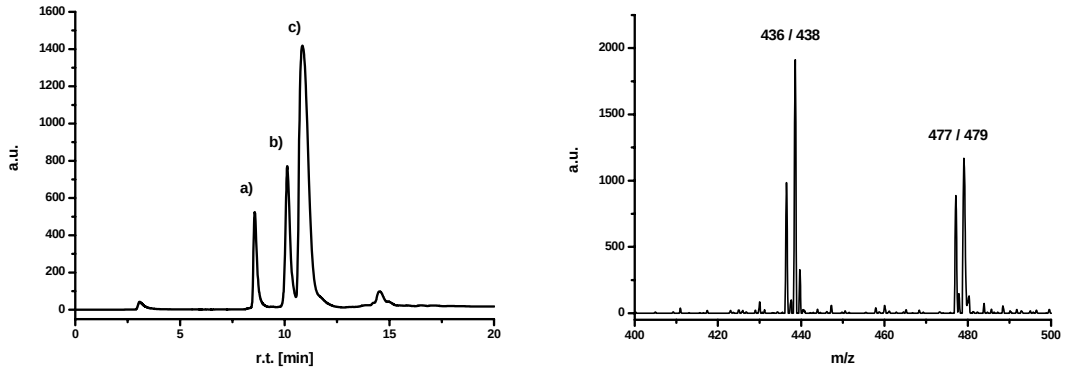

Figure 40: HPLC trace (left) and corresponding ESI-MS spectra (right) of the reaction of **1** with histidine.

It is likely that only bidentate coordination of the tridentate ligand took place. Coordination of the imidazole-nitrogen is favoured due to the stronger binding of aromatic amines to Re(I) carbonyl complexes as compared to the other functional groups. The amine and carboxylate function are in competition to each other resulting in two possible conformations as shown in figure 41, which also explains the two bands in HPLC (figure 40). The amine coordination (N,N-adduct, cationic complex) forms a six-membered ring while oxygen coordination (N,O-adduct, neutral complex) results in a less favoured seven-membered ring. The two products could not be separated due to very similar solubility in all solvents.

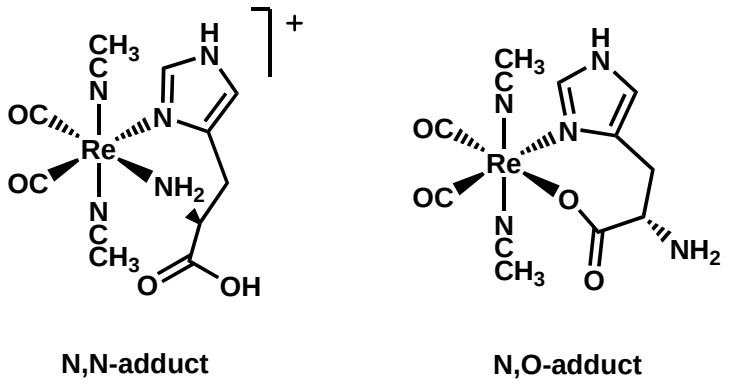

Figure 41: The two most likely coordination modes of histidine to **1**.

The reaction of two equivalents of histidine at 60° C for 4 days gave one major rhenium product according to HPLC with the retention time similar to the later peak in figure 40. The IR spectrum of the crude product showed CO stretching frequencies at 1916 and

1828 cm^{-1}. These frequencies are similar to the other imidazole containing complexes, which is again in line with the assumed coordination via the imidazole.

In summary, imidazole and imidazole containing ligands strongly coordinated to the *cis*-$\{Re(CO)_2\}^+$ moiety. The coordination occurred exclusively in *trans* position to CO whereby bromide or the solvent molecules respectively at these positions, were substituted. Replacing the acetonitrile ligands was not possible even with excess of ligands and at higher temperatures. Denticity of the ligands did not influence this behaviour since even the strong tridentate amino acid histidine did not afford a threefold substitution. Taking all these facts into account, it makes more sense to consider **1** or **2** as a source for complexes with the $\{Re(NCCH_3)_2(CO)_2\}^+$ core then with $\{Re(CO)_2\}^+$.

3.10.2. Synthesis of complexes with α,α'-diimine and terpyridine ligands

Due to favourable photophysical properties such as room-temperature luminescence and tuneable metal-ligand charge transfer (MLCT) excited states, complexes of the type $[ReX(diimine)(CO)_3]$ have been applied in solar-energy conversion schemes. The corresponding bpy and phd complexes were studied for photocatalytic activity like CO_2 → CO conversion.[26-30] It was mentioned that in general, $[ReX(diimine)(CO)_3]$ complexes showed catalytic activity when exhibiting fluorescence, whereas nonfluorescing compounds did not convert CO_2 to CO.[32] The correlation of catalytic activity and spectroscopic or electrochemical properties is difficult so that we restricted our studies on absorption and emission spectra and determination of the redox potential for the two complexes formed with bpy and phd.

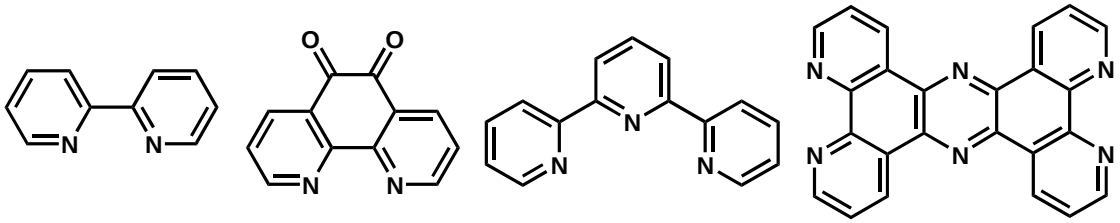

Figure 42: α,α'-diimine ligands used for photochemical investigations.

The terpyridine ligand is one of the most widely used polyaromatic heterocycle in photochemistry. We were interested in the question if a *meridional* coordination with **1** was possible. As mentioned before, the acetonitrile ligands could not be replaced so far by tridentate ligands. Since terpy is a very strong ligand, exchange of the acetonitrile ligands in **1** could occur or, alternatively, only a two fold *cis*-coordination would be possible as found in other systems.[87-90] Starting from such *cis*-coordinated complexes, a *meridional* coordination of the terpy-ligand is only possible under harsh conditions. It is known from literature (see scheme 16, top) that heating up $[ReBr(CO)_3(terpy)]$ in a sealed tube to 240° C for 5 h, one CO ligand is replaced by the terpy which coordinates as a tridentate ligand under formation of *mer*-$[ReBr(CO)_2(terpy)]$.[87] When heating the *trans-cis*-$[RuI_2(CO)_2(terpy)]$ complex in boiling tetrachloroethane (b.p. 146.5° C), the *meridional* coordination of the terpyridine ligand causes the evolving of one more CO to get a monocarbonyl complex $[RuI_2(CO)(terpy)]$ (scheme 16, bottom).[88] Due to the strongly bounded acetonitrile ligands, such a decarbonylation reaction of **1** with terpyridine would also be possible and result in a Re(I)-monocarbonyl complex.

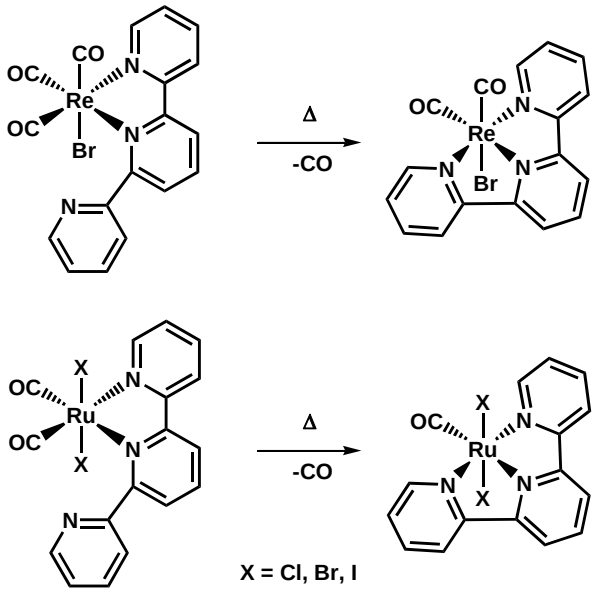

Scheme 16: Cleavage of CO from Re(I) and Ru(II) complexes as caused by *meridional* coordination of the terpyridine ligand.[87, 88]

A few $[Re(CO)_2(diimine)]^+$ complexes are known using phosphines or extremely harsh conditions.[56] Several $[Re(CO)_2(P\text{-}P)(N\text{-}N)]^+$ complexes showed promising results in

photochemical applications due to their long-lived excited-state lifetimes and high quantum yields. $[Re(CO)_2(bpy)_2]^+$ was obtained by melting bpy together with $[Re(CO)_3(bpy)(F_3CSO_3)]$.

3.10.3. Complexes with bipyridine and phenathroline-derivatives as ligands

The aromatic amine ligands 2,2'-bipyridine (bpy) and 7,7'-phenanthroline-dione (phd) ligands reacted with **1** within 16 hours in acetonitrile at RT, forming the corresponding complexes $[Re(NCCH_3)_2(bpy)(CO)_2]Br$ (**8**) and $[Re(NCCH_3)_2(CO)_2(phd)]Br$ (**9**) in 83% and 70% yield respectively. Recrystallisation from ethanol/hexane gave the analytically pure products with ν_{CO} of 1926, 1853 and 1835 cm^{-1} for **8** and 1933 and 1850 cm^{-1} for **9**. Due to the delocalisation of the electron density over the aromatic system, the carbonyl stretching frequencies are blue-shifted by approximate 30 cm^{-1} compared to **1**. The UV/VIS spectra reveal typical MLCT absorption bands at 423 nm (ε = 3000 l mol^{-1} cm^{-1}) for complex **8** and at 420 nm (ε = 5200 l mol^{-1} cm^{-1}) for complex **9** (figure 43). Both complexes did not show luminescence as compared to $[ReBr(CO)_3(bpy)]$ and $[ReBr(CO)_3(phd)]$ under the same conditions (1 mM in DMF under argon at RT).

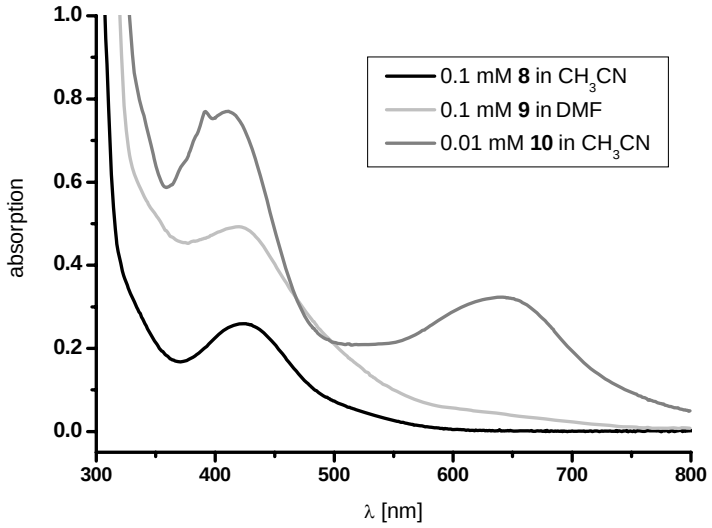

Figure 43: Absorption spectra of **8, 9** and **10** in the visible range.

The reaction of **1** with 7,7'-phenanthroline-diamine (pham) in methanol led to a dark green complex formulated as $[Re(NCCH_3)_2(CO)_2(pham)]Br$ (**10**) according to

spectroscopic and elemental analysis. No fluorescence could be observed but a much stronger extinction in the visible range at 412 nm (ε = 26100 l mol^{-1} cm^{-1}) and at 641 nm (ε = 113000 l mol^{-1} cm^{-1}) respectively.

8 crystallised from EtOH/hexane in the monoclinic space group $P2_1/c$ as red needles and showed a coordination of the bpy ligand again in *trans* position to the carbonyl ligands (figure 44). **9** crystallised under the same conditions in the monoclinic space group $P2_1/n$ as a red block and showed the same feature like **8** with a slightly bended acetonitrile ligands due to crystal packing.

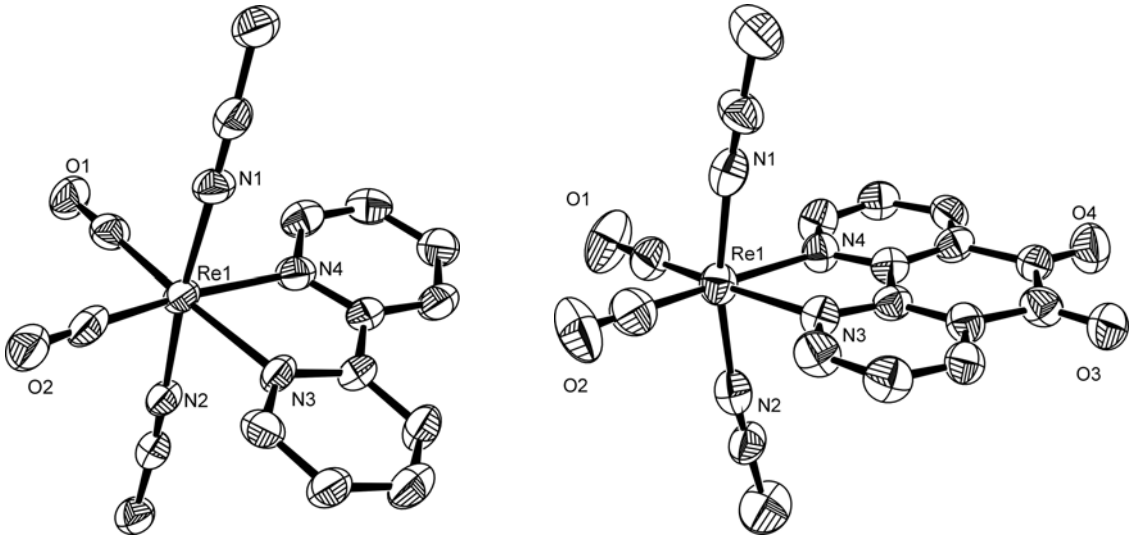

Figure 44: ORTEP plot of complexes **8** and **9** (Ellipsoids are drawn at 50% probability, hydrogen atoms and counter ions are omitted for clarity). Selected bond length are [Å]: **8**; Re(1)-N(1) 2.073(8); Re(1)-N(2) 2.083(8); Re(1)-N(3) 2.192(7) Re(1)-N(4) 2.180(8); **9**; Re(1)-N(1) 2.064(15); Re(1)-N(2) 2.091(15); Re(1)-N(3) 2.189(12); Re(1)-N(4) 2.181(12).

Changing to the *mer*-$Re(CO)_3$ **2** as the starting material, the reaction with bpy or phd in THF proceeded much faster and within 30 min the pure complexes **8** and **9** precipitated from solution. Since only CO formed during the reaction, no purification was necessary and the complexes were received in an analytically pure form.

The ^{1}H-NMR spectrum of **8** and **9** showed one signal for the acetonitrile ligands in both complexes. Four aromatic proton signals in complex **8** and three aromatic proton signals

in complex **9** would be expected based on symmetry considerations. This was confirmed in the spectrum of **8** (figure 45), which shows four signals between 7.6 and 9.2 ppm. Two doublets at 9.1 and 8.6 ppm of the protons A, A' and D, D' and two multiplets at 8.3 and 7.7 ppm for B, B' and C, C'.

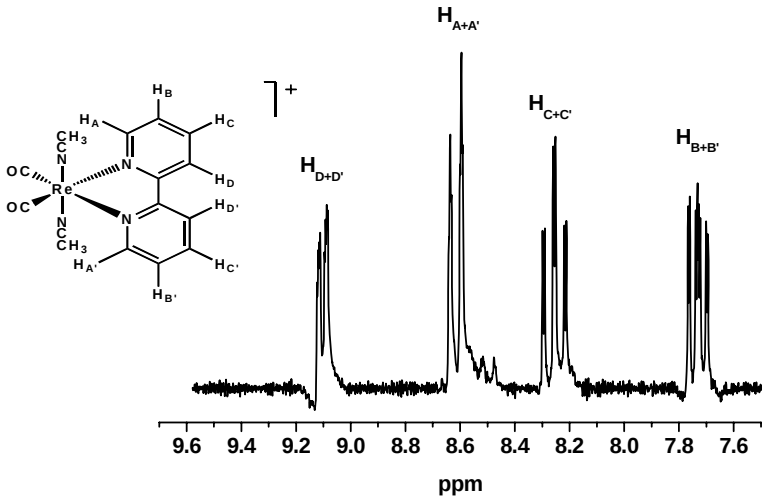

Figure 45: Aromatic proton signals in the ^{1}H-NMR (200 MHz) of complex **8** in CD_3OD.

As well, the ^{1}H-NMR spectrum of **9** in dmso-d6 shows three signals for the aromatic protons (figure 47). Measuring in MeOD, this clear picture was not received. The spectrum in figure 46 shows four sets of aromatic protons. Based in the fact that CO and $NCCH_3$ are very tightly bound, isomerisation is unlikely. Indeed other analyses such as HPLC and IR indicated one single product. The composition $[Re(NCCH_3)_2(CO)_2(phd)]Br$ was confirmed by elemental analysis. A change in the NMR spectra was furthermore not observed even after exposing the NMR sample to daylight for 3 days. Since in mass spectrometry peaks at m/z = 615 $[M+1]^+$, 599 $[M - Br + 2\ MeOH]^+$ and 567 $[M - Br + MeOH]^+$ were detected, acetal or semiacetal formation is most likely.

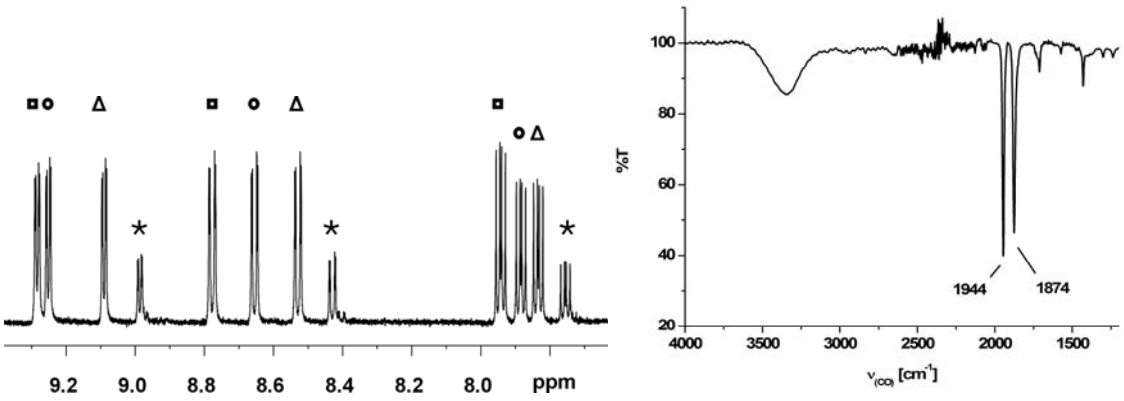

Figure 46: The four sets of aromatic proton signals in the ^{1}H-NMR (500 MHz) of complex **9** in CD_3OD and the liquid IR spectrum of the NMR solution.

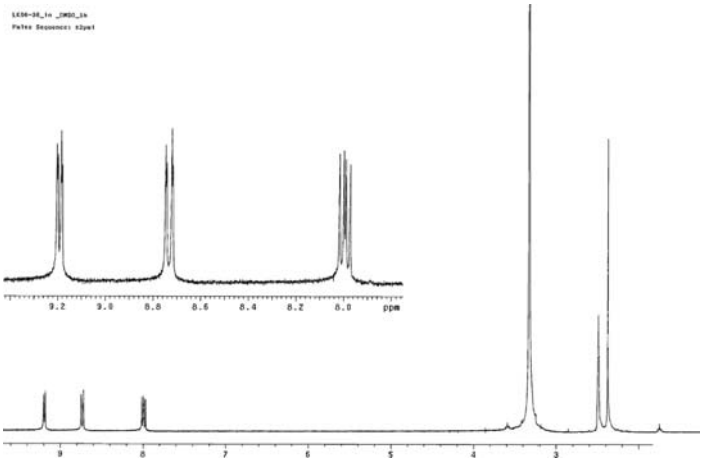

Figure 47: ^{1}H-NMR (300 MHz) of complex **9**, recorded as a dmso-d6 solution; δ_H 9.19 (dd, J = 5.4, 1.5 Hz, 2H), 8.73 (dd, J = 8.1, 1.5 Hz, 2H), 7.99 (dt, J = 5.4, 2.4 Hz, 2H), 2.38 (s, 6H).

Cyclic voltammetry of a 1 mM solution of **9** in DMF with 0.1 M $TBAPF_6$ as electrolyte showed two reversible one-electron reductions corresponding to the formation of the semiquinone and the hydroquinone. (figure 48). The reduction potentials $E°_{1/2}$ = -47 and -669 mV vs. Ag/Ag^+ were comparable with those found for the corresponding complex $[ReBr(CO)_3(phd)]$ with -15 and -755 mV.[29]

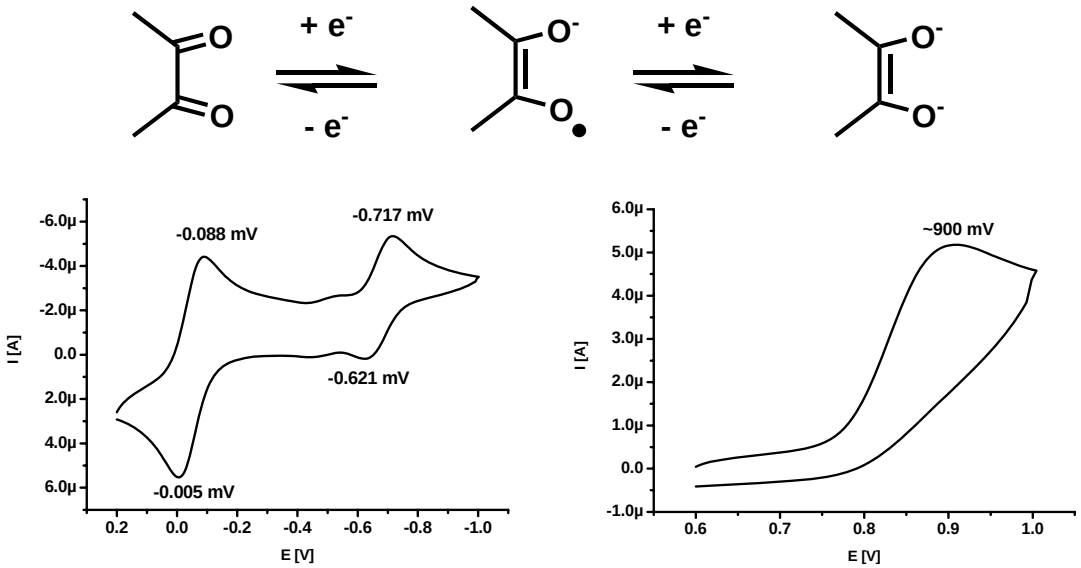

Figure 48: Cyclic voltammogram of complex **9** (1 mM in DMF; 0.1 M $TBAPF_6$) with two reversible one electron reductions at -47 and -669 mV (left) and an irreversible oxidation at around 900 mV (right) vs. Ag/Ag^+.

3.10.4. Synthesis of a dinuclear complex with tpphz as bridging ligand

The increasing interest in homo- and heterodinuclear ruthenium, osmium[91] and rhenium[28, 92] compounds originates mainly in their very intense metal to ligand charge transfer bands and favourable photostability which allows photoinitiated long distance energy transfer. Heterobimetallic catalysts also offer the possibility of tandem catalytic processes as in examples of site specific olefin polymerisation.[93, 94] The complex $[ReBr(CO)_3(tpphz)ReBr(CO)_3]$ (tpphz = tetrapyrido[3,2-a:2',3'-c:3'',2''-h:2''',3'''-j] phenazine) was directly accessible from tpphz and $[ReBr_3(CO)_3]^+$ by a reaction in toluene and showed intense fluorescence properties.[28]

The reaction of 2.1 equivalents of **1** with tpphz in acetonitrile resulted quantitatively in an orange/red precipitate with carbonyl stretching frequencies at 1932 and 1857 cm^{-1}, indicating a symmetric complex. Mass spectroscopy exhibited a signal at m/z = 517 with an isotope-pattern of two rhenium atoms assigned to $[Re_2(NCCH_3)_4(CO)_4(tpphz)]^{2+}$. The UV/VIS spectra reveal a typical MLCT absorption band at 430 nm (ε = 14000 l mol^{-1} cm^{-1}) but did not show luminescence. Crystallisation from acetone gave red plates of the complex $[Re_2(NCCH_3)_4(CO)_4(tpphz)]Br_2$ **11**.

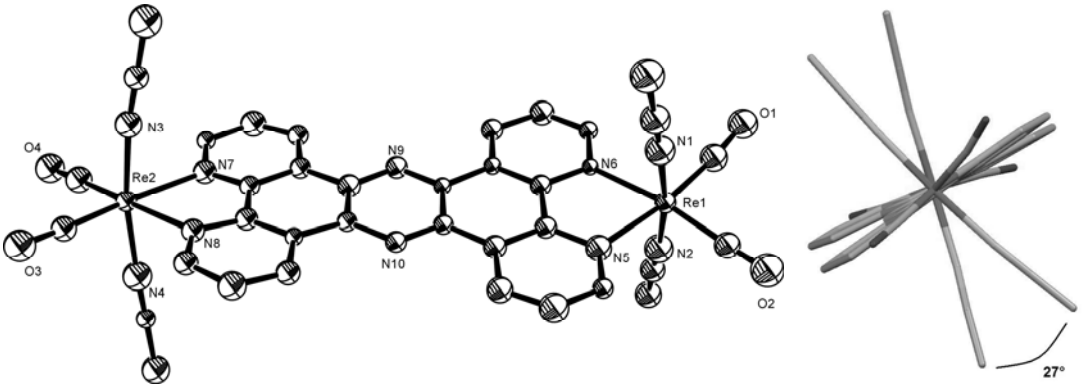

Figure 49: ORTEP plot and view along the Re(1)-Re(2) axis of complex **11** (Ellipsoids are drawn at 50% probability and hydrogen atoms and counter ions are omitted for clarity). Selected bond lengths are [Å]: Re(1)-N(1) 2.065(18); Re(1)-N(2) 2.084(18); Re(1)-N(5) 2.204(16); Re(1)-N(6) 2.178(13); Re(2)-N(3) 2.054(16); Re(2)-N(4) 2.074(18); Re(2)-N(7) 2.273(15); Re(2)-N(8) 2.220(15). The N(1)-Re(1)-Re(2)-N(3) torsion angle is 27°.

The structure of **11** is shown in figure 49. The bond lengths of Re(1) to the tpphz ligand are comparable with the one in complex **8** and **9** (2.17-2.20 Å) but the Re(2)-N(7) and the Re(2)-N(8) bond lengths are with 2.220(15) and 2.273(15) Å quite long even if the error is rather large. The Re(1)-Re(2) distance is 13.10 Å and looking along the Re(1)-Re(2) axis, the two moieties are twisted with a N(1)-Re(1)-Re(2)-N(3) torsion angle of 27°.

3.10.5. Synthesis of complexes with the terpyridine ligand

Due to the strong chelating effect, the reaction of **1** in H_2O with terpyridine is expected to yield a *meridional* coordination of the terpyridine ligand. A meridional coordination would require the substitution of two bromides and one CO or both acetonitrile ligands and one bromide. Starting with **1**, the reaction with terpyridine in water at 40° C led to the formation of one single product with a retention time of the rhenium complex shifted from initial 8.6 to 21.3 minutes in HPLC. After recrystallisation from acetone, $[Re(NCCH_3)_2(CO)_2(terpy)]Br$ (**12**) was obtained as an orange-red powder in 70% yield. Elemental analysis and mass spectrometry were in support of this composition. Single crystals of **12**, suitable for x-ray diffraction analysis, were obtained by slowly evaporating an acetone solution. The structure in figure 50 (left) shows two-fold coordination of the terpyridine ligand and the two acetonitrile ligands remained coordinated. Heating to reflux did not cause tridentate coordination of terpy and the *meridional* coordination could not be obtained. Harsher conditions in higher boiling

solvents or even in molten ligand were not helpful because **1** had limited solubility and decomposed at higher temperatures.

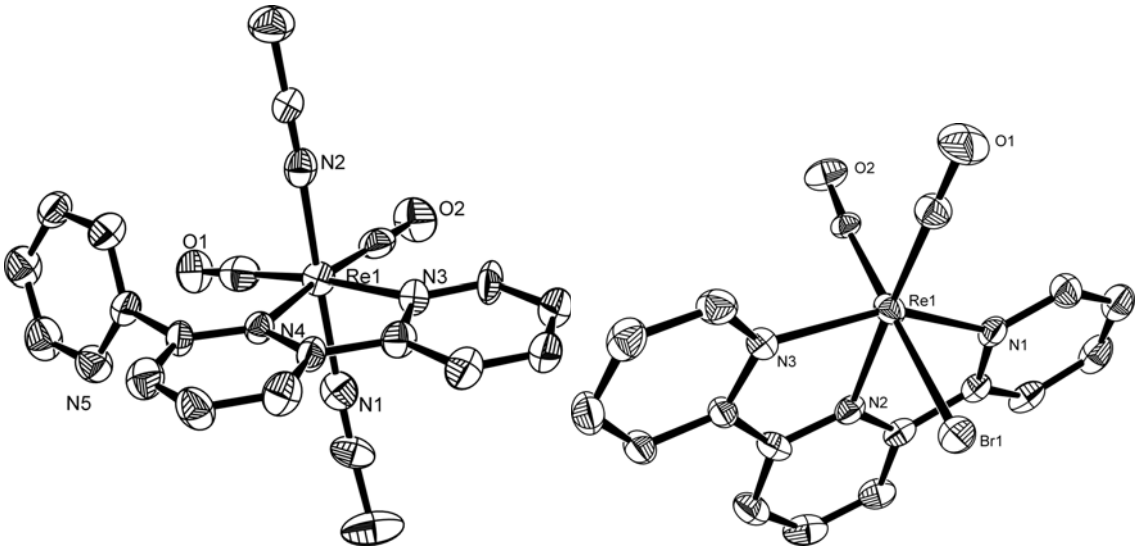

Figure 50: ORTEP plot of the two terpyridine complexes **12** and **12a** (Ellipsoids are drawn at 50% probability and hydrogen atoms and the counter ion in **12** are omitted for clarity). Selected bond lengths are [Å]: **12**; Re(1)-N(1) 2.066(14); Re(1)-N(2) 2.066(13); Re(1)-N(3) 2.164(11); Re(1)-N(4) 2.238(11); **12a**; Re(1)-N(1) 2.123(4); Re(1)-N(2) 2.085(4); Re(1)-N(3) 2.129(4); Re(1)-Br(1) 2.6188(7); The N(1)-Re(1)-N(3) bond angle is 152.69(17)°.

The situation was different when replacing **1** with **2** as a starting material. The reaction with terpyridine in THF gave a black precipitate. The solubility was very limited to DMSO or DMF and slightly in acetone. The proton NMR spectrum showed no acetonitrile signal anymore but exclusively aromatic protons. Elemental analysis, mass spectrometry and IR pointed to a composition $[ReBr(CO)_2(terpy)]$ (**12a**). Carbonyl stretching frequencies of **12a** at 1883 and 1806 cm^{-1} were redshifted by about 40 cm^{-1} as compared with **12.** This redshift is a consequence of substituting the π-accepting acetonitrile ligands by donating pyridine type nitrogens. They were comparable with the values known from literature (1889, 1817 cm^{-1}, liquid film (DMSO)).[87] Single crystals were obtained form acetone and confirmed the nature of **12a** (figure 50, right). The bond angle of 152.69(17)° between N(1)-Re(1)-N(3) is slightly smaller compared to other structures with the terpyridine ligand coordinated in a *meridional* fashion ($[Ru(CH_2OAc)(CO)(terpy)]^+$ 157.08(11)°[90], $[Ru(terpy)(R_2terpy)]^{2+}$ 157.9(3)° and 158.4(3)°[95]). The bromide Br(1) and the C(2)-O(2) carbonyl ligand are disordered with a ratio of 88:12.

To summarise, several α,α'-diimines and terpyridine complexes comprising the *cis*-$\{Re(CO)_2\}^+$ moiety were synthesised and characterised. They all showed a red shift in the MLCT absorption maxima from UV/VIS spectroscopy compared to the corresponding $[ReBr(CO)_3(diimine)]$ complexes, attributed to the reduction in ligand field strength through removal of one CO ligand. With **1**, only the two bromide or solvent ligands trans to the COs could be substituted to obtain complexes **8**, **9**, **10**, **11** and **12**. With **2** however, the reaction with terpyridine led to the *meridional* coordinated complex **12a**.

Table 11: Spectroscopic data of diimine- and terpyridine complexes of **1** and **2**. [a] in DMF, [b] as a KBr pellet, [c] 1 mM in DMF with 0.1 M $TBAPF_6$ as electrolyte.

Complex	λ_{max} [nm][a]	$\nu_{(CO)}$ [cm^{-1}][b]	$E_{1/2, red}$ [mV][c]	colour
bpy (**8**)	423	1926, 1853, 1835	-1165	red
phd (**9**)	420	1933, 1850	-47, -669	dark red
pham (**10**)	412, 641	1926, 1843		green
terpy (**12**)	420	1922, 1853		orange
mer-terpy (**12a**)	400, 470	1883, 1805		black
tpphz (**11**)	430	1932, 1857		red
$[ReBr(CO)_3(bpy)]$[29]	370	2019, 1905	-1190	yellow
$[ReBr(CO)_3(phd)]$[29]	375 sh	2033, 1943	-15, -755	

3.10.6. Synthesis of complexes with pyridine-carboxylic acid ligands

For the labelling of biomolecules with the $\{M(CO)_3\}^+$ core (M = ^{99,99m}Tc, Re), pyridine carboxylic acids are used in the [2+1] approach as linker-molecules between metal centre and (bio)molecule.[17] The bidentate ligand 2,5-dipic or 2,4-dipic can be coupled to targeting molecules by standard peptide synthesis methods. In order to probe the *cis*-$\{M(CO)_2\}^+$ moiety as a potential coordination centre in such a strategy and its possibilities in labelling reactions, **1** was reacted with the two model ligands 2-pyridine carboxylic acid (2-pic) and 2,5-pyridine dicarboxylic acid (2,5-dipic).

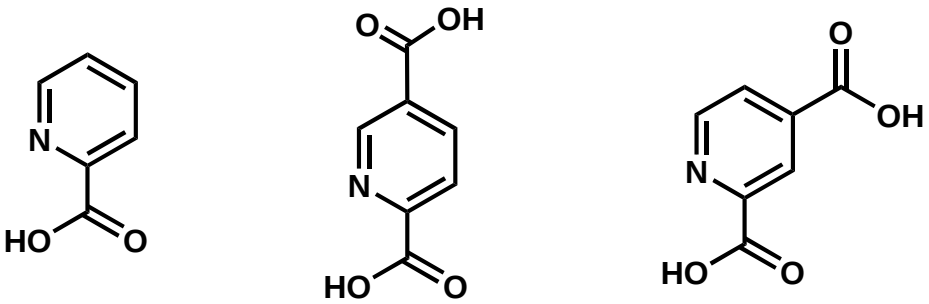

2-pic **2,5-dipic** **2,4-dipic**

Figure 51: Pyridine carboxylic acid ligands used in the [2+1] approach for labelling with $[^{99m}Tc(CO)_3]^+$.

The reaction of **1** with 2-pic in a diluted aqueous solution caused a colour changed from colourless to yellow within 1 hour. After stirring over weekend, the HPLC trace revealed the formation of one single product with a retention time of 18.1'. At 40° C, a more concentrated solution accelerated the reaction and after a few minutes the pure product started to precipitate. By slow evaporation of an aqueous solution of the precipitate with a weak N_2 stream, the neutral product $[Re(2\text{-pic})(NCCH_3)_2(CO)_2]$ (**13**) crystallised as yellow plates. Carbonyl stretching frequencies in the IR spectrum were at 1913 and 1835 cm^{-1} and mass spectroscopy showed a m/z ratio of 447 for $[M]^+$. The structure could be solved by x-ray analysis and a presentation of the molecule is shown in figure 52. It crystallised in the triclinic space group P-1. The bond lengths Re(1)-O(3) and Re(1)-N(3) are comparable with the similar $[Re(2,4\text{-dipic})(OH_2)(CO)_3]$ (**14a**) [17] complexes (see table 12) and the O(3)-Re(1)-N(3) angle (75.0(2)°) is in the normal

range of a five membered ring. The two acetonitrile ligands are strongly bended with a bond angle of 168.3(2)°

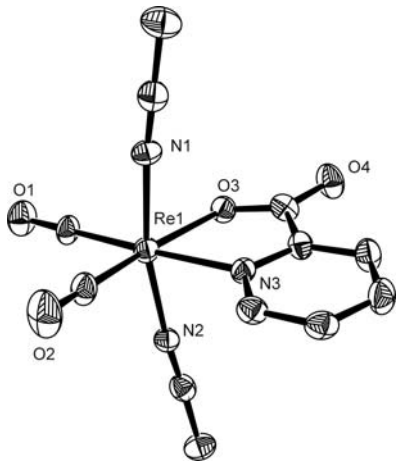

Figure 52: ORTEP plot of complex **13** (Ellipsoids are drawn at 50% probability and hydrogen atoms are omitted for clarity). Selected bond lengths are [Å]: Re(1)-N(1) 2.064(5); Re(1)-N(2) 2.076(5); Re(1)-O(3) 2.147(5); Re(1)-N(3) 2.170(5). The N(1)-Re(1)-N(2) bond angle is 168.3(2)°.

In the reaction of **1** with 2,5-dipicolinic acid (2,5-dipic) in water, the solution turned orange/red within minutes and the product precipitated. After filtration, the neutral product [Re(2,5-dipic)$(NCCH_3)_2(CO)_2$] (**14**) was obtained. Elemental analysis, NMR and ESI-MS (m/z = 492 $[M+H]^+$) confirmed the composition of **14**. With 1939 cm^{-1}, the symmetric carbonyl stretching frequency is shifted to higher wavenumbers compared to **13**. The electron delocalising effect of the additional carboxylic group at the pyridine moiety lowers the electron density at the metal centre.

Table 12: Selected bond length and IR frequencies of 2-pic and 2,5-dipic complexes **13**, **14a**, and **14**.

	Re-N(3) [Å]	Re-O(3) [Å]	IR $\nu_{(CO)}$ [cm^{-1}]	
13	2.170(5)	2.147(5)	1913	1835
14	-	-	1939	1817
14a	2.186(5)	2.163(4)	2036	1920

The labelling of biomolecules with the *cis*-$\{M(CO)_2\}^+$ moiety via a pyridine-carboxylic acid function would be possible since complex **1** reacted under mild conditions in a short time with the corresponding ligands to form stable complexes. For a labelling approach, **1** would be an adequate moiety with substitution labile positions. If a neutral complex is required, 2-pic as a mono-anionic ligand could be used as a linker, if there is a need for a positive charged complex, the labelling via a neutral ligand, *e.g.* a substituted 2,2'-bipyridine, would be a possibility.

3.10.7. Synthesis of a complex with bis(2-pyridylmethyl)glycine

As shown above, picolinic acid type ligands coordinate very well to Re(I)-carbonyl complexes. Thus, strong tetradentate mixed pyridine-carboxylic acid ligands should be able to substitute four ligands in **1**. It is furthermore known from literature that *N*,*N*-substituted tetradentate glycine derivatives (L^4) containing pyridine and/or carboxylic acid functional groups are able to substitute one CO and three halides in $[ReBr_3(CO)_2(NO)]^-$ to form complexes $[Re(CO)(NO)L^4]$ (scheme 17).[50]

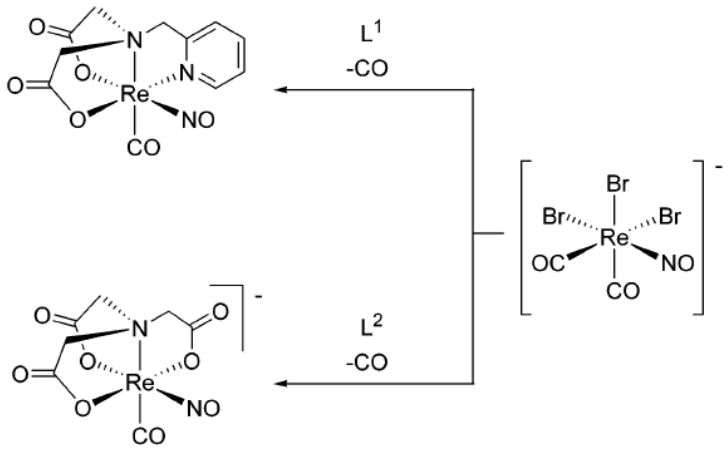

Scheme 17:[50] Substitution reaction of $[ReBr_3(CO)_2(NO)]^-$ with tetradentate N,N,O,O- and O,N,O,O-chelators.

Obviously, these tetradentate ligands L^4 are very strongly chelating and it was expected that such ligands would behave similarly in the reaction with **1**. The bis(2-pyridylmethyl)glycine (**BPG**) ligand was chosen since it combines four type of very good donors for the Re(I) centre. The two aromatic nitrogen atoms are weak π-acceptors and σ-donors the free electron pair of the amine and the carboxylic acid oxygen are σ-

donors. After tetradentate coordination the neutral complex would be expected to precipitate from water.

The reaction of an aqueous solution of **1** with 1 equivalent of BPG at RT resulted in a yellow precipitate. The IR spectrum of the crude product showed two pairs of carbonyl vibrations but no C≡N stretching frequency anymore (figure 53). These two sets of carbonyl stretching frequencies belong to the two possible isomers with the pyridines either in mutual *trans* or in *cis* position. The IR carbonyl frequencies of the major product are at ν_{CO} = 1882, 1788, 1774 cm^{-1} and were assigned to the *trans* isomer. The minor *cis* isomer showed IR carbonyl frequencies at ν_{CO} = 1913, 1821 cm^{-1}. The frequencies are shifted to higher wavenumbers due to the weaker electron donating combination of one pyridine and one amine in *trans* position to the carbonyl ligands compared to one amine and on carboxylic acid group.

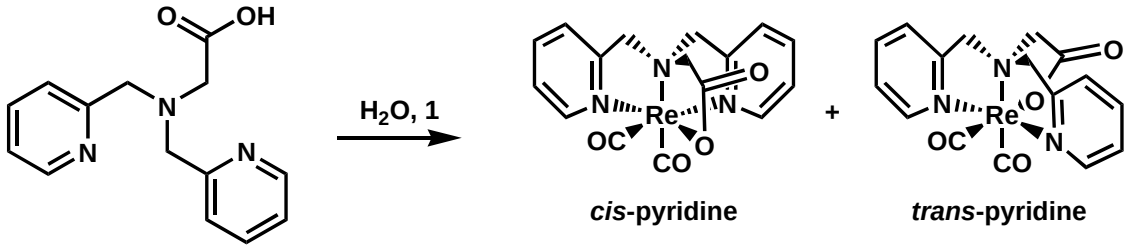

	IR $\nu_{(CO)}$ [cm^{-1}]	
cis-pyridine	1913	1821
trans-pyridine	1882	1774
x-tals (*trans*-pyridine)	1882	1776

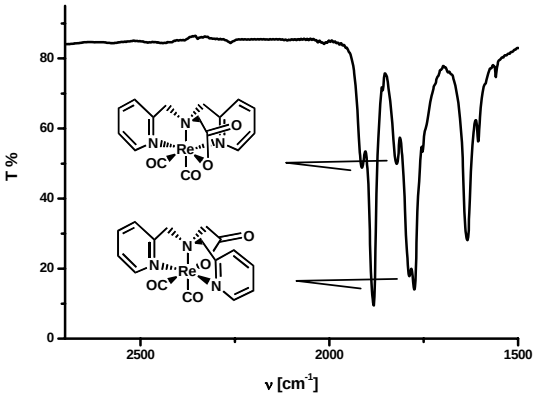

Figure 53: Reaction scheme, IR spectra and ν_{CO} of the two isomers formed by the reaction of **1** with BPG.

The reaction can be directed towards one single product by adding the BPG ligand to a refluxing solution of **1** in water. Single crystals could be obtained from methanol as

yellow needles. The structure in figure 54 shows the two pyridine rings in mutual *trans* position and the IR spectrum of the crystals confirmed the above made assignments of the two sets of stretching frequencies (see table in figure 53). The ligand was able to replace the acetonitrile ligands. The formation of three five-membered rings is bending the bond angles to 78.1° for both N-Re-N angles and to 77.4° for the N(3)-Re(1)-O(3) angle. Nevertheless the bond angle between the two carbonyl ligands is not widened up and is with 86.9° still smaller than 90 degrees. The Re(1)-N(1) and Re(1)-N(2) bond lengths (2.129(6) and 2.130(5) Å) are shorter than the rhenium-pyridine bonds (2.170(5) Å) but longer than the rhenium-acetonitrile bond length in complex **13** (2.070(5) Å in average).

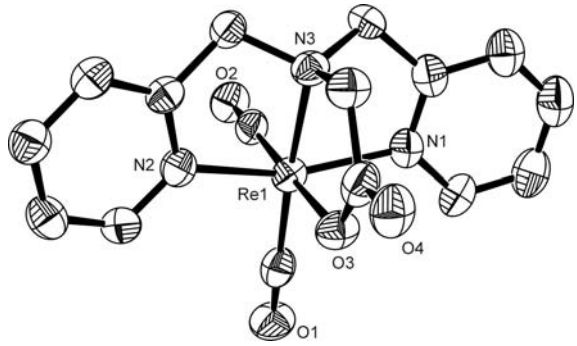

Figure 54: ORTEP presentation of the complex **15** (Ellipsoids are drawn at 50% probability and hydrogen atoms are omitted for clarity). Selected bond lengths are [Å]: Re(1)-N(1) 2.129(6); Re(1)-N(2) 2.130(5); Re(1)-O(3) 2.156(5); Re(1)-N(3) 2.202(6). Selected bond angles are [°]: N(1)-Re(1)-N(3): 78.1(2); N(2)-Re(1)-N(3): 78.1(2); O(3)-Re(1)-N(3): 77.4(2); C(2)-Re(1)-C(1): 86.9(3).

Cyclic voltammetry of a 1 mM solution of **15** in DMF with 0.1 M $TBAPF_6$ as electrolyte, the voltammogram (figure 55) showed a reversible one electron oxidation at +595 mV *vs* Ag/Ag^+.

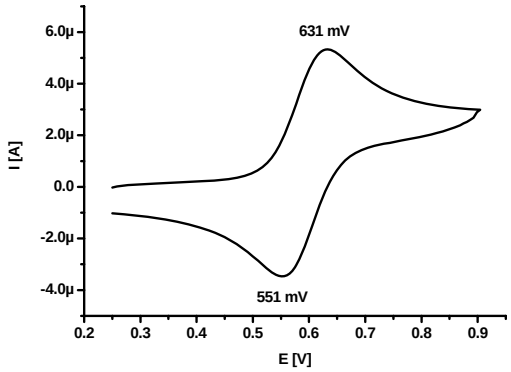

Figure 55: Cyclic voltammogram of complex **15** (1 mM in DMF; 0.1 M $TBAPF_6$) with a reversible one electron oxidation at 595 mV *vs* Ag/Ag^+.

3.11. Substitution reactions with $(Et_4N)[ReBr_2(CO)_2(imz)_2]$

The two-electron reduction of $(Et_4N)[ReBr_4(CO)_2]$ in DME with TDAE and in the presence of imidazole resulted in the complex $(Et_4N)[ReBr_2(CO)_2(imz)_2]$ (**1c)**. **1c** was soluble in CH_3CN, pyridine, alcohol and water and in solution, solvent molecules exchanged with the bromide ligands as discussed in chapter 3.6.4. To investigate further stability and reactivity of **1c**, a few substitution reactions were carried out and followed by HPLC and IR.

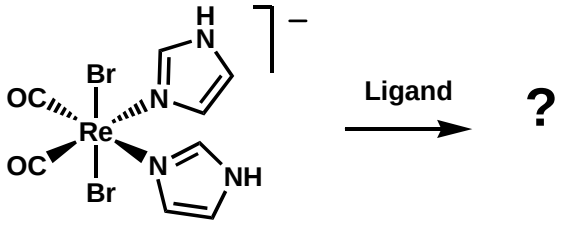

Figure 56: Precursor molecule $(Et_4N)[ReBr_2(CO)_2(imz)_2]$ (**1c**).

3.11.1. Reaction of $[ReBr_2(CO)_2(imz)_2]^-$ with 2-pyridine carboxylic acid

To obtain a bidentate coordination of the 2-pic ligand with **1c**, at least one imidazole ligand had to be substituted. As described for the substitution reactions of 2-pic with **1** (chapter 3.11.6.), the imidazole ligands in **3** were not replaced by other ligands such as e.g. 1-methylimidazole. In addition, the 2-pic ligand can coordinate in different ways (figure 57) and some of the possible isomers also form stereoisomers.

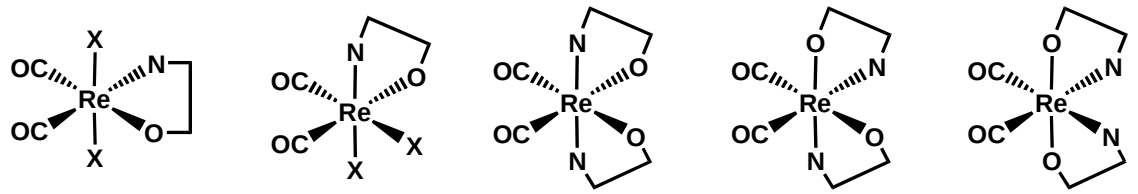

Figure 57: Isomers of 2-pic complexes with **1c** (stereoisomers are not shown).

During the reaction of **1c** with 2 eq. of 2-pic in H_2O, the colour of the solution changed within 2 hours from slightly yellow to dark red. After stirring for another 8 hours, the

solvent was evaporated in vacuum. The IR spectrum of the product showed one pair of carbonyl stretching frequencies at 1878 and 1785 cm^{-1} and two carboxyl vibrations at 1631 and 1593 cm^{-1}.

Single crystals could be obtained from the diffusion of a MeOH layer into a layer with hexane. The complex (HImz)[Re(2-pic)$_2$(CO)$_2$] (**16**) crystallised as red needles. The nitrogen atoms are in mutual *trans* position (figure 2). The centrosymmetric space group indicated a racemic mixture of the two possible enantiomeres. The bond length of the Re(1)-N(1) is only slightly shorter than the Re(1)-N(3) bond length of the 2-pic complex **14**, where only one ligand is coordinated *trans* to the two carbonyl ligands. Due to the strong bonding of the acetonitrile complex in **14**, a stronger bonded pyridine moiety in **16** was expected. Forming two five-membered rings, the angles N(1)-Re(1)-N(1)#1 with 155.6(3)° and O(2)#1-Re(1)-O(2) with 79.5(3)° are strongly distorted from 180° and 90° respectively.

	Re-N [Å]	Re-O [Å]
16	2.119(5)	2.149(4)
14	2.170(5)	2.147(5)

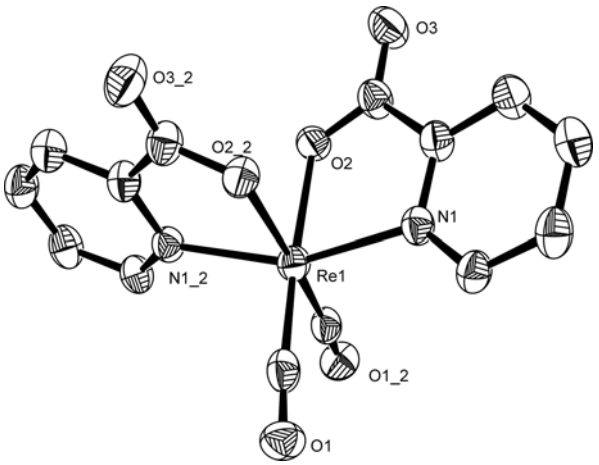

Figure 58: ORTEP plot and selected bond lengths of complex **16** (Ellipsoids are drawn at 50% probability, hydrogen atoms and the counter ion are omitted for clarity). Selected bond lengths are [Å]: Re(1)-N(1) 2.119(5); Re(1)-O(2) 2.149(4).

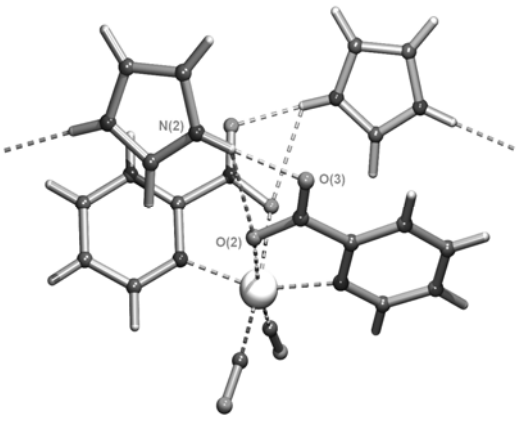

The counter-ion is a protonated imidazole $(Himz)^+$. It shows H-bonding with both nitrogen-protons to the carboxy-groups of neighbouring complexes. The hydrogen bridge N(2)-O(3) [-x-½, y-1, -z-½] is 2.776(9) Å and there is also a weak interaction between N(2) and O(2) [-x-½, y-1, -z-½] with a distance of 3.037(8) Å.

Figure 59: Surrounding of the counter-ion of **16** and its H-bond interactions.

The 500 MHz ^{1}H NMR spectrum shown in figure 60 is in strong support of the conformation found crystallographically in the solid state. It also indicated that no structural changes or substitutions took place in solution. The two doublet signals for $H_{A+A'}$ and $H_{D+D'}$ and the two multiplet signals for $H_{B+B'}$ and $H_{C+C'}$ showed the chemical equivalence of the corresponding protons.

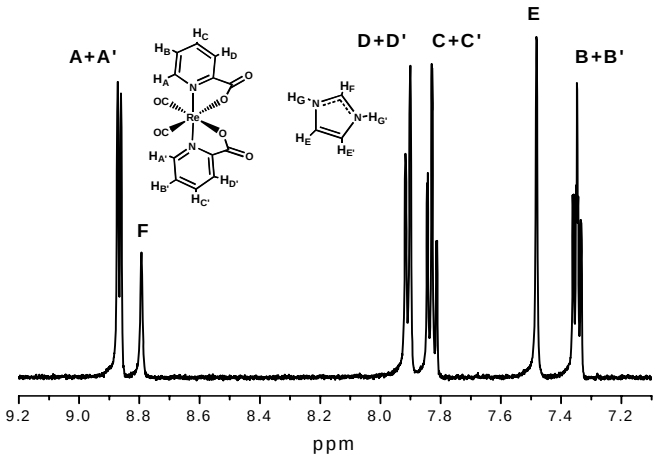

Figure 60: 500 MHz proton NMR spectrum of **16** in MeOH.

The experiment clearly showed, that one conformation is thermodynamically and probably also kinetically preferred. From mechanistic point of view and form the experience with $[Re(CO)_2]^+$ complexes, an initial coordination of the pyridine moiety at

the solvated positions (formerly bromides) was likely, followed by the formation of a five-membered ring by displacement of the imidazole ligands.

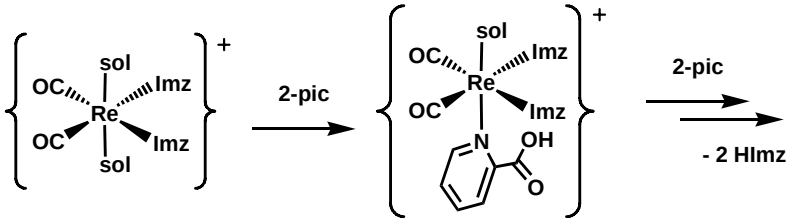

Scheme 18: Initial coordination of the pyridine moiety in the position *cis* to the carbonyl ligands leads to the *trans*-pyridine conformation in the reaction of **1c** with 2-pic.

3.11.2. Reaction of $[ReBr_2(CO)_2(imz)_2]^-$ with 2,2'-bipyridine

As a further bidentate ligand, bpy was chosen since the complex *cis*-$[Re(CO)_2(bpy)_2]^+$ was known from literature.[56] Adding 2.5 equivalents of bipyridine to a methanol solution of **1c** at 70° C induced an immediate colour change from slightly yellow to dark red. After 3 h of stirring, evaporating the solvent in vacuum and recrystallisation from DCM/Et_2O, a dark red powder was obtained. The IR spectrum showed ν_{CO} at 1889 and 1805 cm^{-1} respectively and UV absorptions at 385 and 515 nm. This IR and UV values were not comparable with the literature values for the *cis*-$[Re(CO)_2(bpy)_2]^+$ complex (1922 and 1852 cm^{-1} (liq.) and 364, 400, 492 nm).[56] A substitution of the bromide and imidazole ligands by two bpy ligands could therefore not be assumed. Mass spectrometry gave a m/z of 535 for the obtained complex and indicated the formation of $[Re(CO)_2(bpy)(imz)_2]^+$. Since we started from a complex with imidazole being *trans* to CO and halides are usually weaker ligands in $Re(I)(CO)_x$ chemistry, we predicted a coordination of one of the nitrogens of the bipyridine *cis* to CO. Bidentate coordination needs further first a reorganisation of the imidazole ligands to obtain the *cis* isomer. To get the bipyridine coordination *trans* to CO, an even more complicated mechanism was required. Single crystals were obtained by slowly evaporating a solution of **16a** in methanol. The structure is shown in figure 61. The two imidazole moieties are in *trans* position to each other and the bpy ligand is coordinated *trans* to the carbonyl groups. During the reaction, a reorganisation of the ligands must have taken place.

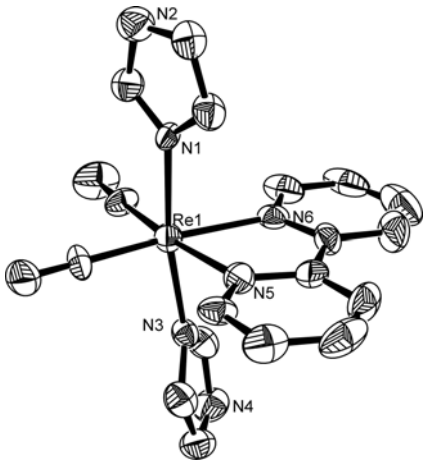

Figure 61: ORTEP plot and selected bond lengths of complex **16a** (Ellipsoids are drawn at 50% probability, hydrogen atoms and the counter ion are omitted for clarity). Selected bond lengths are [Å]: Re(1)-N(3) 2.128(9); Re(1)-N(1) 2.144(8); Re(1)-N(6) 2.187(9); Re(1)-N(5) 2.193(9).

Table 13: IR and absorption spectroscopic data of $[Re(CO)_2]^+$ bipyridine complexes.

	IR $\nu_{(CO)}$ [cm^{-1}]	λ_{max} [nm]	λ_{em} [nm]
16a	1889, 1805 (KBr)	385, 515	372 (ex_{322})
cis-$[Re(CO)_2(bpy)_2]^+$ [56]	1922, 1852 (liq.)	364, 400, 492	704
8	1926, 1853, 1835 (KBr)	425	-

3.12. Summary

The water soluble and air stable complexes $[ReBr_2(NCCH_3)_2(CO)_2]^-$ (**1**) and $[ReBr_2(CO)_2(imz)_2]^-$ (**1c**) showed substitution reactivity with several types of mainly N-based ligands to form stable $\{Re(CO)_2\}^+$ complexes $\{Re(CO)_2\}^+$. In solution, solvent molecules exchanged the bromide ligands and the two positions became labile for substitution.

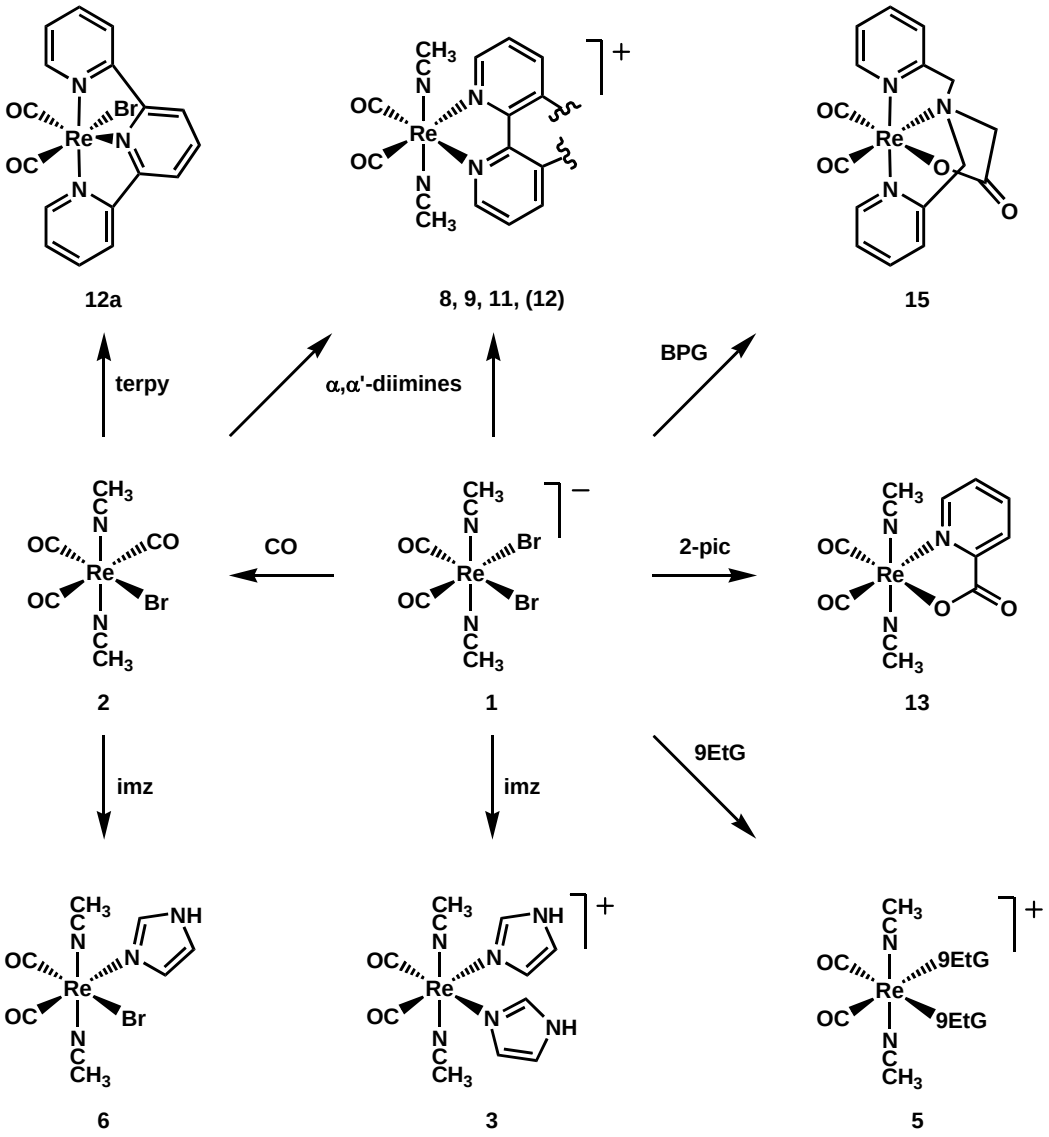

Figure 62: Substitution reactions of **1** and **2** with different types of ligands forming the corresponding complexes. The reactions of **1** were performed in water or methanol, the reaction of **2** in THF. All products were analysed at least by IR, x-ray diffraction and elemental analysis.

Applying CO pressure to a solution of **1** in water, the unexpected *mer*-$[ReBr(NCCH_3)_2(CO)_3]$ complex **2** formed. In **1**, the coordination of ligands such as imidazole, benzimidazole and 9-ethylguanine formed the corresponding complexes **3**, **4** and **5**. The positions *trans* to the carbonyl ligands showed strong affinity with the imidazole moiety, which is present in biomolecules in form of histidine and purine bases such as adenine or guanine although an interaction with plasmid DNA was not observed. Once coordinated, the imidazole ligand in **3** was not substituted by a competing ligand. α,α'-diimines and also terpyridine coordinated in a bidentate fashion to **1.** Substituting two bromides led the complexes **8**, **9**, **11** and **12** in different red colours but without strong luminescence properties. With bidentate mixed pyridine-carboxylic acid containing ligands, neutral complexes such as complex **13** were obtained, again substituting the two bromides in *trans* position to the carbonyl ligands. Finally, with the tetradentate ligand bis-(2-pyridylmethyl)glycine BPG, a four-fold substitution of all non carbonyl ligands in **1** was achieved. The neutral complex $[ReBr(NCCH_3)_3(CO)_2]$ **1a** behaved the same, since in solution, both ligands *trans* to the carbonyl moiety are exchanged by solvent molecules and ready for substitution reactions.

Similar reactions with **2** as a starting material, showed similar results. While reacting with a ligand, one of the carbonyl ligands was replaced and evolves as CO gas. In case of bidentate α,α'-diimine ligands, the products were equal to the reactions with **1**, forming the complexes **8** and **9**. With imidazole, only a single substitution was obtained, because the reaction has to be performed in organic solvents such as THF and the neutral complex **6** precipitates. A big influence of the starting material was observed for the reaction with terpyridine. A *meridional* coordination of the terpyridine ligand replaced in this reaction two acetonitrile and one carbonyl ligand, forming complex **12a**.

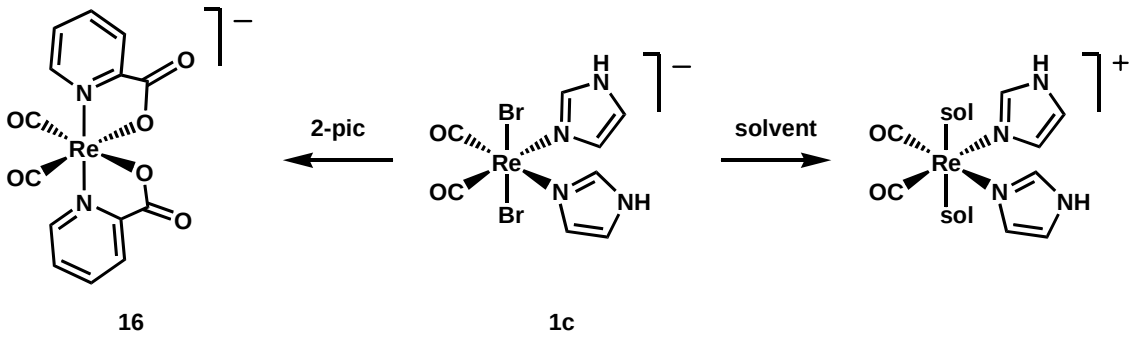

Figure 63: Substitution reaction of **1c** in water/solvent forming complex **16** with the substitution of all non-carbonyl ligands.

Reactions of the other complexes **1b**, **1c** and **1d** were not that well established as **1** and **1a**. It is obvious to assume that the benzonitrile complex **1b** would have similar reactivity as **1** but with different solubility. In the reaction of $[ReBr_2(CO)_2(imz)_2]^-$ (**1c**) with 2-pic the Br- and the imidazole ligands were substituted by two 2-pic ligands and formed complex **16**. With other ligands, no clear results were obtained and these experiments indicated a more complicate reactivity.

3.13. Attempts for the synthesis of $\{^{99m/99}Tc(CO)_2\}^+$ complexes

3.13.1. Carbonylation of $[^{99m}TcO_4]^-$

The labelling of different kind of biomolecules with the γ-emitter ^{99m}Tc is a persistent field of research. Since the development of boranocarbonate as a kit method for the preparation of $[^{99m}Tc(OH_2)_3(CO)_3]^+$, an easy access to label all kind of molecules is available[37] (scheme 19)

The standard kit formulation for the synthesis of $[^{99m}Tc(OH_2)_3(CO)_3]^+$ consists of:

- 4 mg sodium-boranocarbonate (BC)
- 7 mg sodium-tartrate • 2 H_2O (tartrate)
- 7 mg $Na_2B_4O_7$ • 10 H_2O (borate)
- placed in a capped vial flushed with N_2 for 5 min.

The kit is commercially available as "IsoLink™ Carbonyl Labeling Agent" with a slightly different formulation using a mixture of borate and sodiumcarbonate Na_2CO_3 as bases, lyophilised in a sterile vial.

Adding $[^{99m}TcO_4]^-$ containing saline solution to the kit, the BC acts as an *in situ* reducing agent and CO source. Within a 15 minutes at 95° C, $[^{99m}Tc(OH_2)_3(CO)_3]^+$ is obtained in yields higher then 98%.[36] It would be of importance to find a similar procedure for the synthesis of comparable $\{Tc(CO)_2\}^+$ precursors.

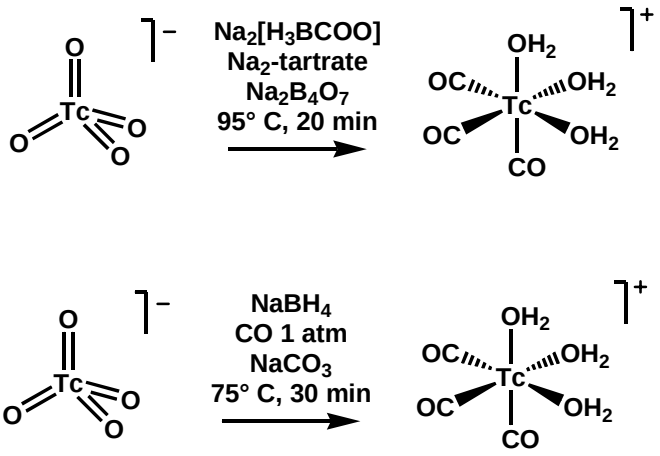

Scheme 19: The two approaches for the synthesis of $[^{99m}Tc(OH_2)_3(CO)_3]^+$.

The reaction mechanism of this carbonylation is unknown. Therefore it is difficult to predict how a change in the reaction conditions will influence nature and yield of products. If a stepwise carbonylation occurred, the addition of acetonitrile to the reaction solution could suppress the coordination of a third CO ligand since the acetonitrile ligands are strongly bound. Besides adding acetonitrile to both of the above-mentioned methods, the influence of changing the reducing agent, the CO ratio or the pH was studied. At tracer level no other analytical method than HPLC comparison of retention times in chromatography is possible. Therefore, to define the nature of newly synthesised complexes containing only H_2O, CO, CH_3CN or halides is ambiguous. The addition of ligands such as imidazole, bipyridine or pyridine-2 carboxylic acid would form well-defined and stable complexes, which could then be compared with model rhenium compounds. The HPLC-γ retention times were compared with the UV retention time of the corresponding $\{Re(CO)_2\}^+$ and $\{Re(CO)_3\}^+$ complexes by coinjection. Since the γ-detector is connected to the UV detector physically by a tube, a delay in retention time of 0.5' to 0.75' of the radioactive peak to the UV peak was acceptable.

3.13.2. Carbonylation of $[^{99m}TcO_4]^-$ with changes in the standard procedure

Addition of CH_3CN

As a primary experiment, the influence of adding acetonitrile to the standard synthesis of $[^{99m}Tc(OH_2)_3(CO)_3]^+$ was investigated. Adding 10% of acetonitrile to the reaction solution led within 60 minutes to two products. One peak at 6.8 minutes for $[^{99m}Tc(OH_2)_3(CO)_3]^+$ and a new, unknown peak $\{^{99m}TcXY\}$ at 10.5 minutes were detected in γ-HPLC (figure 64). Decreasing the amount of acetonitrile to 1%, the peak at 10.5' did not show up anymore. An increase to 50% slowed down the carbonylation reaction drastically and beside the two above mentioned peaks, several small peaks around 19' were detected after 3 hours.

Table 14: Overview of the influence of acetonitrile in the synthesis of $[^{99m}Tc(OH_2)_3(CO)_3]^+$.

change	main peaks [min]	remarks
10% CH_3CN	6.8', 10.5'	1 : 1 in intensity
1% CH_3CN	6.8'	small peak at 23'
50% CH_3CN	6.8', 10.4'	several products with small peaks around 19'

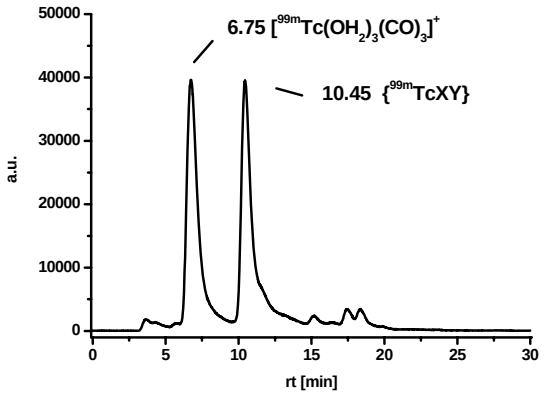

Figure 64: HPLC-γ trace of the carbonylation of $[^{99m}TcO_4]^-$ at 60° C for 1 h with the standard kit formulation but adding 10% acetonitrile; The first peak at 6.75' corresponds to $[^{99m}Tc(OH_2)_3(CO)_3]^+$ the second at 10.45' to the new, unknown product $\{^{99m}TcXY\}^+$.

If CH_3CN was added after the synthesis $[^{99m}Tc(OH_2)_3(CO)_3]^+$, the same main peak at 10,5' was obtained, indicating a tricarbonyl-acetonitrile complex $[^{99m}Tc(NCCH_3)_x(CO)_3]^+$. Since a coinjection of corresponding rhenium complexes $[ReCl(NCCH_3)_2(CO)_3]$ (r.t. = 5.4 min) and $[ReBr(NCCH_3)_3(CO)_2]$ (r.t. = 10.0 min) did not give any improvements about the composition of the peak at 10.5'. Further ligand substitution reactions should help to identify the peak for $\{^{99m}TcXY\}$.

Table 15: Comparison of the retention times in HPLC of the obtained ^{99m}Tc compounds with rhenium complexes by coinjection.

compound	retention time [min]	
^{99m}Tc reaction solution	6.7	10.4
$[^{99m}Tc(CO)_3]^+ + CH_3CN$		10.5
$[ReCl(NCCH_3)_2(CO)_3]$	5.4	
$[ReBr(NCCH_3)_3(CO)_2]$		10.0

Variations in the kit formulation

The commercially available carbonylation kit IsoLink™ has a different formulation, with $Na_2B_4O_7 \cdot 10\ H_2O$ (2.8 mg) and Na_2CO_3 (7.2 mg) as a base making the reaction solution more basic. Lowering the amount of BC delivers less CO but also decreases the amount of reducing agent. This was corrected by adding $NaBH_4$. As a last change, the synthesis of $[^{99m}Tc(CO)_3]^+$ was performed according to the procedure with 5 mg $NaBH_4$, 4 mg $NaCO_3$ and CO gas at atmospheric pressure. To exclude reactions in which other then carbonyl complexes were formed, the reaction was also performed with $NaBH_4$ only and $NaCO_3$ but without CO. All the reactions contained 10% (v/v) of acetonitrile. A summary of the resulting peaks in HPLC is given in table 16.

Changing the kit formulation resulted in a number of new peaks in HPLC. Lowering the amount of BC slowed down the reaction and replacing BC partly or fully by $NaBH_4$ increased the number of peaks without any improvement towards one peak.

Table 16: Overview of the influence of changing the kit formulation in the synthesis of $[^{99m}Tc(OH_2)_3(CO)_3]^+$ with 10% of acetonitrile.

change	main peaks	remarks
less BC (2 mg)	6.7', 10.3'	very slow reaction, a lot of small peaks
IsoLink®	6.2', 9.7'	slow reaction, two peaks
2 mg BC + 3 mg $NaBH_4$	25' broad	many peaks, traces at 6.5' and 10.3'
no base	3.5', 6.3', 9.8'	very hydrophilic compound at 3.5'
CO_3^{2-}, BH_4^-, CO	~17'	single peak
CO_3^{2-}, BH_4^-	3.5'	

3.13.3. Complex formation of $[^{99m}Tc(CO)_3]^+$ and $\{^{99m}TcXY\}$

To better identify the nature of the compounds in the new peaks, aqueous solutions (100 µl, 10^{-3} M) of ligands such as bpy, 2-pic or BPG were added after the formation of $[^{99m}Tc(OH_2)_3(CO)_3]^+$ and $\{^{99m}TcXY\}$. The resulting new peaks at around 20' were compared with corresponding rhenium complexes via coinjection measurements. Additionally, the ligands were added from the beginning as a one-pot synthesis.

Complex formation with of 2,2'bipyridine (bpy)

By the addition of bpy to the reaction solution received according to chapter 3.13.2., the two peaks at 6.8' and 10.5' converted to two new major peaks at 19.7 and 21.4' and a minor at 18.5'. Figure 65 shows in the upper part the γ-trace of the reaction solution after addition of bpy and heating for 30 minutes at 60° C. The lower part the same reaction after 60 minutes at 60° C. $[^{99m}Tc(OH_2)_3(CO)_3]^+$ reacted faster with bpy compared with the $\{^{99m}TcXY\}$. After heating for another half an hour, γ-HPLC showed that out of the peak at 10.5' mainly the peak at 19.7' was formed.

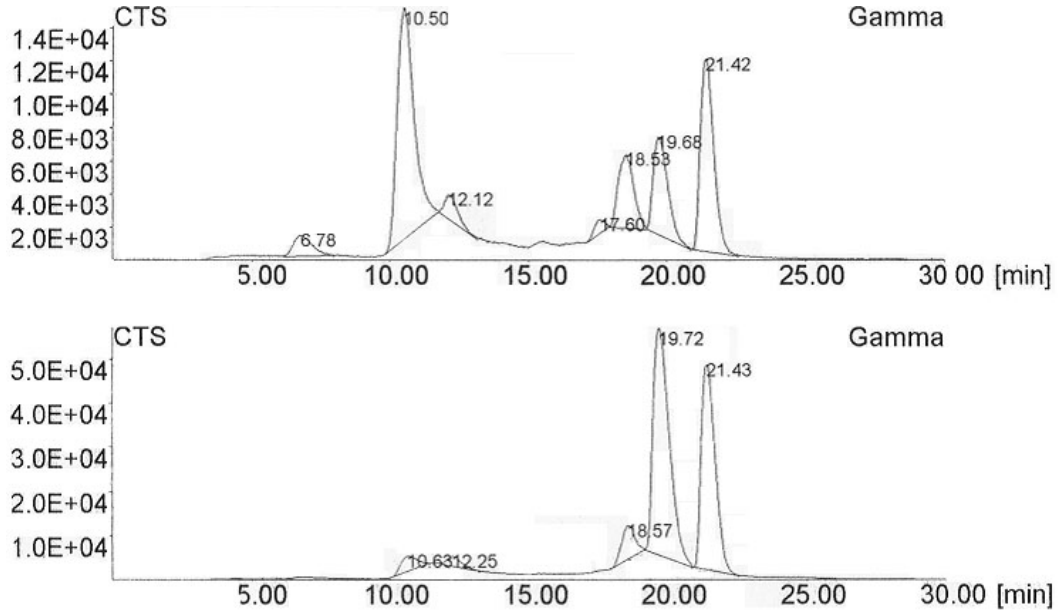

Figure 65: γ-detection of the HPLC chromatogram of the complexation of the two carbonylation products $[^{99m}Tc(OH_2)_3(CO)_3]^+$ and $\{^{99m}TcXY\}$ with bpy. Upper trace: 30 min at 60° C, lower trace: 60 min at 60° C.

A coinjection of a mixture of $[ReBr(CO)_3(bpy)]$ (**8a**) and $[Re(NCCH_3)_2(CO)_2(bpy)]Br$ (**8**) should give evidence about the obtained products. According to the UV trace (figure 66), the peak at 20.9' was assigned to **8a** and the band at 18.1' to **8**. Thus, the γ-peak at 21.4 minutes is the ^{99m}Tc-analogue of **8a** $[^{99m}Tc(OH_2)(CO)_3(bpy)]^+$, delayed by separation of the UV and γ-detector of about 0.5'. With this delay and the obtained retention time, complex **8** would be comparable with the small peak at 18.6'. With 1.6' delay the second major peak at 19.7' could not be assigned to any known complex. If the reaction was performed as a one-pot synthesis, the peak at 19.7' was detected in γ-HPLC. Therefore, there is still no evidence about the composition of the new peaks.

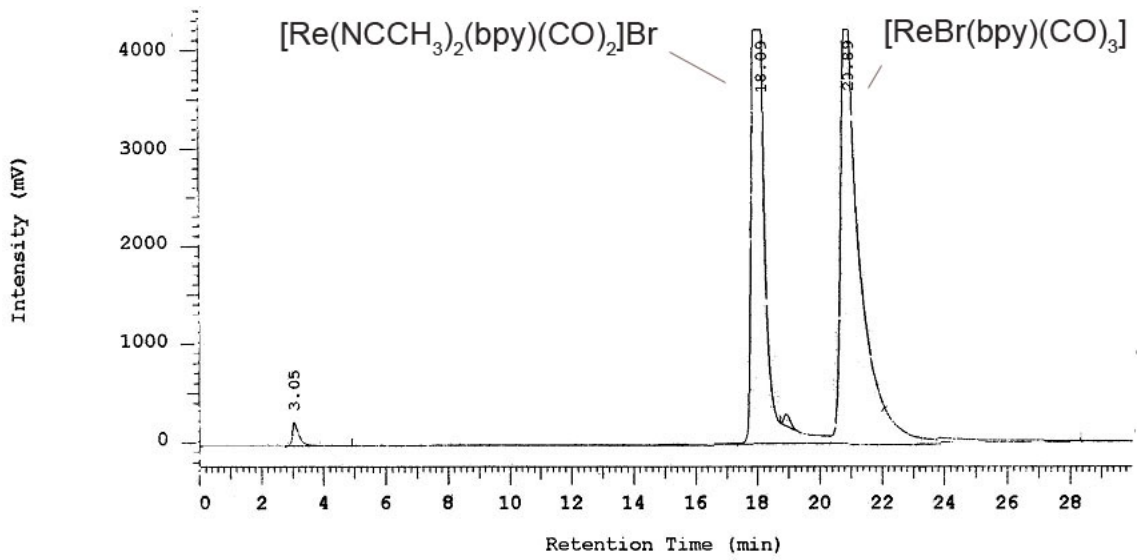

Figure 66: HPLC-UV chromatogram of the coinjection of **8** and **8a**.

Complex formation with 2-picolinic acid (2-pic)

The reaction with 2-pic lead to the formation of one single product. The peak at 19.1' is assigned to [^{99m}Tc(2-pic)(OH_2)($CO)_3$] matching the retention time of the corresponding [Re(2-pic)(OH_2)($CO)_3$] complex with 18.7'.

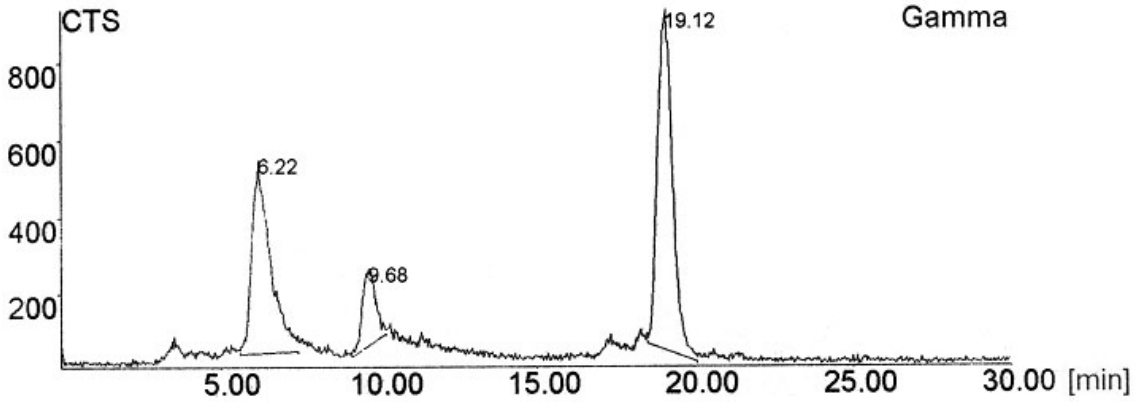

Figure 67: γ-trace of the carbonylation products complexated with 2-pic, 30 min at 60° C.

Complex formation with bis-pyridylmethyl-glycine (BPG)

Replacing tartrate by a strongly chelating tetradentate ligand, we could maybe prevent a threefold carbonylation by forming a {^{99m}Tc($CO)_2L^4$} complex. The chelating power of the BPG ligand was already shown in chapter 3.11.7. Since BPG can afford a

tetradentate coordination with **1** to yield [Re(BPG)$(CO)_2$] (**15**), tartrate was partly or completely replaced by BPG.

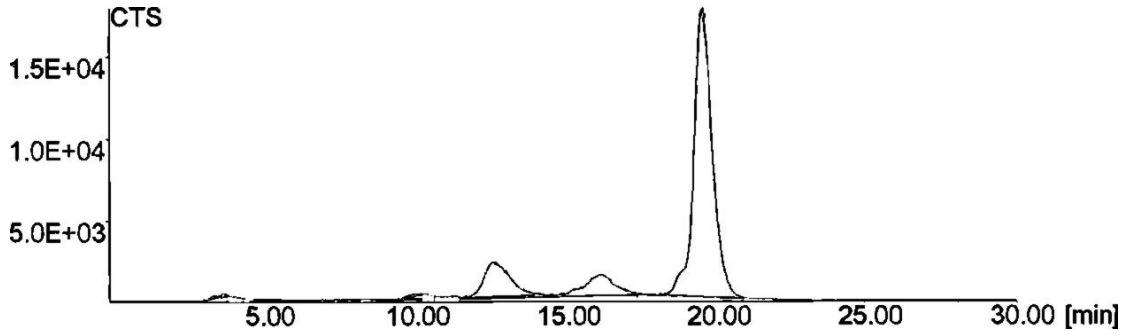

Figure 68: γ-trace of the one-pot reaction of $[^{99m}TcO_4]^-$ with 4 mg BC, 7 mg borate and 4 mg BPG, 60 min at 90° C; the main peak has a retention time of 19.6'.

The one-pot reaction with BPG replacing tartrate partly or completely showed in both cases a single peak at 19.6' in γ-HPLC. Since $[Re(BPG)(CO)_3]^+$ (**15a**) has a retention time of 18.7' and **15** of 17.7', the peak was assigned to the tricarbonyl complex $[^{99m}Tc(BPG)(CO)_3]^+$.

3.13.4. Summary

By adding 10% CH_3CN to the standard synthesis of $[^{99m}Tc(OH_2)_3(CO)_3]^+$ and complexation of the obtained two products with ligands, several new peaks in HPLC appeared. By coinjection of possible analogue $\{Re(CO)_3\}^+$ and $\{Re(CO)_2\}^+$ complexes, some of the new ^{99m}Tc bands were comparable in retention time with known $\{Re(CO)_3\}^+$ complexes only but none of them could be assigned to a retention time of a known $\{Re(CO)_2\}^+$ complex. About the composition of the unknown peaks can only be speculated and the addition of acetonitrile had a much bigger influence of the carbonylation reaction then expected. To obtain $[^{99m}Tc(CO)_2]^+$ at tracer level, a direct method to synthesise $[M(CO)_2]^+$ (M = Re, ^{99}Tc) complexes starting from $[MO_4]^-$ would be helpful, which can then be adapted to ^{99m}Tc chemistry.

3.13.5. Experiments with ^{99}Tc

Synthesis of $(Et_4N)_2[^{99}TcBr_3(CO)_3]$

$(Et_4N)_2[^{99}TcBr_3(CO)_3]$ (**18**) as starting material was synthesised according to the known synthesis of the trichloro complex $(Et_4N)_2[^{99}TcCl_3(CO)_3]$.[18] The procedure had to be adapted for the bromo-compound. $(Bu_4N)[^{99}TcO_4]$ was dissolved in THF and reduced with BH_3-THF under CO atmosphere. This low-pressure carbonylation led after workup with $(Et_4N)Br$ and TFA or HBr in ethanol to **18** in about 68% yield. Purity was determined by HPLC and IR spectroscopy. The two bands of the carbonyl stretching vibrations at 2022 cm^{-1} for the symmetric and the splitted band 1913, 1898 cm^{-1} for the asymmetric vibrations were only weakly shifted compared to $(Et_4N)_2[^{99}TcCl_3(CO)_3]$ (2028, 1902 cm^{-1}).[18]

Oxidation of $(Et_4N)_2[^{99}TcBr_3(CO)_3]$ with Br_2

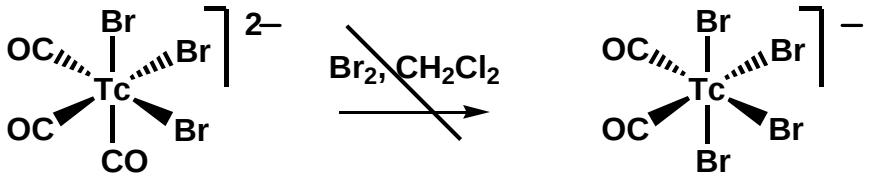

Figure 69: Failed oxidative decarbonylation of **18** with bromine.

As mentioned in chapter 3.4., the oxidation with halogens of $[^{99}TcCl_3(CO)_3]^{2-}$, to $[^{99}TcX_4(CO)_2]^-$ is not well established. The adaptation of the corresponding synthesis of $[ReBr_4(CO)_2]^-$ was not successful. Oxidation to $[TcBr_6]^-$ was the main reaction and further experiments with more diluted solutions and lower temperatures did not improve the yield.

Decarbonylation of $(Et_4N)_2[^{99}TcBr_3(CO)_3]$ with TMNO

According to literature, the decarbonylation with trimethyl amine oxide (TMNO) requires an electrophilic CO carbon. Carbonyl complexes with symmetric stretching frequencies lower than 2000 cm^{-1} do not react anymore with amine oxides.[69, 70] The carbonyl stretching frequency of **18** is with 2022 cm^{-1}, much higher as compared to

$(Et_4N)_2[ReBr_3(CO)_3]$ (1999 cm^{-1}), for which the reaction did not work indeed (see chapter 3.7.1.). Complex **18** was reacted with 2.5 equivalent of TMNO and 2 equivalent $(Et_4N)Br$ in acetonitrile but no change in the HPLC chromatogram was observed indicating that no reaction took place and the TMNO method could not be applied to technetium as well.

Carbonylation of $(Bu_4N)[^{99}TcOCl_4]$

Zn°-powder was suspended in 6 ml CH_3CN and CO was bubbled through the solution. A solution of $[^{99}TcOCl_4]^-$ in 3 ml CH_3CN was added via a syringe pump over 2 h and the solution stirred overnight. The solution got dark red to brown and in HPLC several bands appeared. Zinc was filtered off and the solution dried. The IR spectrum in figure 70 shows three bands which were assigned to a $[^{99}Tc(NCCH_3)_y(CO)_2]^+$ compound with $\nu_{(CN)}$ = 2258, $\nu_{(CO)}$ = 1949, 1857 cm^{-1}. Attempts to isolate and crystallise the compounds were not successful due to the presence of large amounts of borates and other salts. At least, a hint for a possible synthesis method for $\{^{99}Tc(CO)_2\}^+$ complexes could be received.

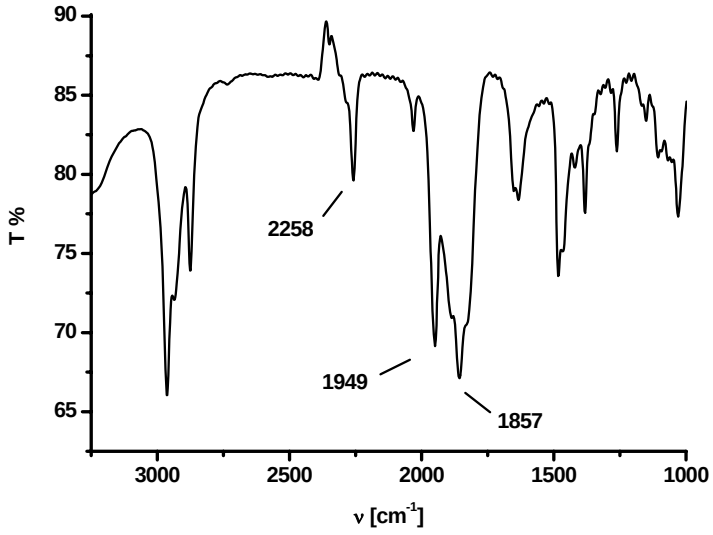

Figure 70: IR spectrum from the reduction of $[^{99}TcOCl_4]^-$ with Zn° in acetonitrile, indicating a possible $\{^{99}Tc(CO)_2\}^+$ complex.

3.13.6. Summary

While the decarbonylation methods did not show any signs for $\{^{99}Tc(CO)_2\}^+$ complexes, the carbonylation reaction in acetonitrile directed towards a two-fold carbonylation. The reaction of $[^{99}TcOCl_4]^-$ with Zn° and CO in acetonitrile indicated the formation of a $\{^{99}Tc(NCCH_3)_x(CO)_2\}^+$ complex. Even if the compound was not structurally characterised, this experiment gave a strong hint in the direction of $[^{99}Tc(CO)_2]^+$ complexes.

3.14. 17-electron Re(II) complexes with the $\{Re(CO)_2\}^{2+}$ fragment

3.14.1. Introduction

Rhenium complexes with the metal centre in the formal oxidation state +II (d^5 configuration) are relatively rare. Most of the known Re(II) complexes contain phosphines or ligands such as aromatic amines or isocyanides with π-acceptor properties dominating Re(II) chemistry.[2] Furthermore, dinuclear compounds with metal-metal bonds are well established.[96] Mononuclear 17-electron complexes of Re(II) are of high interest as precursors for the design of molecular materials with tuneable electronic properties.[97] Many Re(II) compounds originate from photochemical or electrochemical oxidation of Re(I) complexes with MLCT excited states.[98] For the bulk synthesis, the main route to Re(II) compounds involves oxidation of Re(I) or the reduction of Re(III) complexes. A few Re(II) carbonyl complexes are known, especially $[R\text{-}CpRe(CO)_3]^+$, which shows an interesting redox chemistry.[99] To get access to a wide range of complexes, it would be important to have a precursor with substitution labile ligands like $[Re_2(NCCH_3)_{10}]^{4+}$.[97]

In chapter 3.6., the reduction of $[ReBr_4(CO)_2]^-$ to several $\{Re(CO)_2\}^+$ precursors by a variety of reducing agents and solvents was discussed. The most suitable reducing agent was TDAE, a two-electron reductant. In acetonitrile, $[ReBr_2(NCCH_3)_2(CO)_2]^-$ **1** formed and in DME, with imidazole as an additional ligand, $ReBr_2(CO)_2(imz)_2]^-$ **1c**. These two compounds represent the first substitution labile $\{Re(CO)_2\}^+$-precursors. Using the same strategy but reducing by only one electron per rhenium should result in Re(II) complexes provided that they do not immediately disproportionate to Re(I) and Re(III) or form metal-metal bonds.

3.14.2. Synthesis of $[Re(II)Br_2(CO)_2(py)_2]$

$[ReBr_4(CO)_2]^-$ was dissolved in DME in the presence of 20 equivalent of pyridine. Reduction with 0.5 equivalent of TDAE produced a precipitate with carbonyl IR stretching frequencies of 1991 and 1825 cm^{-1}, typical for complexes with a $\{Re(II)(CO)_2\}$ motive. The crude product was washed with methanol removing $(TDAE)Br_2$. A brownish, air stable powder $[ReBr_2(CO)_2(py)_2]$ (**17**) was obtained in 50% yield. After recrystallization, the compound formed red crystals. Single crystals suitable for x-ray structure analysis were obtained from DCM/pentane and the structure is shown in figure 71.

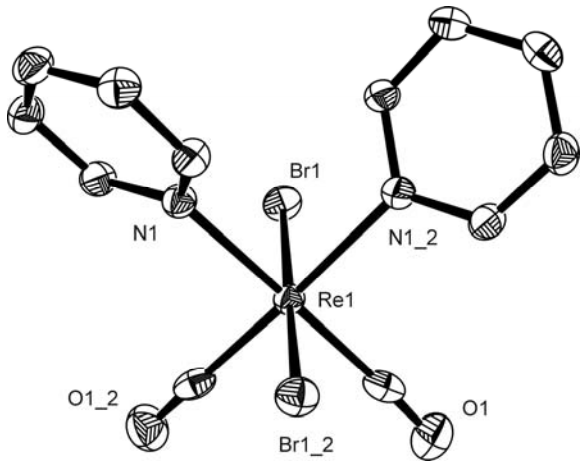

Figure 71: ORTEP plot of complex **17** (Ellipsoids are drawn at 50% probability, hydrogen atoms are omitted for clarity). Selected bond length are [Å]: Re(1)-Br(1) 2.5187(4); Re(1)-N(1) 2.208(3); Re(1)-C(1) 1.971(5).

Complex **17** crystallised in the monoclinic space group C2/*c* as red needles. The structure is comparable with the Re(I) complex **1c** with the two halides in *trans* position to each other and with pyridine ligands instead of imidazole. Therefore, bond lengths for both **17** and **1c** are listed in table 17. The higher oxidation state in **17** lowers the π-back-donation from the metal centre making it thereby more Lewis acidic. This is mirrored by a shorter bond length for both the pyridine and bromide as compared to **1c** (0.087 and 0.023 Å respectively) and a lengthening of the Re-C bond to the carbonyl ligand by 0.122 Å. The carbonyl stretching frequencies in IR are shifted to higher wavenumbers.

Table 17: Selected bond lengths of complex **17** in comparison with **1c**.

bond lengths [Å]	**17**	**1c**
Re(1)-Br(1)	2.5187(4)	2.6054(8)
Re(1)-Br(2)		2.6129(8)
Re(1)-N(1)	2.208(3)	2.231(5)
Re(1)-N(2)		2.226(6)
Re(1)-C(1)	1.971(5)	1.849(8)
Re(1)-C(2)		1.891(9)

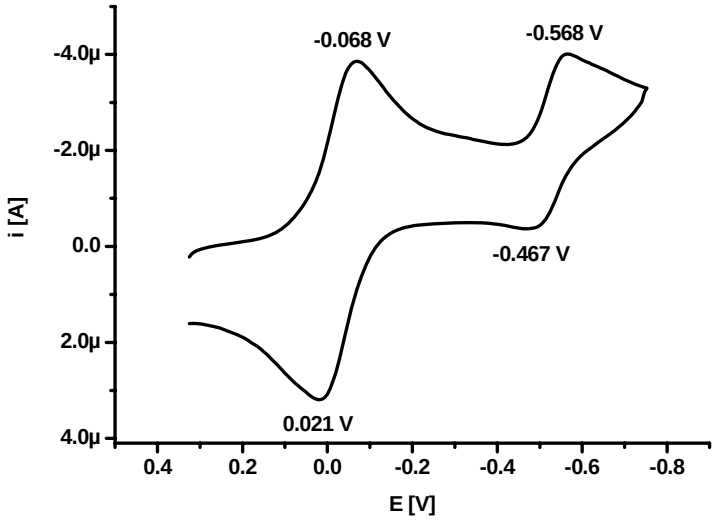

Figure 72: Cyclic voltammogram of **17** in DMF showing two partly reversible reductions at $E_{1/2}$ = -23 mV and –518 mV *vs* Ag/Ag^{+}.

Cyclic voltammetry in DMF with 0.1 M $TBAPF_6$ as an electrolyte depicted a first reversible one-electron reduction at -23 mV and a second, partly reversible reduction at -518 mV. The direct comparison with the one electron oxidation of a corresponding $\{ReBr_2(CO)_2(py)_2\}^{+}$ compound was not possible, because of the uncertainty of similar Re(I) complexes, obtained according the presented methods in chapter 3.6. or by the reduction or **17** with cobaltocene.

3.14.3. Synthesis of $[Re(II)Br_4(CO)_2]^{2-}$

If the reduction of $[ReBr_4(CO)_2]^-$ with 0.5 equivalent TDAE was performed in CH_3CN, the solution colour changed from the original deep red to orange. A precipitate that formed was removed and the solution evaporated. The crude product was washed with DCM to remove remaining starting material. A bright orange solid **18a** was left with IR carbonyl stretching frequencies at 1972 and 1795 cm^{-1} respectively (figure 73).

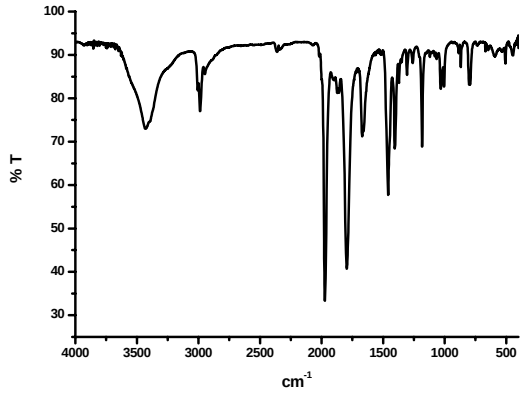

Figure 73: IR spectrum of complex **18a** (KBr) ν_{CO} at 1972 and 1795 cm^{-1}.

Complex **18a** is highly soluble in CH_3CN. Single crystals could be obtained from slowly evaporating an acetonitrile solution. X-ray analysis of the crystal revealed the structure as $(Et_4N)[ReBr_3(NCCH_3)(CO)_2] \cdot (Et_4N)Br$ (**18**, figure 74). Since the crystal grew from acetonitrile, it was well possible that during the crystallisation process one bromide in the original product exchanged for CH_3CN. This implied that the orange product **18a** had the structure $[ReBr_4(CO)_2]^{2-}$. The IR spectrum of **18a** showed no nitrile stretching frequencies, which is in agreement with this formulation. From charge and ion considerations, $[ReBr_4(CO)_2]^{2-}$ could be a possible composition but starting from $(Et_4N)[ReBr_4(CO)_2]$, the charge must be balanced by $(TDAE)^{2+}$ or a mixture of $(Et_4N)^+$ and $(TDAE)^{2+}$ cations. Elemental analysis of **18a** indicated a ratio $(Et_4N)^+$:$(TDAE)^{2+}$ ratio of 13:1.5. Adding $(Et_4N)Br$ to the reaction solution gave higher purity, directing to $(Et_4N)_2[ReBr_4(CO)_2]$ as a suggested structure for **18a**. In IR, the band for $(TDAE)Br_2$ is not visible anymore and elemental analysis confirmed the composition $(Et_4N)_2[ReBr_4(CO)_2]$ **18a**. The high solubility in CH_3CN was an indication of

solvatation effects like ligand exchange. Most likely, one bromide ligand was exchanged by a solvent molecule during crystallisation.

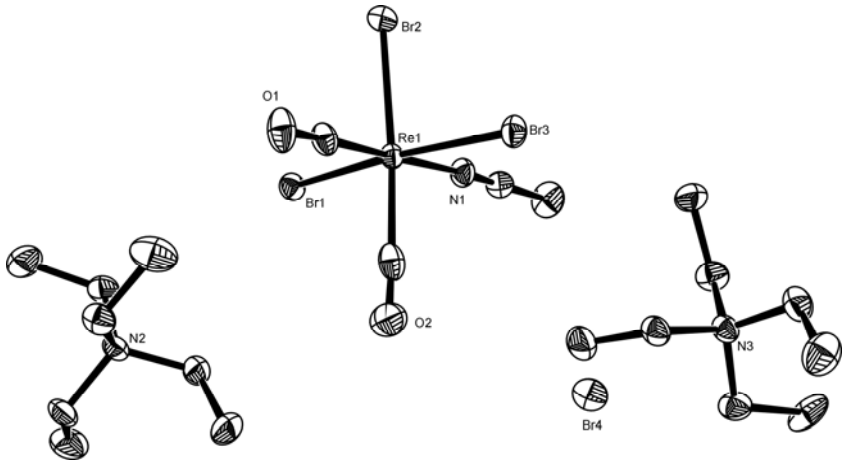

Figure 74: ORTEP plot of complex **18** (Ellipsoids are drawn at 50% probability, hydrogen atoms are omitted for clarity, counter ion and co-crystallised salt are shown for a complete overview). Selected bond lengths [Å] and bond angles [°] are: Re(1)-C(1) 1.903(9); Re(1)-C(2) 1.966(11); Re(1)-N(1) 2.170(7); Re(1)-Br(1) 2.5360(9); Re(1)-Br(2) 2.5867(10); Re(1)-Br(3) 2.5292(9); Br(3)-Re(1)-Br(1) 171.02(3).

The Re(1)-C(1,2) bond lengths are 1.903(9) and 1.966(11) Å respectively and in the same range as found in complex **17**, as well as the Re-Br length with 2.5360(9), 2.5867(10)and 2.5292(9) Å. In comparison, the Re(III) starting material $[ReBr_4(CO)_2]^-$ has a Re-C bond length of 1.978(7) Å, which is again longer compared with **18** and the Re-Br bond lengths are again slightly shorter (2.445(5), 2.498(5) and 2.542(5) Å).[63]

Magnetic susceptibility data of compound **18a** were measured between 5 and 300 K. At low temperature, compound **18a** had a μ_{eff} = 1.77 BM in agreement with a d^5 system with one single unpaired electron (μ = 1.73 BM).

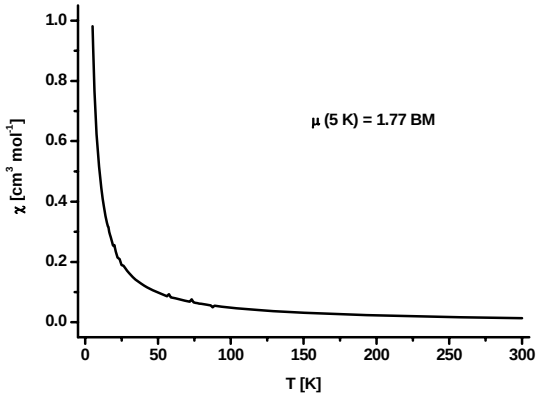

Figure 75: Temperature-dependant magnetic susceptibility data for **18a** recorded in the range 5-300 K showing a μ_{eff} = 1.77 BM.

3.14.4. Summary

A new family of paramagnetic mononuclear 17 electron Re(II) complexes was found. The unexpected stability of complex **17** and **18a** under aerobic conditions showed the potential for further reactions and complexes. Although the exact composition of complex **18a** was not found, structurally characterised **18** as a direct product of **18a** is a versatile starting material for substituting the 4 bromide ligands by all kind of other mono- and bidentate ligands. This opens an avenue for systematically studying the chemistry of Re(II).

4. Experimental Part

4.1. Methods and analysis

All reactions were performed under a nitrogen atmosphere and the chemicals were used without further purification. The phenanthroline like ligands phd, pham and tpphz were synthesised by B. Probst according to slightly modified literature procedures[91, 100, 101], BPG was synthesised according to the literature.[102] The other ligands were purchased either from Fluka, Aldrich or Acros. $NH_4[^{99}TcO_4]$, $Na_2[H_3BCOO]$ and IsoLink™ were a gift from Mallinckrodt. $[^{99m}TcO_4]^-$ was obtained by a $^{99}Mo/^{99m}Tc$ UTK FM generator from Mallinckrodt (Tyco).

4.1.1. Standard analyses

Elemental analyses (EA) were performed on a Leco CHNS-932 elemental analyser. IR spectra were recorded in a PerkinElmer Spectrum BX FT-IR spectrometer. ^{1}H-NMR spectra were recorded on a Varian Mercury 200 MHz or a BrukerDRX500 500 MHz spectrometer. ESI-MS were performed on a Merck-Hitachi M-8000 spectrometer, on a Bruker esquire™/LC spectrometer or on a Bruker esquire™/HCT™ spectrometer. Values are reported for the ^{187}Re isotope.

4.1.2. Additional analyses

UV-Vis spectra were measured using a Cary 50 spectrometer with solution samples (DMF or CH_3CN) in 1 cm quartz cells. Fluorescence measurements were performed with the UV solutions on a PerkinElmer LS50B fluorescence spectrometer. Electrochemical measurements were carried out as a 1 mM solution in DMF or CH_3CN containing 0.1M TBA PF_6 as conducting electrolyte.

High performance liquid chromatography (HPLC) was performed on a Merck L7000 system, using a Macherey-Nagel Nucleosil C18 column. HPLC solvents were 0.1% trifluoroacetic acid (solvent A) and methanol HPLC grade (solvent B). The HPLC

gradient used is as follows: 0-3 minutes: 100% A; 3.1-9 minutes: 75% A, 25% B; 9.1-20 minutes: linear gradient from 66% A (34% B) to 0% A (100% B); 20-28 minutes: 100% B; 28.1-30: 100% A. The flow rate was 0.5 ml/min. Detection was performed at 250 nm. The detection of radioactive ^{99m}Tc/^{99}Tc complexes was performed with a Berthold LB508 radiodetector equipped with a NaI(Tl) scintillation detector.

4.1.3. Crystal structure determination

Crystallographic data were collected at 183(2)° K with Mo K_α radiation (λ = 0.7107 Å) that was monochromated with help of a graphite, on either a Stoe IPDS diffractometer (compounds **1a**, **1c**, **2**, **3**, **5**, **8**, **9**, **12**, **13**, **15,** and **16**) or an Oxford Diffraction Xcalibur system with a Ruby detector (compounds **1d**, **6**, **12a**, **16a, 17**, **18**). Suitable crystals were covered with oil (Infineum V8512, formerly known as Paratone N), mounted on top of a glass fibre and immediately transferred to the diffractometer. In the case of the IPDS, a maximum of eight thousand reflections distributed over the whole limiting sphere were selected by the program SELECT and used for unit cell parameter refinement with the program CELL.[103] Data were corrected for Lorentz and polarisation effects as well as for absorption (numerical). In case of the Oxford system, the program suite CrysAlis^{Pro} was used for data collection, semi-empirical absorption correction and data reduction.[104] Crystallographic data of compound **11** were collected at 183(2)° K on a Stoe IPDS 2T diffractometer with Cu K_α radiation (λ = 1.54186 Å). An extremely thin crystal was mounted with help of MicroMounts™ manufactured by MiTeGen, Ithaca, USA, and immediately transferred to the diffractometer. Reflection data was processed with the help of the program X-Area.[105] Data were corrected for Lorentz and polarisation effects as well as for absorption (numerical).

Structures were solved with direct methods using SIR97[106] and were refined by full-matrix least-squares methods on F^2 with SHELXL-97.[107] The structures were checked for higher symmetry with help of the program Platon.[108]

4.2. Synthetic work

4.2.1. Synthesis of $(Et_4N)[ReBr_2(NCCH_3)_2(CO)_2]$ (1)

Method A

200 mg $(Et_4N)[ReBr_4(CO)_2]$ (0.289 mmol) were dissolved in 9 ml CH_3CN, 700 mg (100 eq.) Mg° (activated with 1 M HCl) added and stirred for 16 h at RT under N_2. The colour changed from dark red to green/brown. Filtering off Mg° and the reaction residue with a celite-filter and evaporating the solvent in vacuum gave the crude product, that was washed in boiling EtOH to get **1** in a yield of 68%.

Method B

200 mg $(Et_4N)[ReBr_4(CO)_2]$ (0.289 mmol) was dissolved in 5 ml CH_3CN, 75 µl (1.1 eq.) TDAE added and stirred for 1 h at RT under N_2. $(TDAE)Br_2$ was removed by filtration and the solution dried in vacuum. The residue was washed in boiling EtOH to get **1** in a yield of 86% (Found: C, 27.18; H, 4.18; N, 6.88. Calc. for $C_{14}H_{26}Br_2N_3O_2Re$: C, 27.37; H, 4.27; N, 6.84); ν_{max} (KBr) [cm^{-1}]: 2274 (CN), 1893 (CO), 1794 (CO); δ_H (D_2O, 200 MHz) 3.13 (q, J = 7.4 Hz, 8H), 2.40 (s, 6H), 1.13 (tt, J = 7.4, 2.0 Hz, 12H); m/z (ESI) 460 $[M - Br]^+$, 419 $[M – Br - CH_3CN]^+$.

4.2.2. Synthesis of $[ReBr(NCCH_3)_3(CO)_2]$ (1a)

Method A

200 mg $(Et_4N)[ReBr_4(CO)_2]$ (0.289 mmol) was dissolved in 9 ml CH_3CN, 700 mg (100 eq.) Mg° (activated with 1 M HCl) added and stirred for 16 h at RT under N_2. The colour changed from dark red to green/brown. Filtering off Mg° and the reaction residue with a celite-filter and evaporating the solvent in vacuum gave the crude product, that was dissolved in 2 ml CH_3CN. The residue was filtered off and the solution cleaned by column separation (silica gel/CH_3CN). After the yellow and orange band, the greenish band was collected and dried in vacuum to get **1a** (73 mg, 56%).

Method B

200 mg $(Et_4N)[ReBr_4(CO)_2]$ (0.289 mmol) were dissolved in 5 ml CH_3CN, 75 µl (1.1 eq.) TDAE added and stirred for 1 h at RT under N_2. Filtering off $(TDAE)Br_2$ and evaporating the solvent in vacuum gave the crude product, which was dissolved in 1 ml CH_3CN. The solution was cleaned by column separation (silica gel/CH_3CN). After the yellow and orange band, the greenish band was collected and dried in vacuum to get **1a** (80 mg, 62%) (Found: C, 21.26; H, 1.96; N, 9.21. Calc. for $C_8H_9BrN_3O_2Re$: C, 21.58; H, 2.04; N, 9.44); ν_{max} (KBr) [cm^{-1}]: 2281 (CN), 1940 (CO), 1840 (CO); m/z (ESI) 366 $[M - Br]^+$.

4.2.3. Synthesis of $(Et_4N)[ReBr_2(NCC_6H_5)_2(CO)_2]$ (1b)

250 mg (0.362 mmol) of $(Et_4N)[ReBr_4(CO)_2]$ were dissolved in 4 ml benzonitrile and 1.5 eq. of TDAE was added. $(TDAE)Br_2$ was removed by filtration and the solution dried in vacuum. The residue was washed with acetone to get **1b** (140 mg, 50%) as a brown powder (Found: C, 38.81; H, 4.16; N, 5.91. Calc. for $C_{24}H_{30}Br_2N_3O_2Re$: C, 39.03; H, 4.09; N, 5.69); ν_{max} (KBr) [cm^{-1}]: 2226 (CN), 1901 (CO), 1815 (CO); δ_H (MeOD, 200 MHz) 7.90-7.52 (10H, m, $NCC_6\mathit{H}_5$), 3.30 (8H, m, $N\text{-}(C\mathit{H}_2CH_3)_4$ + MeOH), 1.29 (12H, m, $N\text{-}(CH_2C\mathit{H}_3)_4$); m/z (ESI) 481 $[M - 2Br + CH_3OH]^+$, 467 $[M - 2Br + H_2O]^+$, 449 $[M - 2Br]^+$.

4.2.4. Synthesis of $(Et_4N)[ReBr_2(CO)_2(imz)_2]$ (1c)

200 mg (0.289 mmol) of $(Et_4N)[ReBr_4(CO)_2]$ were dissolved in 5 ml dimethoxyethane. 100 mg imidazole (5 eq.) and 1 eq. of TDAE were added at once. The red solution turned to colourless and precipitation started immediately. After 30 min, the solution was decanted and the residue dried under vacuum. 3 ml of water was added to the residue and the suspension was stirred for 1 hour. Filtering and washing with water ended in **1c** (104 mg, 49%) as a slightly brownish powder (Found: C, 28.15; H, 3.89; N,

10.77. Calc. for $C_{16}H_{28}Br_2N_5O_2Re$: C, 28.75; H, 4.22; N, 10.48); ν_{max} (KBr) [cm^{-1}]: 1870 (CO), 1781, 1768 (CO); δ_H (MeOD, 200 MHz) 7.90 (s, 2H), 7.20 (t, *J* = 1.4 Hz, 2H), 7.02 (t, *J* = 1.4 Hz, 2H), 2.57 (s, 6H, NCC*H*$_3$).

4.2.5. Synthesis of $[ReBr(CO)_2(py)_3]$ (1d)

150 mg (0.218 mmol) of $(Et_4N)[ReBr_4(CO)_2]$ were dissolved in 5 ml pyridine and 1 eq. of TDAE was added. The red solution turned to brownish and precipitation started immediately. After 30 min, the volume of the solution was reduced to 2 ml under vacuum. The precipitated $(TDAE)Br_2$ was removed by filtration and the remaining solution dried under vacuum. The crude product was dissolved in acetone, the additional remaining $(TDAE)Br_2$ was removed by filtration and the solution was dried to get **1d**. ν_{max} (KBr) [cm^{-1}]: 1873 (CO), 1783 (CO).

4.2.6. Synthesis of *mer*-$[ReBr(NCCH_3)_2(CO)_3]$ (2)

0.2 g (0.33 mmol) **1** were dissolved in a small autoclave in 5 ml H_2O and degassed the system from non CO gases. 40 bar of CO were then applied. After 6 h the CO was removed, and the fine colourless precipitation was centrifuged, washed with H_2O and Et_2O and dried to give 0.127 g (90%) **2** as a white powder (Found: C, 19.38; H, 1.47; N, 6.44. Calc. for $C_7H_6BrN_2O_3Re$: C, 19.45; H, 1.40; N, 6.48); ν_{max} (KBr) [cm^{-1}]: 2285 (CN), 2065 (CO), 1954 (CO), 1887 (CO), 1827 (CO); δ_H ($CDCl_3$, 200 MHz) 2.50 (s).

4.2.7. Synthesis of $[Re(NCCH_3)_2(CO)_2(imz)_2]Br$ (3)

50 mg (82 μmol) of **1** were dissolved in 5 ml MeOH and 22.3 mg (4 eq.) of imidazole added and stirred at 60° C. After 2 h the solvent was evaporated the residue washed twice with THF and CH_2Cl_2 and dried to yield 27.7 mg (51 μmol, 63%) **3** (Found: C,

26.71; H, 2.52; N, 15.58. Calc. for $C_{12}H_{14}BrN_6O_2Re$: C, 26.67; H, 2.61; N, 15.55); ν_{max} (KBr) [cm^{-1}]: 2262 (CN), 1916 (CO), 1827 (CO); δ_H (MeOD, 200 MHz) 7.91 (s, 2H), 7.20 (m, 2H), 7.03 (m, 2H), 2.58 (s, 6H); m/z (ESI) 460 $[M - Br]^+$, 419 $[M – Br - CH_3CN]^+$.

4.2.8. Synthesis of $[Re(NCCH_3)_2(CO)_2(bzimz)_2]Br$ (4)

50 mg (82 µmol) of **1** were dissolved in 3 ml H_2O and 21.2 mg (2.2 eq.) benzimidazole (bzimz) added and stirred under N_2 for 1 h. The precipitation was filtered off, washed with water and dried to get an off-white powder (Found: C, 37.29; H, 3.09; N, 12.96. Calc. for $C_{20}H_{18}BrN_6O_2Re$: C, 37.50; H, 2.83; N, 13.12); ν_{max} (KBr) [cm^{-1}]: 2269 (CN), 1917 (CO), 1828 (CO); m/z (ESI) 561 $[M - Br]^+$, 443 $[M – Br – bzimz]^+$.

4.2.9. Synthesis of $[Re(NCCH_3)_2(CO)_2(9EtG)_2]Br$ (5)

50 mg (82 µmol) of **1** were dissolved in 3 ml H_2O and 29.2 mg (2 eq.) 9EtG added and stirred under N_2 over several days at 60° C. The reaction mixture was cooled to RT and the resulting precipitation was filtered off. ν_{max} (KBr) [cm^{-1}]: 2271 (CN), 1917 (CO), 1834 (CO); m/z (ESI) 684 $[M - Br]^+$, 504 $[M – Br – 9EtG]^+$, 463 $[M – Br – 9EtG - CH_3CN]^+$.

4.2.10. Synthesis of $[ReBr(NCCH_3)_2(CO)_2(imz)]$ (6)

47 mg (110 µmol) of *mer*-$\{Re(CO)_3\}^+$ **2** were dissolved in 5 ml THF, 4 eq. imidazole added and stirred under N_2 at 60° C. The precipitation was filtered off, washed with THF and dried to get **6** (42.2 mg, 82%) as a white powder (Found: C, 23.06; H, 2.19; N, 11.72. Calc. for $C_9H_9BrN_4O_2Re$: C, 22.89; H, 2.13; N, 11.86); ν_{max} (KBr) [cm^{-1}]: 2274

(CN), 1910 (CO), 1819 (CO); δ_H (MeOD, 200 MHz) 8.11 - 7.27 (m, 3H), 2.59 (s, 6H). m/z (ESI) 393 $[M - Br]^+$.

4.2.11. Synthesis of $[Re(NCCH_3)_2(CO)_2(bpy)]Br$ (8)

Method A

50.5 mg (120 μmol) of *mer*-$\{Re(CO)_3\}^+$ **2** were dissolved in 4 ml THF, 36.1 mg (2 eq.) bipyridine added and stirred under N_2 at 50° C. After a few minutes a red precipitation was formed which was filtered off, washed with Et_2O and dried under vacuum to give **8** (59.8 mg, 92%).

Method B

$[ReBr(NCCH_3)_3(CO)_2]$ (**1a**) was dissolved in CH_3CN, 1.1 eq. 2,2'-bipyridyl added and stirred overnight at RT. Evaporating the solvent and recrystallisation from DCM/hexane yields **8** (83 %) (Found: C, 34.27; H, 2.63; N, 9.71. Calc. for $C_{16}H_{14}BrN_4O_2Re$: C, 34.29; H, 2.52; N, 10.00); ν_{max} (KBr) [cm^{-1}]: 2273 (CN), 1926 (CO), 1853, 1835 (CO); δ_H (MeOD, 200 MHz) 9.10 (m, 2H), 8.61 (m, 2H), 8.26 (m, 2H), 7.73 (m, 2H), 2.28 (s, 6H). m/z (ESI) 480 $[M - Br - 1]^+$, 440 $[M - Br - CH_3CN]^+$; λ_{max} [nm] (ε) [l mol^{-1} cm^{-1}]: 423 (3000).

4.2.12. Synthesis of $[Re(NCCH_3)_2(CO)_2(phd)]Br$ (9)

Method A

50.5 mg (117 μmol) of *mer*-$\{Re(CO)_3\}^+$ **2** were dissolved in 5 ml THF, 25 mg (1 eq.) 7,7'phenanthroline-dione (phd) added and stirred under N_2 at 60° C. After a few minutes a dark red precipitation was formed which was filtered off, washed with THF and dried under vacuum to give **9** (66.8 mg, 94%).

Method B

25 mg (56 μmol) of **1a** were dissolved in 3 ml CH_3CN, 14 mg (1.2 eq.) phd added and stirred under N_2 over weekend at RT. The solvent was evaporated in vacuum and the crude product recrystallised with EtOH/hexane to give **9** (25 mg, 70%). (Found: C, 35.00 H, 2.12; N, 9.21. Calc. for $C_{18}H_{12}BrN_4O_4Re$: C, 35.19; H, 1.97; N, 9.12); ν_{max} (KBr) [cm^{-1}]: 2273 (CN), 1933 (CO), 1850 (CO); δ_H (DMSO, 300 MHz) 9.19 (dd, *J* = 5.4, 1.5 Hz, 2H), 8.73 (dd, *J* = 8.1, 1.5 Hz, 2H), 7.99 (dt, *J* = 5.4, 2.4 Hz, 2H), 2.38 (s, 6H); m/z (ESI) 615 $[M+1]^+$, 599 $[M - Br + 2CH_3OH]^+$, 567 $[M - Br + CH_3OH]^+$, 553 $[M - Br + H_2O]^+$, 535 $[M - Br]^+$. λ_{max} [nm] (ε) [l mol^{-1} cm^{-1}]: 420 (5200).

4.2.13. Synthesis of $[Re(NCCH_3)_2(CO)_2(pham)]Br$ (10)

100 mg (164 μmol) of **1** were dissolved in 3 ml MeOH, 34 mg (1 eq.) pham added and stirred under N_2 overnight at RT. The solvent was evaporated in vacuum and the crude product recrystallised with EtOH/hexane to give **10** (61 mg, 61%). ν_{max} (KBr) [cm^{-1}]: 1926 (CO), 1843 (CO); m/z (ESI) 535 $[M - Br]^+$. λ_{max} [nm] (ε) [l mol^{-1} cm^{-1}]: 412 (26100), 641 (113000).

4.2.14. Synthesis of $[(Re(NCCH_3)_2(CO)_2)_2(tpphz)]Br_2$ (11)

20 mg (52 μmol) of tpphz were dissolved in 5 ml CH_3CN, 67 mg (2.1 eq.) **1** added and heated to reflux under N_2. After 1 hour an orange precipitate started forming and after 30 hours the reaction was complete. The precipitate was filtered off, washed with a small amount of cold CH_3CN and dried under vacuum to give **11** almost quantitatively. (Found: C, 36.10 H, 2.31; N, 11.54. Calc. for $C_{36}H_{26}Br_2N_{10}O_4Re_2$: C, 36.19; H, 2.19; N, 11.72); ν_{max} (KBr) [cm^{-1}]: 2280 (CN), 1932 (CO), 1857 (CO); m/z (ESI) 517 $[M-2Br]^{2+}$. λ_{max} [nm] (ε) [l mol^{-1} cm^{-1}]: 430 (14000).

4.2.15. Synthesis of $[Re(NCCH_3)_2(CO)_2(terpy)]Br$ (12)

50 mg **1** were dissolved in 3 ml H_2O, 1 eq. (19 mg) 2,2':6',2''-terpyridine (terpy) added and stirred for 4 h at 60° C. Evaporating the solvent and recrystallisation from acetone ended in **12** (40 mg, 77 %) as an orange/red powder (Found: C, 38.63; H, 3.08; N, 10.43. Calc. for $C_{21}H_{17}BrN_5O_4Re$: C, 39.56; H, 2.69; N, 10.99; ν_{max} (KBr) [cm^{-1}]: 2268 (CN), 1922 (CO), 1853 (CO); m/z (ESI) 558 $[M - Br]^+$, 517 $[M - Br - CH_3CN]^+$, 476 $[M - Br - 2CH_3CN]^+$. λ_{max} [nm] (ε) [l mol^{-1} cm^{-1}]: 420 (10000).

4.2.16. Synthesis of $[ReBr(CO)_2(terpy)]$ (12a)

100 mg (230 μmol) of *mer*-$\{Re(CO)_3\}^+$ **2** were dissolved in 10 ml THF at 60° C, 60 mg (1.1 eq.) terpy added and stirred under N_2 at 60° C for 5 h. The reaction mixture was cooled to RT, the volume reduced to half under vacuum and cooled in the fridge overnight. The resulting suspension was centrifuged, washed with 2 ml THF, centrifuged again and dried under vacuum to give **12a** (92 mg, 71%) (Found: C, 36.82; H, 2.02; N, 7.36. Calc. for $C_{17}H_{11}BrN_3O_2Re$: C, 36.76; H, 2.00; N, 7.57); ν_{max} (KBr) [cm^{-1}]: 1883 (CO), 1806 (CO), 775 (CN_{terpy}); δ_H (DMSO, 200 MHz) 8.87 (m, 2H), 8.56 (m, 4H), 8.20 (t, J = 8 Hz, 1H), 8.01 (m, 2H), 7.46 (s, 6H). m/z (ESI) 578 $[M + Na]^+$, 555 $[M]^+$, 507 $[M - Br + OCH_3]^+$, 476 $[M - Br]^+$. λ_{max} [nm] (ε) [l mol^{-1} cm^{-1}]: 400 (10400), 470 (10400).

4.2.17. Synthesis of $[Re(2\text{-pic})(NCCH_3)_2(CO)_2]$ (13)

50 mg (82 μmol) of **1** were dissolved in 3 ml H_2O and 11 mg (1.1 eq.) of 2-pic added and stirred at 40° C. The solution turned immediately to yellow. After a few minutes, **13** started to precipitate. After 4 h the mixture was cooled to RT. 25 mg (56 μmol, 69%) of **13** was collected by filtration (Found: C, 32.39; H, 2.41; N, 9.58. Calc. for $C_{12}H_{10}N_3O_4Re$: C, 32.28; H, 2.26; N, 9.41); ν_{max} (KBr) [cm^{-1}]: 2272 (CN), 1913 (CO),

1835 (CO); δ_H (MeOD, 200 MHz) 8.86 (m, 1H), 8.15 (m, 2H), 7.72 (m, 1H), 2.37 (s, 6H); m/z (ESI) 447 $[M]^+$, 407 $[M - CH_3CN]^+$.

4.2.18. Synthesis of $[Re(2,5\text{-dipic})(NCCH_3)_2(CO)_2]$ (14)

40 mg (66 μmol) of **1** were dissolved in 1 ml H_2O and 11 mg (1.1 eq.) of 2,5-dipic in 0.5 ml H_2O added and stirred at RT. The solution turned to orange/red and after several minutes, **14** started to precipitate. After a few hours 25 mg (56 μmol, 69%) of **14** was collected by filtration (Found: C, 31.64; H, 2.36; N, 8.34. Calc. for $C_{13}H_{10}N_3O_6Re$: C, 31.84; H, 2.06; N, 8.57); ν_{max} (KBr) [cm^{-1}]: 2284 (CN), 1939 (CO), 1817 (CO); δ_H (d_6-DMSO, 200 MHz) 9.12 (s, 1H), 8.59 (dd, 1H), 8.16 (d, 1H), 2.07 (s, 6H); m/z (ESI) 492 $[M+H]^+$.

4.2.19. Synthesis of $[Re(BPG)(CO)_2]$ (15)

100 mg (163 μmol) of **1** were dissolved in 3 ml H_2O, 47 mg (1.1 eq.) BPG added and heated to 110° C. After refluxing overnight the precipitation was filtered off, washed with water and dried to yield **15** (40 mg, 49%) as a yellow powder (Found: C, 38.41; H, 2.90; N, 8.32. Calc. for $C_{16}H_{14}N_3O_4Re$: C, 38.55; H, 2.83; N, 8.43); ν_{max} (KBr) [cm^{-1}]: 1882 (CO), 1787, 1774 (CO), 1634 (CO); δ_H (MeOD, 200 MHz) 8.72 (d, *J* = 5.5 Hz, 2H), 7.90 (dt, *J* = 7.5, 1.5 Hz, 2H), 7.54 (t, *J* = 8 Hz, 2H), 7.34 (t, *J* = 6.5, 2H), 4.90 (d, *J* = 15 Hz, 2H), 4.39 (d, *J* = 15 Hz, 2H), 3.42 (s, 2H). m/z (ESI) 522 $[M+Na]^+$, 500 $[M + H]^+$; HPLC (TFA / MeOH, C18rp) [min] 17.7.

4.2.20. Synthesis of $(Himz)[Re(2\text{-pic})_2(CO)_2]$ (16)

30 mg (45 μmol) of **1c** were dissolved in 3 ml H_2O and 11 mg (2 eq.) 2-pic added. The solution turns dark red within 2 hours. After stirring overnight, the solvent was removed

in vacuum and the residue dissolved in CH_2Cl_2. Filtering of the $(Et_4N)Br$ and drying the solution gave **16**. Single crystals were obtained by layering of a methanol solution with hexane. ν_{max} (KBr) [cm^{-1}]: 1882 (CO), 1775 (CO), 1631 (CO), 1591 (CO), 1360; HPLC (TFA, C18rp) [min] 15.6; δ_H (MeOD, 500 MHz) 8.96 (d, *J* = 5.5 Hz, 2H), 8.89 (s, 1H), 8.00 (d, *J* = 7.5 Hz, 2H), 7.92 (t, *J* = 7.5 Hz, 2H), 7.57 (s, 2H), 7.44 (t, *J* = 6.5 Hz, 2H), 1.29 (s, 2H); λ_{max} [nm] 393.

4.2.21. Synthesis of $[Re(bpy)(CO)_2(imz)_2]Br$ (16a)

56 mg (84 μmol) of **1c** were dissolved in 5 ml MeOH, 35 mg (2.5 eq.) bpy added and heated at 70° C. The solution turns from slightly yellow to dark red within a few minutes. After stirring for 3 hours, the solvent was removed in vacuum and the residue reprecipitated from CH_2Cl_2 into stirring Et_2O giving $[Re(bpy)(CO)_2(imz)_2]Br$ (**16a**). Single crystals were obtained by slowly evaporating a methanol solution of **16a**. ν_{max} (KBr) [cm^{-1}]: 1881 (CO), 1809 (CO); m/z (ESI) 535 $[M\text{-}Br]^+$; λ_{max} [nm] 385, 515.

4.2.22. Synthesis of $[ReBr_2(CO)_2(py)_2]$ (17)

200 mg of $(Et_4N)[ReBr_4(CO)_2]$ (0.289 mmol) were dissolved in 10 ml DME, 20 eq. (500 μl) of pyridine added together with 34 μl (0.5 eq.) TDAE. The precipitation was separated from the solution and dried. The brown powder was washed with a few MeOH, filtered and dried to yield **17** (90 mg, 50%). (Found: C, 25.51; H, 1.69; N, 5.12. Calc. for $C_{12}H_{10}Br_2N_2O_2Re$: C, 25.73; H, 1.80; N, 5.00); ν_{max} (KBr) [cm^{-1}]: 1991 (CO), 1825 (CO).

4.2.23. Synthesis of $(Et_4N)_2[ReBr_4(CO)_2]$ (18a)

100 mg of $(Et_4N)[ReBr_4(CO)_2]$ (0.145 mmol) and 306 mg $(Et_4N)Br$ (10 eq.) were dissolved in 5 ml CH_3CN and 17 µl (0.5 eq.) TDAE added. After 5 min the precipitate was removed and the solution dried. The brown powder was washed with DCM, filtered and dried to yield **18a** as a bright red solid. (Found: C, 26.20; H, 4.98; N, 3.29. Calc. for $C_{18}H_{40}Br_4N_2O_2Re$: C, 26.29; H, 4.90; N, 3.41); ν_{max} (KBr) [cm^{-1}]: 1973 (CO), 1795 (CO).

4.2.24. Synthesis of $(Et_4N)_2[^{99}TcBr_3(CO)_3]$ (19)

A three-neck flask equipped with a reflux condenser and two septa was flushed with CO for 15 min and 449 mg $(Bu_4N)[^{99}TcO_4]$ (1 mmol) were dissolved in 5 ml THF. 25 ml of a 1 M BH_3-THF solution was added to the three-neck flask and CO bubbled through the solution. The pertechnetate solution was added by a syringe-pump with a rate of about 50 µl per minute. The solution turned dark brown and some slurry was formed. Nevertheless, after the full addition a brown solution remained which was evaporated with a N_2 stream at 40° C. To the residue a solution of 1.28 g $(Et_4N)Br$ in 5 ml EtOH containing 500 µl H_2O was added as well as a solution of 153 µl TFA in 500 µl H_2O. The solution was stirred for 12 hours. An orange precipitate could be filtered off and dried under vacuum to get 337 mg **19** in a 50% yield. The remaining solution was dried and the workup repeated (2 ml EtOH, 0.5 g $(Et_4N)Br$, 200 µl HBr) to get another 130 mg of complex **19**. Total yield: 446 mg (68 %). ν_{max} (KBr) [cm^{-1}]: 2022 (CO), 1913, 1898 (CO); HPLC (TFA/MeOH, C18rp) [min] 5.5.

4.3. Supplementary information

4.3.1. Crystallographic data

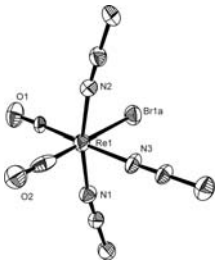

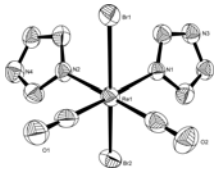

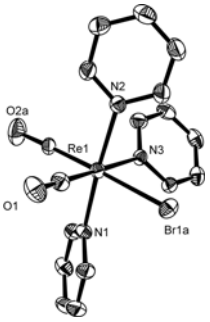

	1a	**1c**	**1d**
	lk060404	lk051006	lk171207
Empirical formula	$C_8H_9BrN_3O_2Re$	$C_{16}H_{28}Br_2N_5O_2Re$	$C_{17}H_{15}BrN_3O_2Re$
Formula weight	445.29	668.45	559.43
Diffractometer	STOE IPDS	STOE IPDS	Oxford Xcalibur
Crystal system	Hexagonal	Monoclinic	Monoclinic
Space group	$P6_3$	$P2_1/n$	$P2_1/n$
a [Å]	16.9076(7)	8.0465(5)	9.35820(10)
b [Å]	16.9076(7)	18.4213(10)	13.2804(2)
c [Å]	7.9231(3)	14.7645(11)	14.3410(2)
α [°]	90	90	90
β [°]	90	99.161(8)	90.3750(13)
γ [°]	120	90	90
Volume [$Å^3$]	1961.51(14)	2160.6(2)	1782.27(4)
Z	6	4	4
Crystal size [mm^3]	0.43 x 0.04 x 0.03	0.45 x 0.13 x 0.09	0.51 x 0.24 x 0.23
Crystal description	pale yellow needle	colourless needle	light red block
Reflections collected	21807	30848	21695
Independent refl. [R(int)]	3967 [0.0914]	4893 [0.0632]	5432 [0.0312]
Refl. observed [I>2σ (I)]	2733	4194	4449
Completeness to Θ [°, %]	30.46°, 99.5%	27.88°, 94.8%	30.51°, 99.9 %
Goodness-of-fit on F^2	0.827	1.154	1.068
Final R indices [I>2σ (I)]	R1 = 0.0318	R1 = 0.0501	R1 = 0.0248
	wR2 = 0.0644	wR2 = 0.1330	wR2 = 0.0531
Diff. peak and hole [e/$Å^3$]	1.088 and –0.578	1.943 and –1.551	1.171 and -2.404

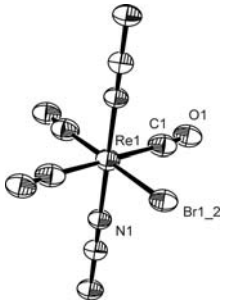

2

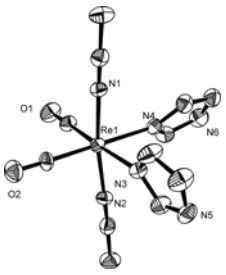

3

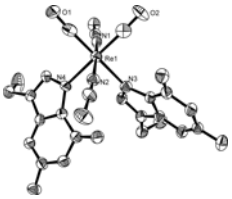

5

	lk130206	lk200904	lk260705
Empirical formula	$C_7H_6BrN_2O_3Re$	$C_{12}H_{14}BrN_6O_2Re$	$C_{22}H_{34}BrN_{12}O_7Re$
Formula weight	432.25	540.4	844.72
Diffractometer	STOE IPDS	STOE IPDS	STOE IPDS
Crystal system	Monoclinic	Monoclinic	Monoclinic
Space group	I2/m	$P2_1/c$	$P2_1/n$
a [Å]	5.9303(4)	14.8912(9)	10.3611(7)
b [Å]	7.8984(4)	6.9874(3)	27.153(2)
c [Å]	11.8361(8)	16.913(1)	11.6030(8)
α [°]	90	90	90
β [°]	102.334(8)	106.203(7)	105.975(7)
γ [°]	90	90	90
Volume [$Å^3$]	541.61(6)	1689.94(16)	3138.2(4)
Z	2	4	4
Crystal size [mm^3]	0.26 x 0.13 x 0.10	0.35 x 0.12 x 0.11	0.32 x 0.19 x 0.06
Crystal description	colourless block	colourless needle	colourless plate
Reflections collected	4657	24560	33748
Independent refl. [R(int)]	862 [0.0625]	5090 [0.1038]	7579 [0.0615]
Refl. observed [I>2σ (I)]	853	3736	6307
Completeness to Θ [°, %]	30.34°, 98.1%	30.45°, 99.3%	28.15°, 98.4%
Goodness-of-fit on F^2	1.204	0.973	1.056
Final R indices [I>2σ (I)]	R1 = 0.0483	R1 = 0.0401	R1 = 0.0609
	wR2 = 0.1085	wR2 = 0.0996	wR2 = 0.1589
Diff. peak and hole [e/$Å^3$]	1.257 and –1.294	1.853 and –1.075	3.639 and –2.244

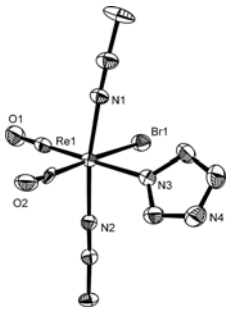

6

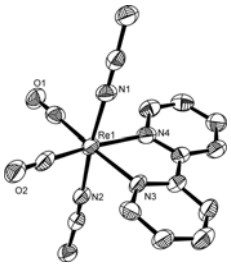

8

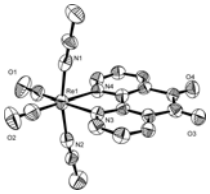

9

	lk180207	lk220404	lk080606
Empirical formula	$C_9H_{10}BrN_4O_4Re$	$C_{16}H_{14}BrN_4O_2Re$	$C_{18}H_{12}BrN_4O_4Re$
Formula weight	504.32	560.42	614.43
Diffractometer	Oxford Xcalibur	STOE IPDS	STOE IPDS
Crystal system	Monoclinic	Monoclinic	Monoclinic
Space group	$P2_1/n$	$P2_1/c$	P2/n
a [Å]	8.9458(1)	13.6113(8)	16.7319(14)
b [Å]	13.2486(2)	9.9206(5)	7.0306(4)
c [Å]	11.8010(1)	14.5778(11)	16.9965(14)
α [°]	90	90	90
β [°]	98.1046(9)	109.508(8)	93.374(10)
γ [°]	90	90	90
Volume [$Å^3$]	1384.68(3)	1855.5(2)	1995.9(3)
Z	4	4	4
Crystal size [mm^3]	0.25 x 0.14 x 0.08	0.48 x 0.07 x 0.03	0.14 x 0.07 x 0.06
Crystal description	colourless needle	red needle	dark block
Reflections collected	38867	19615	12670
Independent refl. [R(int)]	4225 [0.0356]	4936 [0.1399]	3438 [0.0923]
Refl. observed [I>2σ (I)]	2768	3142	2592
Completeness to Θ [°, %]	30.51°, 100%	29.13°, 98.9%	25.03°, 97.3%
Goodness-of-fit on F^2	1.094	0.887	1.058
Final R indices [I>2σ (I)]	R1 = 0.0256	R1 = 0.0554	R1 = 0.0674
	wR2 = 0.0704	wR2 = 0.1259	wR2 = 0.1672
Diff. peak and hole [e/$Å^3$]	2.301 and –1.532	2.795 and –3.569	1.617 and –1.503

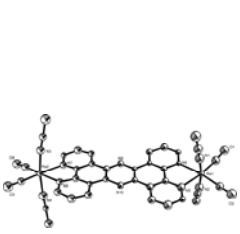
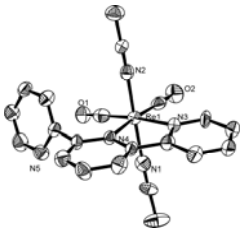
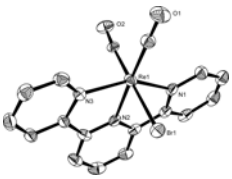

	11	**12**	**12a**
	lk230805	lk011106	lk050407
Empirical formula	$C_{36}H_{24}Br_2N_{10}O_4Re_2$	$C_{24}H_{23}BrN_5O_3Re$	$C_{17}H_{11}BrN_3O_2Re$
Formula weight	1192.87	695.58	555.4
Diffractometer	STOE IPDS 2T	STOE IPDS	Oxford Xcalibur
Crystal system	Triclinic	Monoclinic	Monoclinic
Space group	P-1	$P2_1/c$	$P2_1/n$
a [Å]	11.9779(12)	10.9719(5)	9.3642(2)
b [Å]	13.5611(13)	11.9900(6)	13.4741(2)
c [Å]	16.3820(18)	19.9938(9)	13.5254(3)
α [°]	78.143(8)	90	90
β [°]	69.544(8)	98.851(5)	109.370(2)
γ [°]	74.587(8)	90	90
Volume [$Å^3$]	2384.8(4)	2598.7(2)	1609.96(6)
Z	2	4	4
Crystal size [mm^3]	0.23 x 0.08 x 0.01	0.36 x 0.10 x 0.06	0.20 x 0.12 x 0.07
Crystal description	red plate	red needle	dark prism
Reflections collected	16357	20189	9885
Independent refl. [R(int)]	7006 [0.0710]	5513 [0.1061]	4057 [0.0215]
Refl. observed [I>2σ (I)]	5899	4275	3209
Completeness to Θ [°, %]	61.16°, 95.4%	26.73°, 99.9%	28.69°, 97.5 %
Goodness-of-fit on F^2	1.089	1.164	1.071
Final R indices [I>2σ (I)]	R1 = 0.0761	R1 = 0.0857	R1 = 0.0315
	wR2 = 0.1897	wR2 = 0.1911	wR2 = 0.0653
Diff. peak and hole [e/$Å^3$]	2.500 and –1.821	3.593 and –1.687	3.295 and -3.140

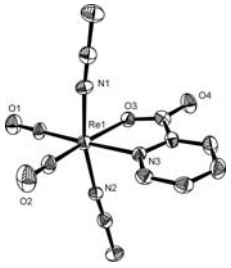

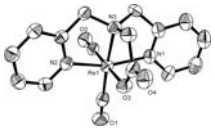

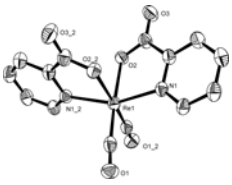

	13	**15**	**16**
	lk221004	lk291106	lk231006
Empirical formula	$C_{12}H_{10}N_3O_4Re$	$C_{17}H_{18}N_3O_5Re$	$C_{17}H_{13}N_4O_6Re$
Formula weight	446.43	530.54	555.51
Diffractometer	STOE IPDS	STOE IPDS	STOE IPDS
Crystal system	Triclinic	Monoclinic	Monoclinic
Space group	P-1	$P2_1/c$	P2/n
a [Å]	7.8212(6)	8.7181(6)	6.7596(6)
b [Å]	8.2437(7)	13.3999(10)	10.6665(7)
c [Å]	12.195(1)	15.7069(11)	12.7163(12)
α [°]	99.07(1)	90	90
β [°]	91.83(1)	100.189(8)	94.564(11)
γ [°]	115.964(9)	90	90
Volume [$Å^3$]	693.5(1)	1806.0(2)	913.95(13)
Z	2	4	2
Crystal size [mm^3]	0.31 x 0.17 x 0.03	0.32 x 0.05 x 0.04	0.33 x 0.10 x 0.08
Crystal description	yellow plate	yellow needle	red needle
Reflections collected	15124	22719	12942
Independent refl. [R(int)]	3862 [0.0811]	4291 [0.0569]	2115 [0.1000]
Refl. observed [I>2σ (I)]	3285	3611	1953
Completeness to Θ [°, %]	30.48°, 91.4%	27.87°, 99.8%	28.27°, 93.4%
Goodness-of-fit on F^2	1.068	1.088	1.084
Final R indices [I>2σ (I)]	R1 = 0.0476	R1 = 0.0493	R1 = 0.0457
	wR2 = 0.1156	wR2 = 0.1387	wR2 = 0.1060
Diff. peak and hole [e/$Å^3$]	2.139 and –1.425	2.041 and –1.293	1.930 and –2.028

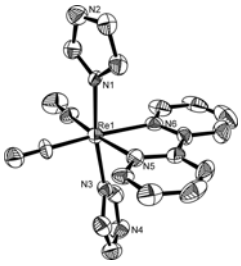

16a

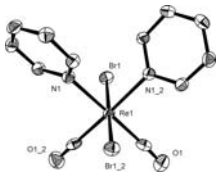

17

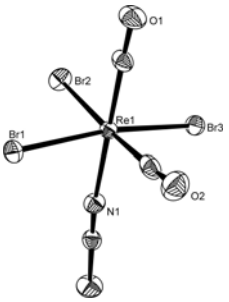

18

	lk030608	lk090307	lk120707
Empirical formula	$C_{18}H_{16}BrN_6O_2Re$	$C_{12}H_{10}Br_2N_2O_2Re$	$C_{20}H_{43}Br_4N_3O_2Re$
Formula weight	614.48	560.24	863.41
Diffractometer	Oxford Xcalibur	Oxford Xcalibur	Oxford Xcalibur
Crystal system	Orthorhombic	Monoclinic	Monoclinic
Space group	Pccn	C2/c	$P2_1/n$
a [Å]	19.1932(3)	7.5498(1)	8.9079(1)
b [Å]	15.7913(4)	14.6102(2)	13.8634(2)
c [Å]	13.9187(3)	12.9991(2)	23.8045(3)
α [°]	90	90	90
β [°]	90	91.924(1)	95.309(2)
γ [°]	90	90	90
Volume [$Å^3$]	4218.56(16)	1433.05(4)	2927.10(6)
Z	8	4	4
Crystal size [mm^3]	0.29 x 0.05 x 0.04	0.25 x 0.04 x 0.02	0.31 x 0.21 x 0.10
Crystal description	purple needle	red needle	red plate
Reflections collected	31584	31002	51064
Independent refl. [R(int)]	3856 [0.0817]	2184 [0.0413]	8929 [0.0331]
Refl. observed [I>2σ (I)]	2308	1836	7420
Completeness to Θ [°, %]	25.35°, 99.9%	30.51°, 100.0 %	30.51°, 99.9 %
Goodness-of-fit on F^2	0.943	1.091	1.277
Final R indices [I>2σ (I)]	R1 = 0.0458	R1 = 0.0252	R1 = 0.0526
	wR2 = 0.1101	wR2 = 0.0603	wR2 = 0.1342
Diff. peak and hole [e/$Å^3$]	1.635 and -1.201	2.786 and -1.410	8.024 and -2.823

4.3.2. Suggested structures of compounds not confirmed by x-ray analysis

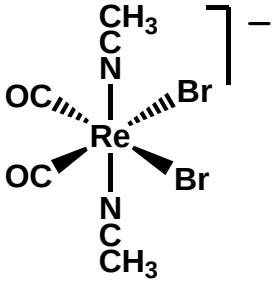

1

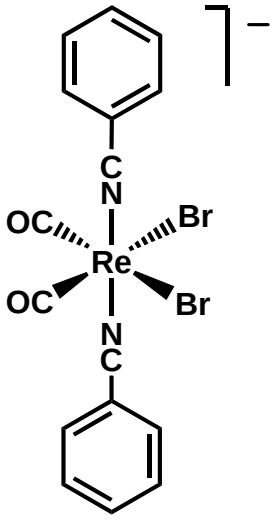

1b

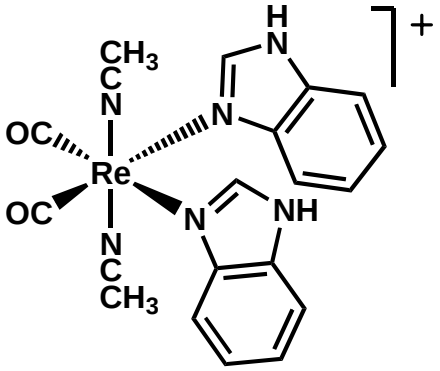

4

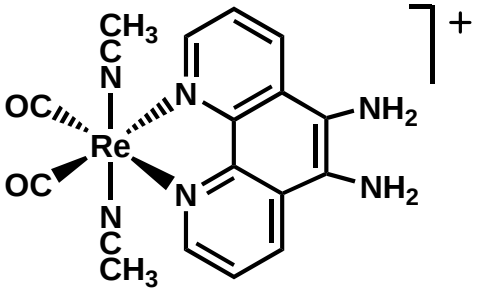

10

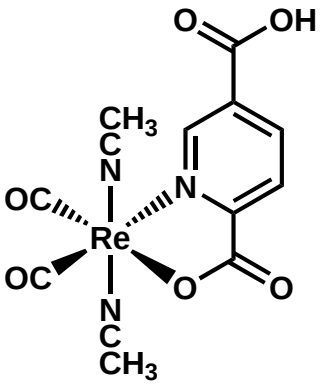

14

5. References

1. Hollemann-Wiberg, *Lehrbuch der Anorganischen Chemie*, Walter de Gruyter, Berlin, 1995.
2. U. Abram, in *Comprehensive Coordination Chemistry II*, eds. J. A. McCleverty and T. J. Meyer, Elsevier Pergamon, Amsterdam, Editon edn., 2003, vol. 5, pp. 271-402.
3. R. Alberto, in *Comprehensive Coordination Chemistry II*, eds. J. A. McCleverty and T. J. Meyer, Elsevier Pergamon, Amsterdam, Editon edn., 2003, vol. 5, pp. 127-270.
4. K. Schwochau, *Technetium*, WILEY-VCH, Weinheim, 2000.
5. D. Copplestone, D. Jackson, R. G. Hartnoll, M. S. Johnson, P. McDonald and N. Wood, *J. Environ. Radioact.*, 2004, **73**, 29-48.
6. R. J. M. Konings and R. Conrad, *J. Nucl. Mater.*, 1999, **274**, 336-340.
7. A. Besserguenev and M. T. Pope, *C. R. Chim.*, 2005, **8**, 933-955.
8. , American Chemical Society, Editon edn., 2006.
9. L. Mond, C. Langer and F. Quincke, *J. Organomet. Chem.* , 1990, **383**, 1-5.
10. W. Hieber and H. Fuchs, *Z. Anorg. Allg. Chem.* , 1941, **248**, 256-268.
11. M. I. Bruce, in *Comprehensive Organometallic Chemistry*, ed. G. Wilkinson, Pergamon Press Ltd, Oxfortd, Editon edn., 1982, vol. 4.
12. W. S. Greenlee and M. F. Farona, *Inorg. Chem.*, 1976, **15**, 2129-2134.
13. J. L. Jiang and R. M. Hua, *Chem. Res. Chin. Univ.*, 2007, **23**, 374-376.
14. J. L. Morgan, A. H. Flood, K. C. Gordon, B. H. Robinson and J. Simpson, *J. Organomet. Chem.* , 2003, **675**, 57-64.
15. E. Palma, J. D. G. Correia, A. Domingos, I. Santos, R. Alberto and H. Spies, *J. Organomet. Chem.* , 2004, **689**, 4811-4819.
16. J. R. Dilworth and S. J. Parrott, *Chem. Soc. Rev.*, 1998, **27**, 43-55.
17. S. Mundwiler, M. Kundig, K. Ortner and R. Alberto, *Dalton Trans.*, 2004, 1320-1328.
18. R. Alberto, R. Schibli, A. Egli, P. A. Schubiger, W. A. Herrmann, G. Artus, U. Abram and T. A. Kaden, *J. Organomet. Chem.* , 1995, **493**, 119-127.

19. V. V. Grushin, *Chem. Rev.* , 1996, **96**, 2011-2034.
20. M. Ephritikhine, *Chem. Rev.* , 1997, **97**, 2193-2242.
21. D. M. Heinekey, B. M. Schomber and C. E. Radzewich, *J. Am. Chem. Soc.* , 1994, **116**, 4515-4516.
22. D. G. Gusev, D. Nietlispach, I. L. Eremenko and H. Berke, *Inorg. Chem.*, 1993, **32**, 3628-3636.
23. X. Y. Liu, K. Venkatesan, H. W. Schmalle and H. Berke, *Organometallics*, 2004, **23**, 3153-3163.
24. D. Walther, *Coord. Chem. Rev.*, 1987, **79**, 135-174.
25. D. Walther, U. Ritter, Z. Undeutsch, R. Kempe and J. Sieler, *Chem. Ber.*, 1992, **125**, 1529-1536.
26. J. Hawecker, J. M. Lehn and R. Ziessel, *J. Chem. Soc., Chem. Commun.*, 1983, 536-538.
27. J. Hawecker, J. M. Lehn and R. Ziessel, *Helv. Chim. Acta*, 1986, **69**, 1990-2012.
28. B. Probst, University of Zürich, 2005.
29. P. Kurz, B. Probst, B. Spingler and R. Alberto, *Eur. J. Inorg. Chem.*, 2006, 2966-2974.
30. Y. Hayashi, S. Kita, B. S. Brunschwig and E. Fujita, *J. Am. Chem. Soc.* , 2003, **125**, 11976-11987.
31. W. L. Wong, K. C. Cheung, P. H. Chan, Z. Y. Zhou, K. H. Lee and K. Y. Wong, *Chem. Commun.*, 2007, 2175-2177.
32. P. Kurz, University of Zürich, 2005.
33. S. P. Schmidt, W. C. Trogler, F. Basolo, M. A. Urbancic and J. R. Shapley, in *Inorganic Syntheses*, ed. J. A. Robert, Editon edn., 2007, pp. 160-165.
34. R. Alberto, A. Egli, U. Abram, K. Hegetschweiler, V. Gramlich and P. A. Schubiger, *J. Chem. Soc., Dalton Trans.*, 1994, 2815-2820.
35. R. Alberto, R. Schibli, D. Angst, P. A. Schubiger, U. Abram, S. Abram and T. A. Kaden, *Transition Met. Chem.*, 1997, **22**, 597-601.
36. R. Alberto, R. Schibli, A. Egli, A. P. Schubiger, U. Abram and T. A. Kaden, *J. Am. Chem. Soc.* , 1998, **120**, 7987-7988.
37. R. Alberto, K. Ortner, N. Wheatley, R. Schibli and A. P. Schubiger, *J. Am. Chem. Soc.* , 2001, **123**, 3135-3136.

38. R. Schibli, R. Alberto, U. Abram, S. Abram, A. Egli, P. A. Schubiger and T. A. Kaden, *Inorg. Chem.*, 1998, **37**, 3509-3516.
39. I. Santos, A. Paulo and J. D. G. Correia, *Contrast Agents III: Radiopharmaceuticals - from Diagnostics to Therapeutics*, 2005, **252**, 45-84.
40. B. Salignac, P. V. Grundler, S. Cayemittes, U. Frey, R. Scopelliti, A. E. Merbach, R. Hedinger, K. Hegetschweiler, R. Alberto, U. Prinz, G. Raabe, U. Kolle and S. Hall, *Inorg. Chem.*, 2003, **42**, 3516-3526.
41. M. Kosel, C. Frick, S. H. Lisanby, H.-U. Fisch and T. E. Schlaepfer, *Neuropsychopharmacology*, 2003, **28**, 2045-2048.
42. M. Allali, E. Benoist, N. Habbadi, M. Gressier, A. Souizi and M. Dartiguenave, *Tetrahedron*, 2004, **60**, 1167-1174.
43. S. R. Banerjee, J. W. Babich and J. Zubieta, *Inorg. Chem. Commun.*, 2004, **7**, 481-484.
44. H. J. Pietzsch, A. Gupta, M. Reisgys, A. Drews, S. Seifert, R. Syhre, H. Spies, R. Alberto, U. Abram, P. A. Schubiger and B. Johannsen, *Bioconjugate Chem.*, 2000, **11**, 414-424.
45. M. Saidi, S. Seifert, M. Kretzschmar, R. Bergmann and H. J. Pietzsch, *J. Organomet. Chem.* , 2004, **689**, 4739-4744.
46. R. F. Vitor, S. Alves, J. D. G. Correia, A. Paulo and I. Santos, *J. Organomet. Chem.* , 2004, **689**, 4764-4774.
47. M. M. Saw, P. Kurz, N. Agorastos, T. S. A. Hor, F. X. Sundram, Y. K. Yan and R. Alberto, *Inorg. Chim. Acta*, 2006, **359**, 4087-4094.
48. J. K. Pak, P. Benny, B. Spingler, K. Ortner and R. Alberto, *Chem. -Eur. J.* , 2003, **9**, 2053-2061.
49. P. Hafliger, N. Agorastos, B. Spingler, O. Georgiev, G. Viola and R. Alberto, *Chembiochem*, 2005, **6**, 414-421.
50. N. Marti, B. Spingler, F. Breher and R. Schibli, *Inorg. Chem.*, 2005, **44**, 6082-6091.
51. P. Haefliger, N. Agorastos, A. Renard, G. Giambonini-Brugnoli, C. Marty and R. Alberto, *Bioconjugate Chem.*, 2005, **16**, 582-587.

52. P. Hafliger, S. Mundwiler, K. Ortner, B. Spingler, R. Alberto, G. Andocs, L. Balogh and K. Bodo, *Synth. React. Inorg., Met.-Org., Nano-Met. Chem.*, 2005, **35**, 27-34.
53. N. Agorastos, L. Borsig, A. Renard, P. Antoni, G. Viola, B. Spingler, P. Kurz and R. Alberto, *Chem. -Eur. J.* , 2007, **13**, 3842-3852.
54. S. Kunze, T. Zobi, P. Kurz, B. Spingler and R. Alberto, *Angew. Chem., Int. Ed.*, 2004, **43**, 5025-5029.
55. G. Jaouen, S. Top, A. Vessieres and R. Alberto, *J. Organomet. Chem.* , 2000, **600**, 23-36.
56. J. L. Smithback, J. B. Helms, E. Schutte, S. M. Woessner and B. P. Sullivan, *Inorg. Chem.*, 2006, **45**, 2163-2174.
57. H. A. Klahn, C. Leiva, K. Mossert and X. Zhang, *Polyhedron*, 1991, **10**, 1873-1876.
58. E. Campazzi, M. Cattabriga, L. Marvelli, A. Marchi, R. Rossi, M. R. Pieragnoli and M. Fogagnolo, *Inorg. Chim. Acta*, 1999, **286**, 46-54.
59. E. Schutte, J. B. Helms, S. M. Woessner, J. Bowen and B. P. Sullivan, *Inorg. Chem.*, 1998, **37**, 2618-2619.
60. S. Sato, T. Morimoto and O. Ishitani, *Inorg. Chem.*, 2007, **46**, 9051-9053.
61. J. V. Caspar, B. P. Sullivan and T. J. Meyer, *Inorg. Chem.*, 1984, **23**, 2104-2109.
62. R. Alberto, W. A. Herrmann, P. Kiprof and F. Baumgartner, *Inorg. Chem.*, 1992, **31**, 895-899.
63. U. Abram, R. Hubener, R. Alberto and R. Schibli, *Z. Anorg. Allg. Chem.* , 1996, **622**, 813-818.
64. N. G. Connelly and W. E. Geiger, *Chem. Rev.* , 1996, **96**, 877-910.
65. N. Wiberg, *Angew. Chem., Int. Ed.*, 1968, **7**, 766-779.
66. K. Kuwata and D. H. Geske, *J. Am. Chem. Soc.* , 1964, **86**, 2101-2105.
67. R. B. King, *Inorg. Chem.*, 1965, **4**, 1518-1520.
68. L. Kromer, B. Spingler and R. Alberto, *J. Organomet. Chem.* , 2007, **692**, 1372-1376.
69. U. Koelle, *J. Organomet. Chem.* , 1977, **133**, 53-58.
70. P. J. Schlom, A. M. Morken, D. P. Eyman, N. C. Baenziger and S. J. Schauer, *Organometallics*, 1993, **12**, 3461-3467.

71. F. W. B. Einstein, A. H. Klahn-Oliva, D. Sutton and K. G. Tyers, *Organometallics*, 1986, **5**, 53-59.
72. R. M. Pearlstein, W. M. Davis, A. G. Jones and A. Davison, *Inorg. Chem.*, 1989, **28**, 3332-3334.
73. R. Alberto, R. Schibli, R. Waibel, U. Abram and A. P. Schubiger, *Coord. Chem. Rev.*, 1999, **192**, 901-919.
74. A. Egli, K. Hegetschweiler, R. Alberto, U. Abram, R. Schibli, R. Hedinger, V. Gramlich, R. Kissner and P. A. Schubiger, *Organometallics*, 1997, **16**, 1833-1840.
75. B. Cudney, S. Patel and A. Mcpherson, *Acta Crystallogr. Sect. D: Biol. Crystallogr.*, 1994, **50**, 479-483.
76. B. Safi, J. Mertens, F. De Proft and P. Geerlings, *J. Phys. Chem. A*, 2006, **110**, 9240-9246.
77. X. Y. Wang, Y. Wang, X. Q. Liu, T. W. Chu, S. W. Hu, X. H. Wei and B. L. Liu, *Phys. Chem. Chem. Phys.*, 2003, **5**, 456-460.
78. W. W. Wang, Y. K. Yan, T. S. A. Hor, J. J. Vittal, J. R. Wheaton and I. H. Hall, *Polyhedron*, 2002, **21**, 1991-1999.
79. F. Zobi, B. Spingler and R. Alberto, *Chembiochem*, 2005, **6**, 1397-1405.
80. S. E. Sherman and S. J. Lippard, *Chem. Rev.*, 1987, **87**, 1153-1181.
81. D. J. Stufkens, *Comments Inorg. Chem.*, 1992, **13**, 359 - 385.
82. D. J. Stufkens and A. Vlcek, *Coord. Chem. Rev.*, 1998, **177**, 127-179.
83. F. Zobi, O. Blacque, H. W. Schmalle, B. Spingler and R. Alberto, *Inorg. Chem.*, 2004, **43**, 2087-2096.
84. M. Howegrant, K. C. Wu, W. R. Bauer and S. J. Lippard, *Biochemistry*, 1976, **15**, 4339-4346.
85. M. Milkevitch, H. Storrie, E. Brauns, K. J. Brewer and B. W. Shirley, *Inorg. Chem.*, 1997, **36**, 4534-4538.
86. G. L. Cohen, J. A. Ledner, W. R. Bauer, H. M. Ushay, C. Caravana and S. J. Lippard, *J. Am. Chem. Soc.*, 1980, **102**, 2487-2488.
87. E. W. Abel, V. S. Dimitrov, N. J. Long, K. G. Orrell, A. G. Osborne, H. M. Pain, V. Sik, M. B. Hursthouse and M. A. Mazid, *J. Chem. Soc., Dalton Trans.*, 1993, 597-603.

88. E. W. Abel, K. G. Orrell, A. G. Osborne, H. M. Pain and V. Sik, *J. Chem. Soc., Dalton Trans.*, 1994, 111-116.
89. P. A. Anderson, F. R. Keene, E. Horn and E. R. T. Tiekink, *Appl. Organomet. Chem.*, 1990, **4**, 523-533.
90. D. H. Gibson, J. Wu, J. G. Andino and M. S. Mashuta, *J. Chem. Crystallogr.*, 2006, **36**, 769-775.
91. J. Bolger, A. Gourdon, E. Ishow and J. Launay, *Inorg. Chem.*, 1996, **35**, 2937-2944.
92. D. L. Reger, R. P. Watson, M. D. Smith and P. J. Pellechia, *Organometallics*, 2005, **24**, 1544-1555.
93. G. P. Abramo, L. Li and T. J. Marks, *J. Am. Chem. Soc.*, 2002, **124**, 13966-13967.
94. J. Wang, H. Li, N. Guo, L. Li, C. L. Stern and T. J. Marks, *Organometallics*, 2004, **23**, 5112-5114.
95. M. Ziegler, V. Monney, H. Stoeckli-Evans, A. Von Zelewsky, I. Sasaki, G. Dupic, J. C. Daran and G. G. A. Balavoine, *J. Chem. Soc., Dalton Trans.*, 1999, 667-675.
96. E. J. Schelter, A. V. Prosvirin and K. R. Dunbar, *J. Am. Chem. Soc.* , 2004, **126**, 15004-15005.
97. E. J. Schelter, J. K. Bera, J. Bacsa, J. R. Galan-Mascaros and K. R. Dunbar, *Inorg. Chem.*, 2003, **42**, 4256-4258.
98. G. Xiong, K. N. Po and K. C. Wai, *Adv. Mater.*, 1998, **10**, 1337-1340.
99. D. Chong, D. R. Laws, A. Nafady, P. J. Costa, A. L. Rheingold, M. J. Calhorda and W. E. Geiger, *J. Am. Chem. Soc.* , 2008, **130**, 2692-2703.
100. C. Hiort, P. Lincoln and B. Norden, *J. Am. Chem. Soc.* , 1993, **115**, 3448-3454.
101. S. Bodige and F. MacDonnell, *Tetrahedron Lett.*, 1997, **38**, 8159-8160.
102. Y. H. Chiu and J. W. Canary, *Inorg. Chem.*, 2003, **42**, 5107-5116.
103. , STOE & Cie, GmbH, Darmstadt, Germany, Editon edn., 1999.
104. Oxford Diffraction Ltd., Oxford, UK, Editon edn., 2007, p. Xcalibur CCD system.
105. , STOE & Cie, GmbH, Darmstadt, Germany, Editon edn., 2006.

106. A. Altomare, M. C. Burla, M. Camalli, G. L. Cascarano, C. Giacovazzo, A. Guagliardi, A. G. G. Moliterni, G. Polidori and R. Spagna, *Journal of Applied Crystallography*, 1999, **32**, 115-119.

107. G. M. Sheldrick, *Acta Crystallogr. Sect. A*, 2008, **64**, 112-122.

108. A. L. Spek, *J. Appl. Cryst.*, 2003, **36**, 7-13.

Acknowledgements

I would like to thank Prof. Roger Alberto for giving me the opportunity to work on this fascinating project in his group. His continuous dedication for chemistry but also for education and social programs is admirable. His support during all the years is greatly appreciated. Also his efforts for the children's university gave me two wonderful Saturday mornings with a bunch of children in the lab. Special thanks for the confidence to leave me the responsibility for the radiochemistry labs and radioprotection, although it's a lot of work.

Many thanks go to the whole Alberto group for the friendly atmosphere. In particular Henrik Braband, Benjamin Probst, Pilar Ruiz-Sanchez, Philipp Antoni, Yuji Tooyama, Yu Liu, Paul Schmutz, Bernhard Spingler, Felix Zelder, Daniel Can, Miguel Guttentag, Christine Croisé, Stefan Mundwiler, Pascal Häfliger, Selvi Pitchumony, Patricia Antunes, Susanne Kunze, Peter Kunz, Jae Kyoung Pak, Nikos Agorastos, Philipp Kurz, Chiara Da Pieve, Fabio Zobi, Alfredo Medina, Naresh Kumar Krishnamoorthi and all the students and short term coworkers from all over the world.

Furthermore, I would like to thank the Institute of Inorganic Chemistry at the University of Zürich and its important people: Nathalie Fichter, Patricia Allegro, Sylvia Wyss, Tanja Spörri, Susanna Sprokereef and Beatrice Spichtig for secretary work, Manfred Jöhri, Ferdinand Wild and Hanspeter Stalder for electronic and mechanistic help, Bernhard Spingler, Helmut Schmalle and Olivier Blacque for the help with the x-ray analysis, Thomas Fox and Paul Schmutz for NMR measurements, the people as well as the professors of the groups of Prof. Heinz Berke and Prof. Roland Sigel for the friendly atmosphere, all people working in the radiolabs for proper working and not making me more work as radioprotection officer as well as everyone else I forgot to mention.

Finally, I want to thank my family and best friends. Without my parents Marianne and Thomas, my brother's family Nick, Corinne, Tim and Anouk, my sister Anna with Samuel and my grandpa Max, none of this would have been possible. Patricia, thanks for your love, your support and everything else you give me even from 2000 km away. Thanks to all the people from the gym club TV Pflanzschule, to Jacqueline as well as the flat share community to be my friends and to make my leisure as comfortable as possible.

All of these people have greatly helped to reach this point.

Curriculum Vitae

Personal data

Name:	Lukas KROMER
Date of birth:	23.10.1975
Place of citizenship:	Winterthur ZH
Nationality:	Swiss

Education

1982-1991	Volksschule, Schulkreis Mattenbach, Winterthur, Switzerland.
1991-1997	Kantonsschule Im Lee, Winterthur, Switzerland.
Feb. 1997	Matura Typ C (natural sciences).
1997	Military service, basic education in medical service.
1997-2003	Study of Chemistry, University of Zürich, Switzerland.
2002-2003	Diploma thesis under the title „Untersuchungen zur Konstruktion von Neuronalen Netzwerken“ with Prof. Seeger at the Institute of Physical Chemistry, University of Zürich, Switzerland.
April 2003	Diploma degree (dipl. chem.), University of Zürich, Switzerland.
2004-2008	Research and teaching assistant with Prof. Roger Alberto, Institute of Inorganic Chemistry, University of Zürich, Switzerland. “Synthesis of Organometallic Rhenium/ Technetium Carbonyl Complexes.
May 2006	Federal Expert in Radiation Protection, Schule für Strahlenschutz, PSI, Würenlingen, Switzerland.
December 2008	PhD degree (Dissertation) at the University of Zürich, Switzerland.

Grants

November 2008	Swiss National Science Foundation (SNF), Post-doc grant for two years at ITQB, Oeiras, Portugal. "Metalcarbonyl Complexes as CO Releasing Molecules" with Prof. Dr. Carlos Romão.

Teaching / Committees

2004 - 2005	Teaching assistant in the Basic Chemistry Laboratory Course for Biology Students (GPC) at the University of Zürich, Switzerland.
2004 - 2007	Teaching assistant in several Laboratory Course in Inorganic Chemistry and Lecture assistant in Basic Chemistry and Radiochemistry.
2006 + 2007	Supervising of a student research project during the Advanced Inorganic Laboratory Course in Inorganic Chemistry.
2007 - 2008	Member of the Promotion Committee for the promotion of Prof. Dr. Roland Sigel to an Associate Professor of the Institute of Inorganic Chemistry at the University of Zürich.

List of Publications

"Synthesis and reactivity of $(Et_4N)[ReBr_2(NCCH_3)_2(CO)_2]$: A new precursor for bioorganometallic chemistry"; Lukas Kromer, Bernhard Spingler, Roger Alberto, *Journal of Organometallic Chemistry* 692 (2007) 1372-1376.

"Substitution reactions with $[ReBr_2(CO)_2(NCCH_3)_2]^-$: a convenient route to complexes with the *cis*-$[Re(CO)_2]^+$ core"; Lukas Kromer, Bernhard Spingler, Roger Alberto, *Dalton Transactions,* (2008) 5800-5808.

"Synthesis, structure and reactivities of the paramagnetic, 17 e^- complex $[ReBr_4(CO)_2]^{2-}$: A convenient precursor for Rhenium(II) and Rhenium(I) chemistry."; Lukas Kromer, Fabio Zobi, Bernhard Spingler, Roger Alberto, in preparation.

List of Contributions to Scientific Conferences

Oral presentations and invited oral presentations

"Stable $Re^{I/II}(CO)_2$ complexes: Reflection on a series of new precursors for organometallic chemistry"
Lukas Kromer (oral presentation), Bernhard Spingler and Roger Alberto; Joint research seminar: Oxford (J.R.Dilworth) – Zürich (R.Alberto), Trin, Switzerland, January 23-26, 2008.

"Stable $Re^{I/II}(CO)_2$ complexes: Reflection on a series of new precursors for organometallic chemistry"
Lukas Kromer (invited oral presentation), Bernhard Spingler and Roger Alberto; Abstract of the RheManTec: International Symposium on the Mn-triade in Life Science and Catalysis, Bloemfontein, South Africa, November 19-24, 2007.

"A New Fragment for Organometallic and Radiopharmaceutical Chemistry"
Lukas Kromer (oral presentation), Bernhard Spingler and Roger Alberto; Joint research seminar: Oxford (J.R.Dilworth) – Zürich (R.Alberto), Trin, Switzerland, March 29-April 01, 2006.

Other contributions

"Synthesis and reactivity of 17-e$^-$ "[$Re^{(II)}(CO)_2$]" based complexes"
Lukas Kromer (Poster), Bernhard Spingler, Roger Alberto; Abstract of the Fall Meeting of the Swiss Chemical Society, Lausanne, Switzerland, September 12, 2007; published in CHIMIA 2007, 61, No. 7/8.

"Water soluble $[Re(CO)_2]^+$ precursors for bioinorganic and radiopharmaceutical chemistry"
Lukas Kromer (Poster), Bernhard Spingler, Roger Alberto; Abstract of the 13th International Conference on Biological Inorganic Chemistry, Vienna, Austria, July 15-20, 2007; published in *J. Biol. Inorg. Chem.* 2007, 12 (Suppl. 1).

"*mer*-$ReBr(NCCH_3)_2(CO)_3$: A Precursor for $Re(CO)_2$ complexes"
Lukas Kromer (Poster), Bernhard Spingler, Patrick Schmartz, Roger Alberto; Abstract of the Fall Meeting of the Swiss Chemical Society, Zürich, Switzerland, October 13, 2006; published in CHIMIA 2006, 60, No. 7/8.

"Complexes with the *cis*-$[Re(CO)_2]^+$ and *mer*-$[Re(CO)_3]^+$ Cores"
Lukas Kromer (Poster, Summary), Roger Alberto; Abstract of the 7th International Symposium on TECHNETIUM in CHEMISTRY and NUCLEAR MEDICINE, Bressanone, Italy, September 6-9, 2006.

"New high affinity organometallic tamoxifen derivatives for diagnosis and therapy of breast cancer"
A. Nguyen (Poster), S. Top, A. Vessières, M. Huché, P. Pigeon, V. Marsaud, J.M. Renoir, L. Kromer, R. Alberto, G. Jaouen; 1st European Chemistry Congress, Budapest, Hungary, August 27-31, 2006.

"New high affinity organometallic tamoxifen derivatives for diagnosis and therapy of breast cancer"
A. Nguyen (Poster), S. Top, A. Vessières, M. Huché, P. Pigeon, V. Marsaud, J.M. Renoir, L. Kromer, R. Alberto, G. Jaouen; International Conference on Organometallic Chemistry, Zaragoza, Spain, July 23-28, 2006.

"$(Et_4N)[ReBr_2(NCCH_3)_2(CO)_2]$ as a New Precursor for Bioorganometallic and Radiopharmaceutical Chemistry"
Lukas Kromer (Poster), Bernhard Spingler, Roger Alberto; Abstract of the 3rd International Symposium on Bioorganometallic Chemistry, Milano, Italy, July 5-8, 2006.

"Reactions of the $[Re(CO)_2]^+$ core with different ligands"
Lukas Kromer (Poster), Bernhard Spingler, Roger Alberto; Abstract of the Fall Meeting of the Swiss Chemical Society, Lausanne, Switzerland, October 13, 2005; published in CHIMIA 2005, 59, No. 7/8.

"A New Fragment for Organometallic and Radiopharmaceutical Chemistry"
Lukas Kromer (Poster), Roger Alberto; Abstract of the Fall Meeting of the Swiss Chemical Society, Zürich, Switzerland, October 7, 2004; published in CHIMIA 2004, 58, No. 7/8.